

**REAL-TIME SAFETY ASSISTANCE TO IMPROVE OPERATORS' SITUATION
AWARENESS IN CRANE LIFTING OPERATIONS**

A Dissertation
Presented to
The Academic Faculty

by

Yihai Fang

In Partial Fulfillment
of the Requirements for the Degree
Doctor of Philosophy in the
School of Civil and Environmental Engineering

Georgia Institute of Technology

December 2016

Copyright © 2016 by Yihai Fang

**REAL-TIME SAFETY ASSISTANCE TO IMPROVE OPERATORS' SITUATION
AWARENESS IN CRANE LIFTING OPERATIONS**

Approved by:

Dr. Yong K. Cho, Advisor
School of Civil and Environmental Engineering
Georgia Institute of Technology

Dr. Daniel Castro-Lacouture
School of Building Construction
Georgia Institute of Technology

Dr. Iris Tien
School of Civil and Environmental Engineering
Georgia Institute of Technology

Dr. Francis T. Durso
School of Psychology
Georgia Institute of Technology

Dr. Chimay J. Anumba
College of Design, Construction & Planning
University of Florida

Dr. Feniosky A. Peña-Mora
School of Engineering and Applied
Science
Columbia University

Date Approved: November 8, 2016

ACKNOWLEDGEMENTS

The achievement of my past five years would not have been possible without the advisory and support of numerous professors, colleagues, friends, and family members. First and foremost, I would like to express my sincere gratitude to my advisor, Dr. Yong K. Cho, for the advisory and support he gave me throughout my doctoral study and research. His vision, passion, and knowledge inspired my research and established my enthusiasm in academia and will continue to motivate me in my future career. I would also like to thank other professors and mentors of mine, Dr. Chimay Anumba, Dr. Daniel Castro, Dr. Francis Durso, Dr. Feniosky Pena-Mora, Dr. Jochen Teizer, and Dr. Iris Tien, for their constant encouragement, insightful comments, and constructive criticism.

I would like to express my gratitude to my fellow colleagues at the RICAL and RAPID labs, Tao Cheng, Nipesh Pradhananga, Sijie Zhang, Chao Wang, Kyungki Kim, JeeWoong (Jay) Park, Jingdao Chen, and Rahul Ramachandran among all the others. We together overcame numerous physical and mental challenges, such as 20-hour straight driving, weeklong field tests in extreme weather, and tedious grading tasks. Studying in such a distinguished institution is very demanding and stressful. I will always remember and cherish all the joyful and exiting moments with my dear friends, Xinjun Dong, Xia Li, Dan Li, Zhen Huang, Yu Liu, Penzi Yu, Xiaoxi Liu, Jiaying Su, and Yan Li.

Finally, I would like to dedicate this dissertation to my family who supports me with no reservation. I consider myself very lucky and blessed to be the son of Dongping Fang and Lin Lin. Besides being incredible parents, they showed me what a true researcher and educator looks like and supported my dream to continue this family tradition. I am so

grateful to have the support and companion of my wife, Ruyi Jiang, who always has confidence in me and cheers me up with her unconditional love.

TABLE OF CONTENTS

ACKNOWLEDGEMENTS	iii
LIST OF TABLES	ix
LIST OF FIGURES	x
SUMMARY	xiii
CHAPTER I INTRODUCTION	1
1.1. Motivation and Background	1
1.1.1. Crane lifting operations and the safety issues	1
1.1.2. Direct and root causes of crane-related accidents	2
1.2. Research Objectives and Scope	5
1.3. Dissertation Organization	6
CHAPTER II LITERATURE REVIEW	8
2.1. Current Practices in Crane Lifting Planning	8
2.2. Existing Technologies for Real-time Lifting Assistance	11
2.2.1. Anti-overturn devices	11
2.2.2. Camera system for enhancing operator visibility	12
2.2.3. RTLS-based crane motion tracking	13
2.2.4. Vision and LiDAR-based equipment pose monitoring methods	15
2.2.5. Critical motion capturing using Encoder Sensors	18
2.3. Effectiveness of Lift Assistance Systems	22
2.3.1. Interactions between operators and assistance systems	22
2.3.2. Evaluation of assistance effectiveness	23

2.4. Operator Error and Situation Awareness	24
2.4.1. Operator error analysis from a cognitive perspective	24
2.4.2. Situation awareness in crane lifting operations	26
2.4.3. Measures of situation awareness.....	27
2.5. Point of Departure.....	29
CHAPTER III RESEARCH FRAMEWORK	31
3.1. Technical framework	31
3.2. System Architecture.....	32
CHAPTER IV REAL-TIME CRANE MOTION CAPTURING	35
4.1. Direct Measurement of Crane Motion Using Sensors	35
4.1.1. Critical motion analysis of crane manipulation and suspension modules	35
4.1.2. Manipulation module motion capturing using rotary encoders	37
4.1.3. Suspension module motion capturing using an inertia measurement unit.....	37
4.4. Error Estimation and Sensitivity Analysis for Crane Pose Reconstruction	40
4.5. Field Test and Discussion	44
4.7. Conclusions.....	51
CHAPTER V AS-IS SITE CONDITION MODELING AND UPDATING	52
5.1. As-is Geometric Data Collection	52
5.2. Site Condition Modeling based on Point Cloud	53
5.3. Site Condition Updating Using a Point Cloud-Vision Hybrid Approach.....	55
5.5. Conclusions.....	61
CHAPTER VI HAZARD ANALYSIS AND REAL-TIME VISUALIZATION.....	62
6.1. Hazard Analysis based on Crane Motion and Site Condition.....	62

6.2. Real-time Visualization and Warnings	64
6.3. Conclusions.....	66
CHAPTER VII EFFECTIVENESS VALIDATION OF LIFTING ASSISTANCE	68
7.1. Effectiveness Assessment Approach	68
7.1.1. Assessment of perceived workload.....	68
7.1.2. Quantitative assessment of lifting performance.....	70
7.1.3. Online assessment of situation awareness	73
7.2. Field Tests and Validation Results	75
7.2.1. Field test 1 overview	75
7.2.2. Assessment of effectiveness in lift performance improvement	77
7.2.3. Impact analysis of individual characteristics	81
7.2.4. Field test 2 overview	84
7.2.5. Workload indexes for two lifting tasks.....	88
7.2.6. Assistance effectiveness in improving lift performance	89
7.2.7. Assistance effectiveness in improving operator's SA	92
7.2.8. General feedback from the operators.....	96
7.3. Conclusions.....	100
CHAPTER VIII ECONOMIC ANALYSIS	102
8.1. Cost estimate.....	102
8.2. Return estimate	103
8.2.1. Benefits in safety improvement	103
8.2.2. Benefits in efficiency improvement.....	105
8.3. Return of investment analysis.....	106

8.4. Conclusions.....	106
CHAPTER IX CONCLUSIONS AND DISCUSSION	107
9.1. Summary	107
9.2. Research Contribution and Impacts	108
9.3. Discussion and Recommendation for Future Research	110
REFERENCES	112
VITA	119

LIST OF TABLES

Table 1: Summary of state-of-the-art real-time lift assistance.....	21
Table 2: Accuracy and range of sensor measurements.....	41
Table 3: Proximity thresholds in the hazard analysis based on level of severity	63
Table 4: Query list for online SA measurement	74
Table 5: Mean and standard deviation of five KPIs in three test scenarios.....	79
Table 6: Results of general feedback survey in five Likert scale	97
Table 7: Cost breakdown for a single assistance system	103

LIST OF FIGURES

Figure 1: Fatalities in crane-related accidents from 1997 to 2014 [3]	2
Figure 2: Sources of information to be processed by a crane operator.....	4
Figure 3: Crane lift path planning using RRT [26].....	10
Figure 4: Load Moment Indicator [34]	12
Figure 5: UWB sensor and tag deployment for crane motion tracking [34]	14
Figure 6: SmartDig system using computer vision technique [40].....	16
Figure 7: Time-elapsed 3D scenes of the workspace [42].....	17
Figure 8: Sensor setup and user interface design in a crane cabin [44]	19
Figure 9: User interface for collecting obstacle data [45].....	19
Figure 10: Sequential model of accident development from a hazard cognition perspective (adapted from [54])	25
Figure 11: Situation awareness (SA) in crane operation and the relationship between SA and working memory (WM)	27
Figure 12: Framework for real-time lift safety assistance	32
Figure 13: System Architecture	33
Figure 14: Kinematics configuration of a typical telescopic boom mobile crane	36
Figure 15: Transforming the angular measurements to absolute positions	38
Figure 16: Error estimation using Monte Carlo Method	43
Figure 17: Sensitivity analysis of load positioning in X-axis	44
Figure 18: Sensor configuration for critical motion capturing	45

Figure 19: IMU sensor configuration for load position measurement.....	46
Figure 20: Comparison between actual lifting (upper) and reconstructed lifting process (lower) in site overview	33
Figure 21: Comparison between actual load sway motion (upper) and reconstructed load sway motion (lower) from the boom's top view.....	33
Figure 22: Errors of virtual lift reconstruction during 92 lifting tasks	50
Figure 23: Lifting site condition modeling process based on point cloud data	55
Figure 24: (a) synthetic image and (b) depth buffer generated from point cloud.....	56
Figure 25: Object detection using feature point matching with a reference image, (a) objects of interest, (b) feature points identified.....	57
Figure 26: Projection of image coordinates into 3D space from camera origin	58
Figure 27: Results of 3D location updating of two vehicles: image captured from UAV (left) and updated 3D site model (right)	60
Figure 28: Flowchart of collision hazard identification.....	63
Figure 29: A Graphical User interface (GUI) for real-time visualization and warning....	47
Figure 30: Graphical user interface deployed in a mobile crane cabin.....	66
Figure 31: Query process in online SA measurement	73
Figure 32: Illustration of Task #1 in top view	76
Figure 33: Illustration of Task #2 in isometric view.....	76
Figure 34: Boxplot of five key performance indexes (KPIs) in no assistance, optional assistance, and full assistance scenarios	78
Figure 35: Relationship between system usage (percentage of total lift time in seconds) and the lift performance of each individual operator.....	82

Figure 36: Illustration of lifting task#1 in top view	86
Figure 37: Illustration of lifting task#1 in isometric view	86
Figure 38: Illustration of lifting task#2 in top view	87
Figure 39: Illustration of lifting task#2 in isometric view	87
Figure 40: Key performance indexes (KPIs) in two lifting tasks under control and test scenarios.....	90
Figure 41: Average response time in two lifting tasks under control and test scenarios..	93
Figure 42: Average response correctness in two lifting tasks under control and test scenarios.....	94
Figure 43: Average response time breakdown in each query	95
Figure 44: Average response correctness breakdown in each query	96
Figure 45: Incident pyramid [82]	104

SUMMARY

Operating a crane is a sophisticated job that not only requires the operators to have extensive skills and experience, but more importantly a comprehensive situation awareness (SA) of the crane and its surroundings throughout the operation. Despite that several real-time assistance systems exist, they cannot reliably monitor crane motion in real-time and fail to fully consider environmental constraints and changes. In addition, very few of them explored the actual impact of the system on lift performance and operators' SA.

This doctoral research creates a framework for enabling real-time safety assistance for mobile crane lifting operations, and to explore a quantitative method to validate the impact of such assistance system on lift performance and the operator's SA. Based on the framework, a practical system architecture is created featuring three major components: real-time crane motion capturing, as-is site condition modeling and updating, and hazard analysis and real-time visualization. First, crane poses are reconstructed in real-time based on the critical motions of crane parts captured by a hybrid sensor system. Second, as-is lifting site conditions are modeled based on point cloud data and updated using a point cloud-vision hybrid approach. Lastly, the risk of colliding the crane parts and lifted load into nearby obstructions is pro-actively analyzed and warnings are provided to the operator through a graphical user interface. A prototype assistance system implementing the system architecture is developed and deployed on a real mobile crane. A series of field tests in realistic lift scenarios revealed that this system was able to capture and visualize crane motion in real-time with an accuracy of 0.43 m. Based on crane motion and as-is site conditions, the system was able to identify the potential collision hazards and provide

timely warnings to the operator to mitigate the risk. The effectiveness of the assistance system is quantitatively validated by the improvement in lift performance and SA, where lift performance is quantified by five key performance indexes (KPIs) and SA is measured using an online query-based technique.

The major contribution of this research is the creation of a technical framework and a practical system architecture toward providing effective safety assistance to crane operators during lifting operations. The findings in this research have the potential to complement existing safety measures in crane lifting practices by providing an additional layer of technology to prevent human error-related crane accidents.

CHAPTER I INTRODUCTION

This chapter examines crane accident records and prominent challenges in crane safety. According to the investigation of past crane accidents, this chapter unveils the direct and root causes of crane accidents and outlines the research objectives and scope in this thesis.

1.1. Motivation and Background

1.1.1. Crane lifting operations and the safety issues

A crane is one of the most essential and commonly used type of machinery in the construction industry. The global crane market is anticipated to exceed \$45 billion in 2016, an increase of more than 25% over 2012 [1]. In the United States alone, approximately 125,000 cranes of different types are in operation every day among all sectors of the construction industry, from single houses to international mega projects [2]. Throughout the entire construction phase of a project, cranes are responsible for a great portion of vertical and horizontal transportations of construction resources including materials, equipment, and personnel.

Compared to other types of accidents, crane-related accidents are less common; however, once they occur, the consequences are much more significant as they very often result in significant cost increase, schedule delay, and most importantly and commonly, serious injuries and fatalities. From 1997 to 2014, the number of fatalities in crane-related accidents totaled 1215 for all industry sectors [3] (Figure 1). It should be noted that the construction industry was responsible for 566 fatalities (47%) in that period, within which 306 deaths (54%) related to mobile cranes. Another source reported that 632 construction workers were killed in crane-related accidents from 1992 to 2006, 78% of which were

associated with mobile cranes [4]. Responsible Behind these numbers are more than 250,000 crane operators and a very large but undetermined number of other workers and even the general public. Unlike other accidents on construction sites, the victims in crane-related accidents are not necessarily limited to construction labors and crane operators but also pedestrians as observed in many crane-related accidents [5].

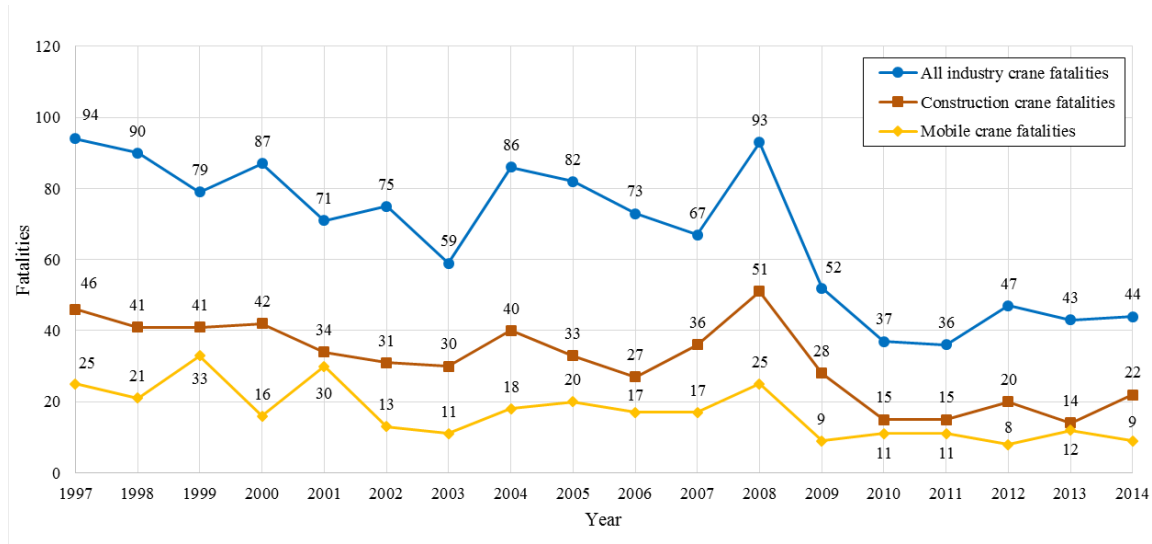


Figure 1: Fatalities in crane-related accidents from 1997 to 2014 [3]

1.1.2. Direct and root causes of crane-related accidents

Construction sites are often very congested with obstructions such as materials, equipment, and structures of different heights and shapes. The Center for Construction Research and Training (CPWR) reported that 61% crane accidents involved crane parts or loads colliding with obstructions (e.g., power lines, personnel, structure) [4]. Similarly, Beavers et al. concluded that struck by the load (32%) and failure of boom/cable (12%) together accounted for 44% of the total number of fatalities [6]. In most cases, collision

accidents occur mainly due to spatial conflicts existing between crane parts and the surrounding obstructions. Within the large workspace of cranes, the presence of built building structure, storage of materials, and power lines introduces massive potential spatial conflicts in crane lifting operations. Suruda et al. [7] reported that 40% of the deaths in crane-related accidents were related to spatial conflicts. Furthermore, when analyzing crane-related spatial conflicts, one must consider the dynamic crane motions and changes in the surrounding environment as the project proceeds [8].

In addition to spatial conflicts, these obstructions introduce blind spots into crane lifting operations, which significantly limits the operator's visibility. Sitting high in a tower crane cabin or low in a mobile crane cabin, operators often find it difficult to determine the absolute height or relative distances between the lifted load and surrounding objects. The limited visibility and depth perception lead to the poor situation awareness of the hazards associated with the lifting operation, which greatly limits the operators' ability to identify potential hazards, choose risk-free paths, and timely react to emergencies [9]. It has been well recognized that real-time information and assistance for decision-making are necessary and sometimes critical for many construction tasks involving human-machine interaction [10].

As spatial conflicts being one of the major direct causes of crane-related accidents, human errors are considered an underlying source of risks [11]. King found that 32 out of the 75 crane accidents from 2004 to 2010 (43%) were due to the operator failure in their responsibilities [12], while Neitzel et al. pointed out that 75% of crane overturn accidents are due to operator error [5]. A recent investigation on risk factors in crane-related near-misses and accidents reveals that inattention is the most prevalent type of risk that accounts

for 19% of incidents [13]. In addition, signal person error and operator error total 24% of the 212 investigated incidents. Crane lifting operations are inherently a sophisticated job that imposes significant mental workload to crane operators. In any given second during a lifting operation, a crane operator is required to process the information from multiple scattered sources simultaneously (Figure 2). During the lift, a crane operator needs to continuously monitor the environment changes such as wind speed and the presence of foreign objects (e.g., unauthorized equipment and personnel), based on which the operator adjusts the crane maneuver speed or alters the lifting strategy. At the same time, the operator has to understand the crane's capacity and status using the load chart, boom angle indicator, or load moment indicator. In addition, lifting operations usually involve the coordination with the riggers or signal people. However, the information the operator receives from these sources is not always accurate or complete due to various reasons such as obstructed line-of-sight, poor communication or misunderstanding.

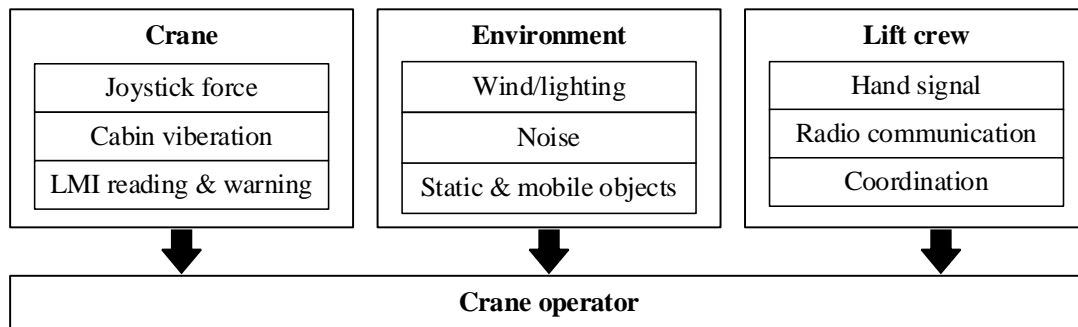


Figure 2: Sources of information to be processed by a crane operator

1.2. Research Objectives and Scope

Despite significant attention and extensive research efforts on crane safety, crane remains one of the major sources of construction fatalities in recent decades. Although direct causes may vary in different accidents, the underlying cause is often related to operator errors. The primary research goal is to design, test, and validate a framework for providing real-time safety assistance that reduces crane accidents related to operator errors. To achieve the research goal, two critical research questions need to be answered:

- 1) What components, requirements and expectations constitute effective and reliable safety assistance for crane lifting operations?
- 2) How to validate the effectiveness of a safety assistance system in improving lift performance and operators' situation awareness?

In order to achieve the primary goal and to answer the research questions, three research objectives have been set as follows:

- To develop a framework that identifies major technical components to realize effective real-time safety assistance
- To create sensor systems and processing algorithms that enable real-time crane motion capturing, as-is site condition modeling and updating, and hazard analysis and visualization
- To create assessment techniques that validate the effectiveness of assistance systems in improving lift performance and operator's situation awareness

This research will focus on mobile cranes as they are the most commonly used type of cranes in construction and more prone to accidents than other types. The hazards

considered in this research will be limited to collisions between crane parts and surrounding obstructions.

1.3. Dissertation Organization

Chapter 1 introduces the challenges in crane safety, explores the direct and root causes of crane accidents, and outlines the research objectives in this thesis.

Chapter 2 summarizes the current practices in crane safety, critically reviews the state-of-the-art in real-time lift assistance, and highlights the importance of human factor in the design and validation of assistance systems.

Chapter 3 presents a technical framework for enabling real-time safety assistance and a practical system architecture to facilitate implementation.

Chapter 4 describes the design, development and deployment of a sensor system for real-time crane motion capturing. This chapter highlights a computation algorithm that monitors and tracks crane load position using a wireless IMU sensor.

Chapter 5 introduces a method to automate 3D modeling and updating of as-is lifting site condition enabled by a point cloud processing pipeline and a point cloud-vision hybrid method for 3D scene updating.

Chapter 6 introduces a pro-active hazard analysis algorithm and a visualization framework for effective safety warning and user interaction.

Chapter 7 describes a quantitative assessment technique for validating the improvement of lift performance and operators' situation awareness. Two field tests are introduced to validate the effectiveness of the developed safety assistance system.

Chapter 8 presents an indicative economic analysis of the real-time safety assistance framework to explore the potential return of investment on such assistance system.

Chapter 9 summarizes the work in this research and outlines the future research directions.

This chapter highlights the research findings and limitations and emphasizes the intellectual merits and broader impact on the construction industry.

CHAPTER II LITERATURE REVIEW

Crane safety has been a great concern in both construction industry and academia. Closely related to the techniques employed in this research, this chapter thoroughly reviews and evaluates the previous research efforts in crane safety including crane lifting planning, real-time crane motion monitoring, construction visualization and simulation, and operator situation awareness analysis. Limitations in previous research and the needs for the proposed research are concluded based on the review findings.

2.1. Current Practices in Crane Lifting Planning

Crane lifting planning is an essential planning task that is critical for the productivity and safety of the entire project [14]. Tasks in crane lifting planning usually include three basic components: crane location planning, lifting path planning, and lifting visualization and simulation.

The goal of crane location or layout planning aims to maximize crane utilization in transporting construction resources. This is a complicated optimization problem involving various spatial-temporal constraints. In current practices, a crane location is typically determined by experienced lift coordinators through trial and error given the site shape and topography, and the distribution of anticipated lifting tasks [15]. This manual process can be assisted or validated by simulation technologies [16] [17] and optimization algorithms [18][19][20][21].

The objective of path planning is to plan a collision-free and efficient lift path based on load data (e.g., size, weight) and site geometric constraints. Traditionally, the lift path is planned mainly depending on the planners' intuition and experience and this process is

often labor intensive and error prone [22]. Recently, researchers have adopted the knowledge and techniques in robotic motion planning to automate the lift planning process. In this approach, a crane is treated as a multi-degree-of-freedom robotic manipulator and various algorithms, such as Heuristic Search [23][24], Probabilistic Road Map [25], Rapidly Exploring Random Tree (RRT) [26][27][28][29], were tested to optimize a lift path to ensure a collision-free travel while guaranteeing a respectively short lift path (Figure 3). It should be noted that the computer-aided path planning only works when provided with accurate and comprehensive site geometric information. Site geometry, however, is not always available or accurate in the early planning phase. In addition to static obstructions, when analyzing crane-related spatial conflicts, one must consider the dynamic crane motions and changes in the surrounding environment as the project proceeds [8]. Design changes occur throughout the planning phase and even during the construction phase, and thus site drawings or models used for lift path planning no longer represent all the geometric constraints existing in the actual lifting site. These variances between planned and actual site conditions inevitably compromise the validity of the planned lift paths.

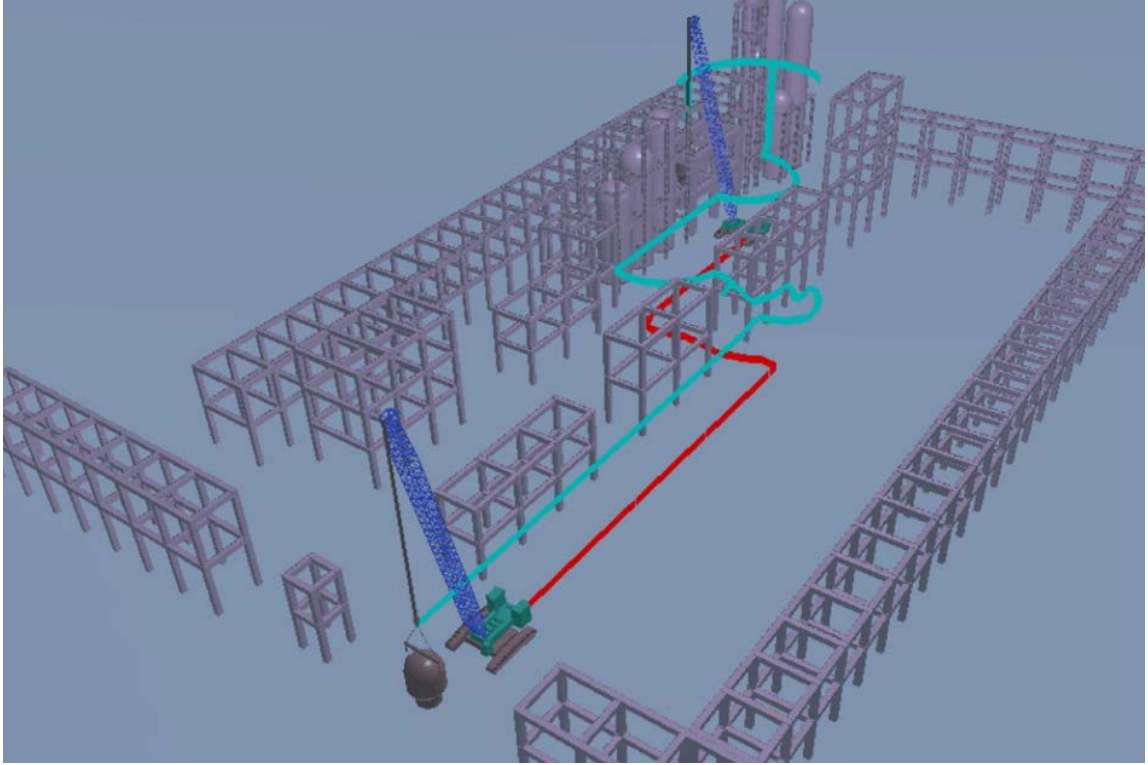


Figure 3: Crane lift path planning using RRT [26]

Simulating and visualizing lifting process are critical tasks in crane lifting planning. Detailed simulation and close-to-reality visualization help the management team and the operator to understand constraints and hazards associated with lifting tasks [30]. In the past decades, the developments in kinematics and dynamic modeling for crane motion simulation and collision detection enables a wide range of applications in visualization and simulation in crane operations [31]. Configurable models that consist of multiple rigid bodies and different joint constraints were introduced to represent multi-body dynamics among different crane parts (e.g., cabin, boom, load) in physics engines [32].

2.2. Existing Technologies for Real-time Lifting Assistance

With the development of information technology, researchers realized that technology can provide another layer of protection in construction safety [33]. Crane operations can benefit from technologies similar to the advanced driver assistance systems implemented on vehicles that provide real-time support to the driver based on surrounding situations. The following sections introduce technologies that have been investigated or implemented in crane lifting operations.

2.2.1. Anti-overturn devices

Mobile cranes can overturn as a result of lifting excessive loads, overreaching, high winds and/or swinging loads, which increase the load radius and overturning moment. Overturns can also happen when the crane is erected with unstable ground conditions (e.g., slope, loose soil) or when the outriggers are not used properly. Although crane overturns are caused by various reasons, 75% of overturn accidents are related to human errors [7]. Referring to the load charts is the most straightforward way for the crane operator to understand the crane's capacity under different configurations. However, it is not easy for the operator to know the crane's states such as boom angle and horizontal reach, especially during the lifting operation. Therefore, load moment indicator (LMI) was introduced to aid the crane operator by measuring the overturning moment on the crane, i.e., load multiplied by radius. It compares the current lifting condition to the crane's rated capacity or load chart and indicates to the operator the percentage of capacity at which the equipment is working and sends warnings if the percentage exceeds a safe limit. Many anti-upset devices such as anti-two-block devices, boom stops, and LMI systems have become standard or

mandatory for most cranes, especially heavy-duty cranes (Figure 4). Active anti-overturn devices, such as the LMI system, send warnings to the operator when a potential overturn incident is detected. Upon receiving the warning, the operator needs to determine what measures need to be taken and then correctly take the actions to mitigate the potential hazards. Therefore, the use of active systems such as LMI will adversely increase the cognitive workload during the lifting operations.



Figure 4: Load Moment Indicator [34]

2.2.2. Camera system for enhancing operator visibility

Providing additional view angles using cameras is a straightforward solution to increase operators' visibility. Typically, a camera system includes a wireless camera mounted on crane trolley or hook block directed downwards, and a monitor in the crane cabin showing the lifted load and the workspace underneath [28] [29]. Despite much positive feedback from the users, whether the camera system will increase the operator's SA is controversial. Since the monitor in the cabin provides only 2-dimensional images without depth

perception, the operator cannot determine the height of load at the lower level or the proximity from the load to surrounding objects. In addition, the cameras are fixed to the crane parts, which makes it less flexible in complicated lifting scenarios such as blind lifts. Furthermore, camera systems provide no automatic warning function, and thus the operator has to constantly check the monitor while operating the crane. This introduces additional workload and distractions to the operator, which could ironically increase the risk of accidents.

2.2.3. RTLS-based crane motion tracking

A real-time location system (RTLS) is a technology that tracks the location of tagged objects in real-time. In construction, RTLS technology has been used for site security, resource location tracking, and equipment safety. In crane operation domain, Luo et al. discussed the requirements for autonomous crane safety monitoring[34]. They envisioned the requirements and strategies to leverage RTLS technology for autonomous crane safety monitoring. To estimate mobile crane poses in near real-time, Zhang et al. employed a high-precision RTLS technology named Ultra-wide band (UWB) with UWB readers deployed around the lifting site and UWB tags mounted on different spots of crane boom and lifted load [35] (Figure 5). The system is able to estimate crane poses in near real-time through noise filtering and missing data filling. Using the similar technology, Hwang studied the characteristics of different collision types and developed a computer program for monitoring crane motions and sending warnings if a potential collision hazard was detected [36]. Li et al. took advantage of Global Positioning System (GPS) and Radio Frequency Identification (RFID) for developing a real-time crane motion monitoring

system [37]. Tracking crane parts and construction workers, this system aims to assist the safety operation in blind lifts by detecting the presence of unauthorized workers within a risk zone. Luo et al. analyzed the impact of RTLS sensor errors on autonomous crane safety monitoring [38]. They proposed a three-level safety zone for incorporating RTLS-based location data in the identification of wing-above-worker incidents.

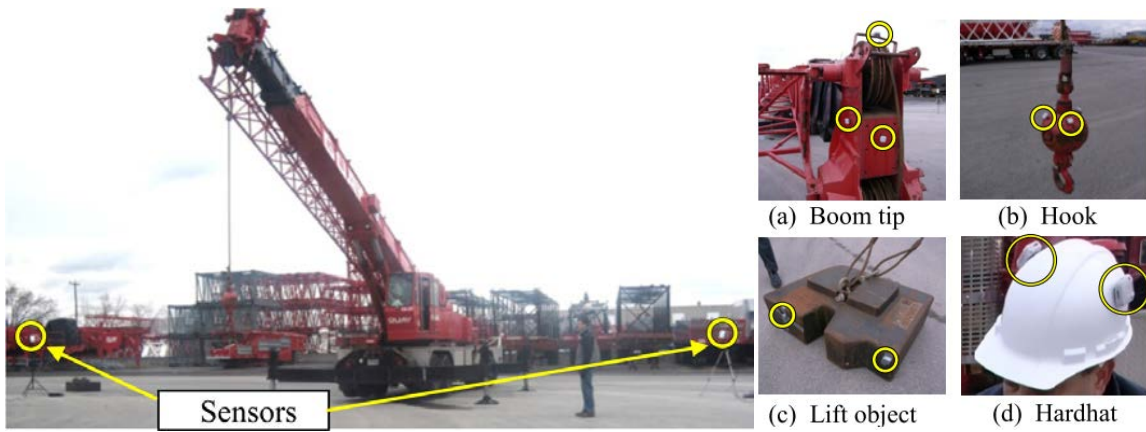


Figure 5: UWB sensor and tag deployment for crane motion tracking [34]

These efforts demonstrated the feasibility of using RTLS for crane pose/motion monitoring. However, the RTLS technology suffers from several limitations that compromise its performance in crane motion monitoring. Firstly, most RTLS system requires setting up hardware including readers, cables for data transmission and synchronization, power supply, and computer for data collection and processing. Depending on the range of the RTLS readers, the number of readers needed to cover the site needs to increase accordingly as the size of the crane to be monitored increases. In addition, crane lifting is a 3-dimensional operation that requires the RTLS system to be

deployed at various heights in order to track the vertical movement of crane parts and load. This not only requires setting up a big amount of RTLS antennas around the lifting site ahead of time, but also means a big investment in hardware given that the cost of UWB is approximately \$140/m² [39]. Secondly, the site security and vandalism for the installed sensing system would be another concern unless the components are installed and retrieved every day. Thirdly, the RTLS technology inherently suffers from signal interference due to multi-path propagation, fading and scattering of signals [40]. These problems become more significant in metallic and densely packed construction environment. As recognized by Zhang et al., their UWB tracking system failed to reliably track the load position because the tags on the crane load cannot be detected and tracked continuously due to serious signal loss [35].

2.2.4. Vision and LiDAR-based equipment pose monitoring methods

Computer vision techniques extract high-dimensional data from digital images or videos and it has been widely used for robot pose tracking in robotics research. Feng et al. introduced a computer vision based approach that uses a set of cameras and markers to identify the pose of articulated equipment [41]. This method requires to set up at least two cameras and multiple planer markers on each of the articulated part and on a pre-survey fixed location near the equipment (Figure 6). This method is able to yield centimeter-level tracking accuracy with a flexible and cost-effective system comprised of ordinary cameras and markers. Although this method performed well in tracking the pose of an excavator in a small workspace, limitations such as sensitivity to occlusions and increased complexity in system setup can be expected when this method is applied to tracking crane pose on a

much larger scale and more dynamic workspace. Instead of using markers, Yang et al. proposed an algorithm to track the job pose of a tower crane by processing and analyzing the images captured by a single site surveillance camera [42]. With the known locations of the surveillance camera and the configuration of the tower crane, a set of synthetic images were generated using a virtual 3D model of the crane. The crane poses in actual images can be identified by comparing them to the synthetic images. This method requires pre-surveying the location of the camera and crane, which is possible for tower crane settings but is challenging for mobile crane setting as the system needs to re-setup every time the mobile crane moves.



Figure 6: SmartDig system using computer vision technique [40]

LiDAR or Laser scanning is a non-destructive sensing technology that rapidly and accurately captures the shape physical objects in a form of point cloud. To help equipment

operators rapidly perceive the crane pose and surrounding environment, Cho and Gai introduced a dynamic object recognition and registration methods using computer vision and laser scanning technologies [43]. The 3D point cloud is projected to a 2D space where the geometric features represented by a local SURF descriptor are compared to a prepared template database for recognition. This method is effective and efficient for recognizing target objects that are known to be present on the construction site. For unknown objects with high shape variance, however, the performance of this method is limited. In addition, the refresh rate of the time-elapsd 3D visualization, which is limited by the scanning speed of LiDAR system, is considered inadequate for many real-time applications (Figure 7).

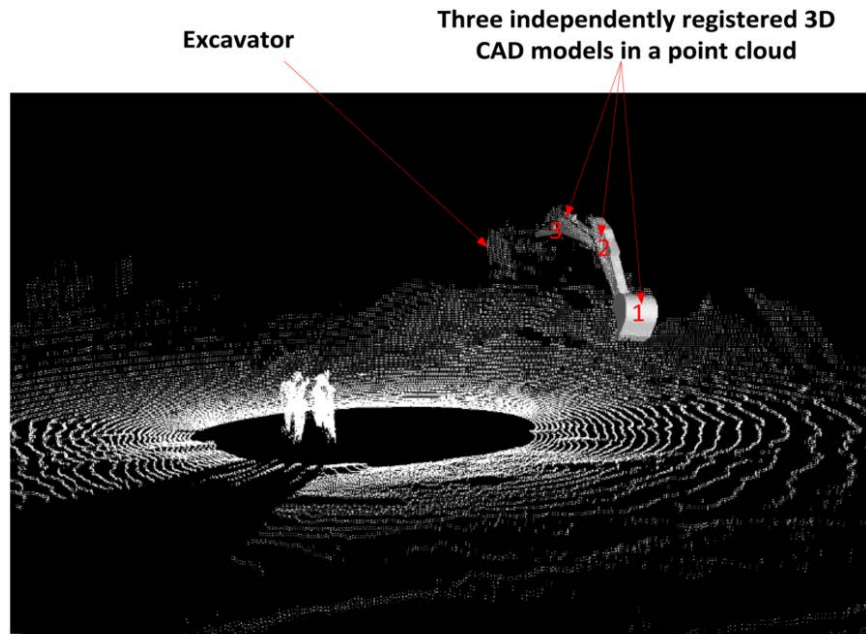


Figure 7: Time-elapsd 3D scenes of the workspace [42]

Wang and Cho proposed a smart scanning technique for tracking the location and pose of construction equipment as well as modeling the dynamic workspace [44]. By

updating the target object's point cloud data while keeping the previously scanned static workspace data, this method greatly improves the modeling and visualization rate, which makes it suitable for real-time visualization and decision-making support. The biggest benefit of LiDAR-based pose monitoring methods is that it is non-invasive, meaning that there is no need to deploy any sensors or devices on the equipment. Instead, it requires a data acquisition system to operate in proximity to the equipment, and sophisticated infrastructure setup for real-time data processing and transmission.

2.2.5. Critical motion capturing using Encoder Sensors

Critical crane motions stand for the key freedoms of major crane parts that, when combined are able to represent most possibilities of crane maneuvers. Lee et al. proposed a crane motion monitoring system using multiple encoders and laser sensors, which successfully captured and visualized the motion of a tower crane in real-time [45] (Figure 8). However, this system does not consider the load sway, and the configuration of a laser sensor and reflection board cannot reliably measure the load elevation during excessive load sway. Ren and Wu developed a real-time anti-collision system that creates a safe lift zone during lifting based on the location and shape of static obstacles collected prior to the lift [46]. However, this process involves extensive manual input and additional data collection time prior to the lift (Figure 9).



Figure 8: Sensor setup and user interface design in a crane cabin [44]

Real-Time State: RotationAngle: 79.4; ElevationAngle: 48.4; BoomLength:43.5m;

Choose object class to start collecting

- Wall Object
 - Horizontal
 - Vertical
 - Inclined
 - Outward
 - Inward
- Ordinary Object
 - Hanging
 - Ground
 - Cylinder
 - Cube
 - Incline

Real-time top view

Data Collecting

Class: Ground Cylinder

	Rotation Angle	Elevation Angle	Boom Length	
Left-most	325.4	25.3	57.6	Recollect
High-most	321.2	39.6	67.5	Recollect
Right-most	316.4	23.7	55.0	Recollect

Finish collection

Mend&Del Con-collect Back

Figure 9: User interface for collecting obstacle data [45]

Compared to the RTLS-based and camera-based crane monitoring methods, the direct motion capturing method hold several apparent advantages. Firstly, hardware employed in the systems is usually more cost-effective and durable in long-term use. Once securely installed on the crane, the sensors require little maintenance and with proper enclosure they can work properly in harsh environmental conditions. Secondly, sensor-based methods do not require external hardware deployment on the site, and thus it introduces minimal interruption to other construction activities.

Table 1 summarizes the characteristics of the aforementioned technologies that are available to provide real-time lift assistance to the operators. There is no doubt that each of these technologies to a certain extent or on certain aspect improves the operator's SA in understanding the crane status as well as the environment conditions. However, these technologies are subject to limitations including compromised accuracy and reliability in harsh construction environment, inadequate modeling and representation of lifting site conditions, and time-consuming and demanding system setup process prior to the lift. Another issue that hinders the industry from adopting such technologies in the field is a lack of scientific and systematic validation of these systems' effectiveness in field experiments. The following section introduces the current body of knowledge and practices in effectiveness evaluation of existing assistance systems.

Table 1: Summary of state-of-the-art real-time lift assistance

	RTLS-based	Camera-based	Vision and LiDAR-based	Encoder-based
Occlusion-resistant				✓
Simple & durable setup		✓		✓
As-is environment		✓	✓	
Graphical user interface		✓	✓	✓
Analysis & warning	✓		✓	✓
References	[34] [36] [35] [37] [38]	[47] [48] [49]	[10] [43] [44]	[45] [46] [50] [51]

2.3. Effectiveness of Lift Assistance Systems

2.3.1. Interactions between operators and assistance systems

The interaction between the operator and the assistance system is an important factor in the effectiveness of operational assistive systems. Most assistance systems such as the Load Moment Indicator (LMI) system provide only numerical feedback, failing to give operators contextual awareness. In such cases, operators must rely on their understanding of the current operating conditions (e.g., crane pose and orientation) to interpret feedback without more descriptive information. This under-interpreted feedback causes increased cognitive load, which may adversely offset the benefits provided by the assistance system. Therefore, it is important to design a user interface (UI) that is processed peripherally, requiring minimal interpretation and integration. For example, the screen size and location of the UI screen within a cabin can greatly affect the users' perception of the content (e.g., models, numbers) displayed by the assistance system. In the development of a tower crane navigation system, Lee et al. (2012) assessed the usefulness of different screen sizes in visualizing real-time crane information. Based on the feedback from operators, they determined that a 13-inch screen most effectively maximized the screen visibility in the confined space of a crane cabin. Also, they attempted to simplify the control of the system by replacing a sluggish touch screen with a 19-key mini keypad. This solution, however, still requires hand control, which distracts the operator from the main lifting task. In addition, a system that provides poorly or excessively presented feedback can increase operator workload, thus reducing the benefits of the assistance system. In such circumstances, selective feedback that provides warnings only when a potential hazard is

detected becomes very useful as it reduces the overall cognitive load, especially when the system turns “transparent.”

2.3.2. Evaluation of assistance effectiveness

Although crane users currently have an array of safety devices available for use, the effectiveness and utilization of these devices are unclear [52]. It is important to evaluate the effectiveness of these safety devices in actual lifting tasks in order to identify potential challenges and suggest further improvement. Previous efforts predominantly focused on the technology side, while the measurable impacts of such systems on lift safety and efficiency from an operational performance perspective remains unknown. In addition, most of these tests were validated in a simulated environment instead of utilizing real lifting tasks with actual pressure and constraints [36] [37] [53].

Chi et al. (2012) designed two UIs to improve the effectiveness of a tele-operated crane system [36]. The first UI design provided multiple views captured by video cameras, and the second UI design featured additional guidance enabled by augmented reality (AR) technology. The effectiveness of the developed UIs was evaluated by a subject test that consisted of novice and expert groups; these evaluations included both subjective (i.e., NASA task loading index) and objective (i.e., completion time for a lifting task) evaluation methods. Although the completion time reflects the lift efficiency to some extent, it is not comprehensive as it cannot reflect how the UIs will affect safety performance. Lee et al. (2012) introduced a tower crane navigation system that visualizes real-time crane motion captured by sensors and the surrounding buildings extracted from BIM models. The usefulness of the system was analyzed by measuring how often the operators use it as

compared to use rates of an LMI system. Previous studies in the field of human behavior and psychology indicate that the visual focus of attention is a good indicator of a worker's actual focus [54]. Videos recorded in the crane cabin were analyzed to measure the duration of operator use of the navigation system as well as the conventional LMI system. The results after 71 days of implementation showed that 93.3% of the operators solely relied on the navigation system compared to only 6.7% who solely relied on the traditional LMI system. This evaluation focused on the perceived ease of use and usefulness of the developed system from the operator's subjective perspective. Although these results somewhat reflected the effectiveness of the proposed system, an objective and quantitative evaluation method for assessing the system's actual impacts on crane lift performance was not investigated.

2.4. Operator Error and Situation Awareness

2.4.1. Operator error analysis from a cognitive perspective

In the field of cognitive psychology, human error is considered a result of failures in the cognition process, which will lead to unexpected or unsafe behaviors. High-risk industries such as nuclear power, aviation, transportation, and mining have taken advantage of cognitive analysis in risk control and safety management. The human cognition process can be simulated by various information processing models, among which the sequential stage model by Furnham precisely describes the cognition process of the equipment operators [55]. This model simulates operator cognition process as a sequential chain that consists of three cognition stages: hazard perception, hazard recognition, and decision/ability to avoid hazard (Figure 10).

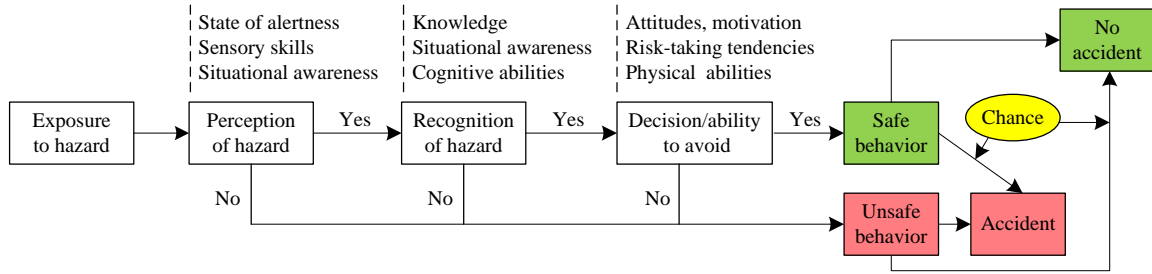


Figure 10: Sequential model of accident development from a hazard cognition perspective (adapted from [54])

This model can be applied to the cognition and decision-making processes of crane operators and the development of crane-related accidents. When crane operators are exposed to one or multiple hazards, they need to first perceive the presence of the hazards through the status, attributes, and dynamics of relevant elements in the environment. Successful hazard perception involves an acute state of alertness and high level of sensory skill from the operators, and it requires them to maintain a good SA during the operation. Once the operators perceive the hazard and proceed to the next stage of hazard recognition, they need to correctly recognize the type and severity of the hazards using their experience and knowledge as well as a comprehensive SA. Based on the information acquired, the operators need to make appropriate decisions and actions to mitigate or avoid the hazard from further development. Operator success in all of the cognition states will result in safe behavior. Failure in any of the stages will result in unsafe behavior. Nevertheless, it should be noted that there is always a chance that safe behavior may result in an accident or that unsafe behavior may not lead to an accident.

2.4.2. Situation awareness in crane lifting operations

The sequential model of accident development shown in Figure 10 shows that the stages of hazard perception and hazard recognition are largely dependent on whether operators have a good SA of the crane and the environment around them, as well as whether they have an adequate cognitive capability to process the information they perceive, as well as the cognitive capacity to prioritize which is the most pressing hazard requiring action. Failures to detect and recognize hazards is generally categorized as an SA problem [56], one which has a high likelihood of leading to performance failure [57]. Situation awareness (SA) is defined by Endsley as “a person's perception of the elements of the environment within a volume of time and space, the comprehension of their meaning and the projection of their status in the near future” [58]. During crane operations, crane operators’ SA depends on an understanding of both the crane (e.g., crane motion, capacity, malfunctions) and the physical characteristics of the environment (e.g., wind speed, blind spots, clearances to obstructions) (Figure 11). Although SA is difficult to quantify, it can be described by its boundaries: the upper limit is determined by the environment, while the lower limit is determined by the cognitive resources of individual operators [59].

To maintain a good SA, an operator needs to determine which objects and/or actions in the environment require the most focus. This can be aided by well-designed bottom-up analysis, warning, and display assistances, and/or well-practiced and educated top-down scanning patterns. Meanwhile, SA can be harmed due to time stress or the increasing number of hazards present. These effects are explained by the relationship between SA and working memory (WM), as shown in Figure 4. Maintaining a good SA

demands a certain amount of cognitive resources or executive processing capabilities that come from WM.

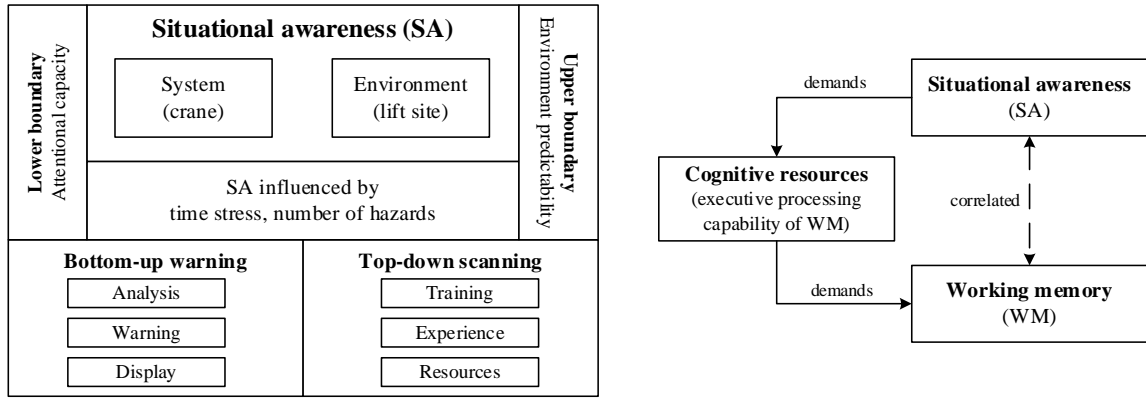


Figure 11: Situation awareness (SA) in crane operation and the relationship between SA and working memory (WM)

Based on the concept of SA and the relationship between SA and WM, the overall SA of an operator should be improved by an effective crane assistance system. Specifically, the assistance system should behave as a supplement to the operator recognition process that helps the operator identify the most significant hazards from a massive amount of information being received from multiple sources. In addition, the system should be capable of informing the operator of the existence of a hazard through an effective warning method or a combination of different warning methods.

2.4.3. Measures of situation awareness

Over the years, a number of measurement methods for situation awareness have been developed and each measure has its advantages and disadvantages. These measures can be

classified into three categories: 1) process indices-based, 2) performance-based, and 3) query-based techniques.

Process indices-based techniques examine the way subjects process information obtained from the environment such as by analyzing gaze movement using eye tracking technology [60][61]. Another type of process indices is physiological measures such as electroencephalographic (EEG) activity, eye blinks, and cardiac activity, which represent the subject's overall functional state [62][63][64]. Although the changes in the subject's physiological states may be associated with cognitive activities, there is not necessarily a direct link between physiological states and the level of SA.

In performance-based techniques, the level of SA is inferred from the performance outcomes based on the assumption that better performance indicates better SA. Commonly used performance metrics include productivity level, time to perform the task, and the accuracy of the response or, conversely, the number of errors committed. The main advantage of performance measures is that they yield objective, quantitative results without disrupting task performance. Although in many cases there is a positive relation between SA and performance, this connection is not always direct and explicit [65].

In query-based techniques, subjects are asked directly about their perception of certain aspects of the situation. The queries are usually designed by domain experts based on the characteristics of the tasks. One of the most widely used query-based techniques is the Situation Awareness Global Assessment Technique (SAGAT) [66]. The operation is frozen at randomly selected times and subjects are queried about their perception of the situation at that instant. SAGAT is popular as it produces a quantitative assessment of SA and it can benchmark the result with similar data in a similar context [67]. However,

SAGAT is criticized as it interrupts the natural flow of the task. To address these limitations, Durso et al. developed the Situation Present Assessment Method (SPAM) based on the premise that SA involves simply knowing where to find a particular piece of information in the environment [68]. In addition to being less intrusive than other techniques [69], the benefits of using SPAM lie in it uses response time to indicate the level of SA so that the results reflect the real-time dynamic SA of the operator.

Despite that each SA measure technique available has their advantages in certain circumstances, no single measure is able to effectively reflect the level of SA given the multivariate nature of SA. Therefore, valid and reliable measurement of SA should utilize a combination of distinct yet related measures that complement each other [70].

2.5. Point of Departure

Despite many safety considerations embedded in lift pre-planning, the ability to provide real-time safety assistance to crane operators during the lifting is inadequate. Although multiple technologies have been introduced to provide safety assistance to the operator, very few of them were actually adopted in the practice. Based on a throughout review of the state-of-the-art in crane safety technologies, gaps in the knowledge are identified including the lack of a reliable real-time crane motion capturing method, inadequate consideration of environmental constraints and changes, and missing validation of the assistance systems' impact on lift performance and operators' situation awareness. Each of these limitations in the state-of-the-art and shortcomings in existing technologies will be addressed in this research. The following chapters will introduce the research framework

and system architecture, as well as the research methodology that enables an effective safety assistance system for crane lifting operation.

CHAPTER III RESEARCH FRAMEWORK

This chapter presents a framework that outlines the technical steps and requirements for enabling real-time safety assistance for crane operations. To facilitate the implementation of this framework, a thorough system architecture is proposed.

3.1. Technical framework

To address the limitations in the state-of-the-art and advance the body of knowledge in lift safety assistance, this research designed and created a framework that enables real-time pro-active safety assistance for mobile crane lifting operations. As shown in Figure 12, this framework consists of five layers (i.e., object, sensing, processing, analyzing, and UI layer) and two objects of interest (i.e., crane and environment). The framework outlines the major tasks or requirements in each layer. In the object layer, crane motion can be represented by the angle and length measurements of a crane's manipulation and suspension modules, and the environment constraints can be modeled by the dimension and location of the obstructions present in the lifting site. In the sensing layer, suitable sensors need to be selected to directly measure the crane critical motions identified in the object layer. A method for acquiring 3D geometry is needed to capture the as-is conditions of the lifting site. In the processing layer, sensing data captured by the sensors need to be synchronized and synthesized in real-time, and the obstructions need to be automatically identified based on the as-is geometric data. Based on the processed data that represents the crane motion and site condition, hazards associated with the current condition analyzed based on the clearances between crane modules and the obstructions. In the UI layer, crane motion, site condition, and the identified hazards are visualized in real-time. The UI should

automatically warn the operator once a hazard is detected, as well as allow the operators to obtain information pertinent to their needs through interaction.

	Crane	Environment
Object layer	Manipulation and suspension module (Angle and length measurement)	Obstructions (dimension, location)
Sensing layer	Direct measurement by sensors	As-is 3D geometry acquisition
Processing layer	Sensor data synchronization	Obstruction identification
Analyzing layer	Hazard analysis based on proximity thresholds	
UI layer	Visualization, interaction, and warning	

Figure 12: Framework for real-time lift safety assistance

3.2. System Architecture

Based on the framework, a system architecture is developed to facilitate the implementation of the real-time lifting assistance. The system architecture consists of three components: crane motion capturing, site condition modeling and updating, and user interface and interaction (Figure 13). To capture crane motion in real-time, a combination of wired rotary encoder sensors and a wireless inertia measurement unit (IMU) sensor are adopted to measure the critical motions of crane modules (e.g., boom lift angle, boom extension length, boom slew angle, load sway). The data from the encoders are first synchronized in a processing unit so that the game engine program on the tablet receives

the packet that includes the measurements from all encoders. In addition, the processing unit will detect and reject corrupted or incomplete packets. In site condition modeling and updating, the format of a point cloud, collected by a laser scanner or other photogrammetry technologies, is used to represent the as-is lifting site condition as it can be efficiently acquired. To reconstruct an as-is lifting site, the site point cloud needs to be converted to bounding box objects to represent site obstructions. Bounding boxes will be automatically constructed to represent the obstruction through multiple steps of point cloud processing. With the point cloud and bounding boxes serving as base 3D information, updating the lifting site condition, more precisely the location change of obstructions (e.g., vehicles, materials), can be achieved by correlating the 2D images captured by a camera with the known 3D information. Based on the crane motion data and the site condition data, the on-board computer will virtually reconstruct and realistically visualize the lift scene using a game engine, and analyze the hazards based on the real-time data. Once a hazard is detected, warnings will be delivered to the operator through both visual and auditory means. Throughout the operation, the operator is able to interact with the UI through voice commands.

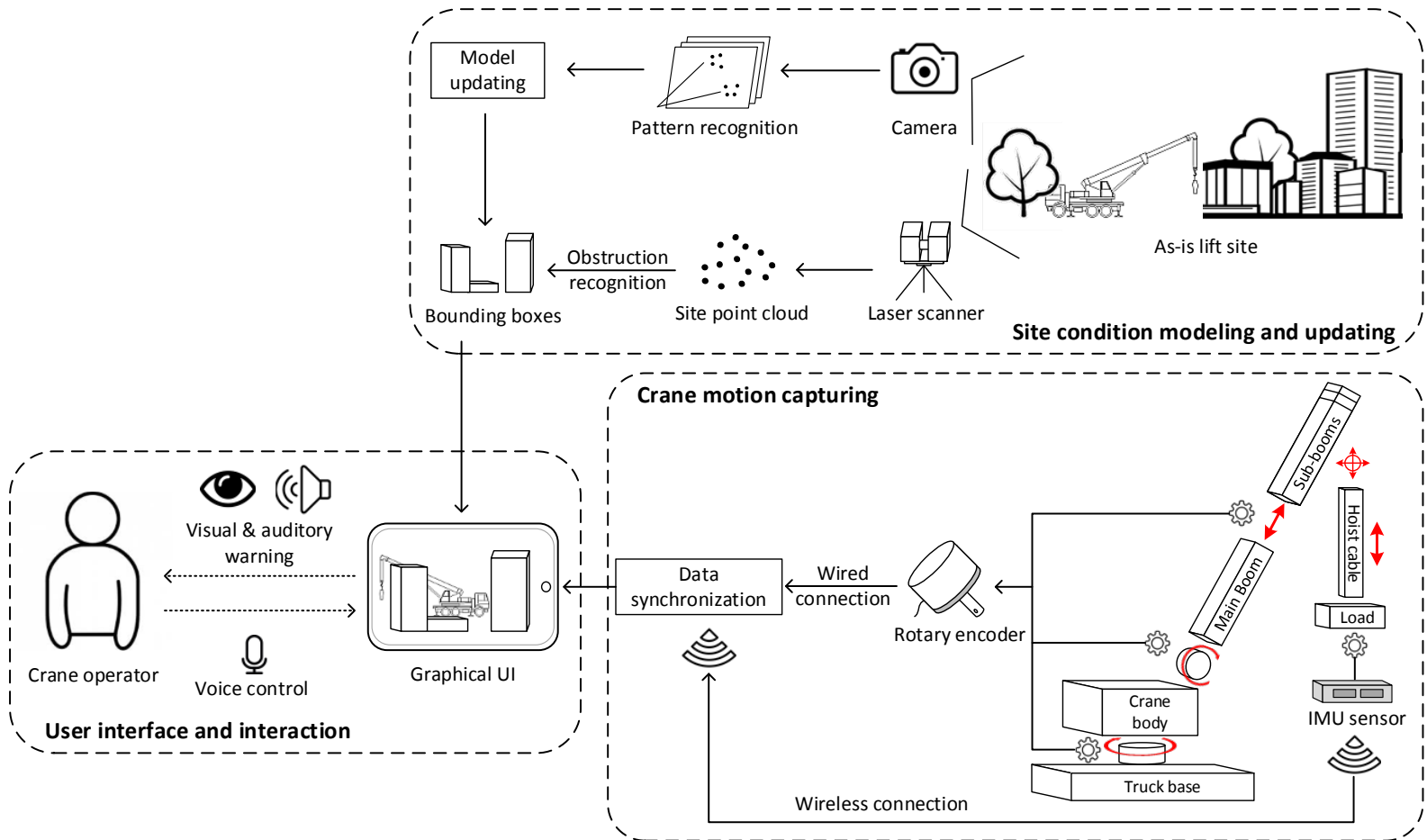


Figure 13: System Architecture

CHAPTER IV REAL-TIME CRANE MOTION CAPTURING

This chapter introduces the design, development, and deployment of a sensor system for real-time crane motion capturing. Two methods and different types of sensor are employed for measuring the critical motions for crane manipulation and suspension modules. Based on the accuracy of each sensor measurement, the load positioning error is estimated and compared to the actual error in a series of field tests.

4.1. Direct Measurement of Crane Motion Using Sensors

4.1.1. Critical motion analysis of crane manipulation and suspension modules

A crane can be understood as an entity comprised of multiple rigid bodies connected by different types of joints, depending on the crane type and configuration. This simplification makes it possible to represent any possible crane pose by measuring critical the angle or length of a particular joint that connects two rigid bodies. For example, a telescopic boom mobile crane can be decomposed to two independent modules: the manipulation module and the suspension module (Figure 14). The manipulation module is comprised of three rigid bodies including a truck base, a crane body, and a telescopic boom. Then, the telescopic boom is further broken down into two rigid bodies (i.e., main boom and sub-booms) connected a prismatic joint that only allows translational movement between these two rigid bodies. The connection between the truck base and the crane body as well as the connection between the crane body and the main boom are modeled by a revolute joint that only allows one rotational degree of freedom between the two rigid bodies. The suspension module consists of a normal rigid body, the lifted load, and an extensible rigid body for the hoist line. Although hoist line itself is elastic and can be hardly considered a rigid body,

when used in a pulley system where double or triple tackles serve together, the cable bundle is resistant to twisting and bending, especially when the lifted load performs a 3-dimensional pendulum motion in a very small magnitude. The connection between the suspension module and the sub-booms is modeled by a spherical joint that allows rotation in all direction and only constraints translational movement. Based on the critical motion analysis, a telescopic boom mobile crane is simplified as six rigid bodies connected by five joints. This means that any motion that can be possibly performed by a crane can be represented and reconstructed by measuring the boom slew angle, boom lift angle and boom extension length in the manipulation module and the length of the hoist line and load sway in the suspension module.

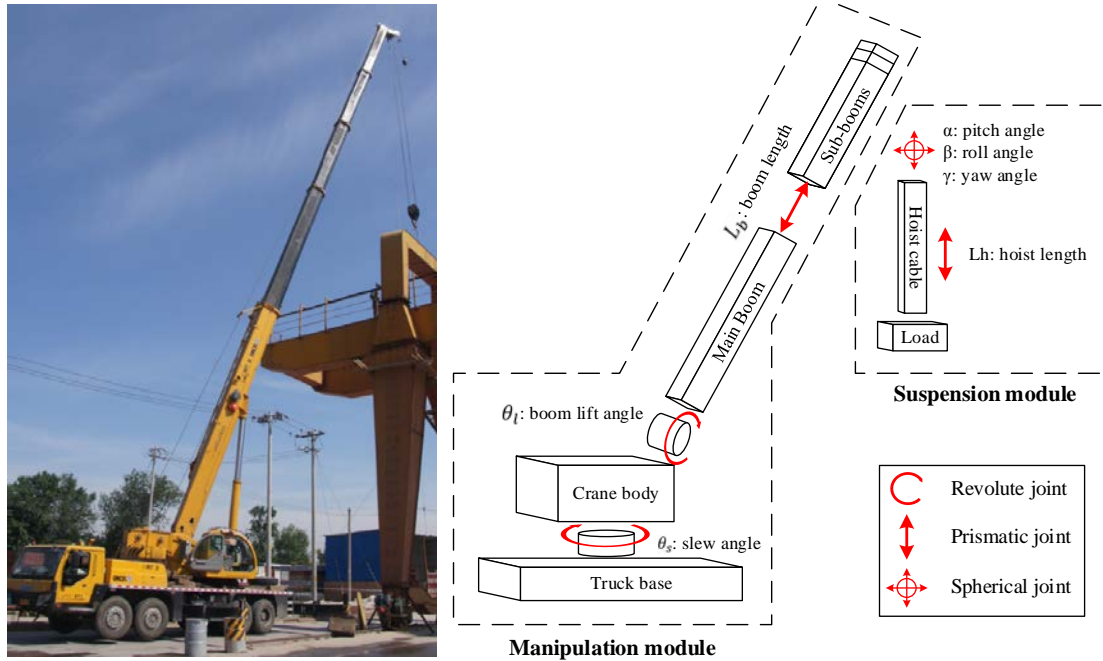


Figure 14: Kinematics configuration of a typical telescopic boom mobile crane

4.1.2. Manipulation module motion capturing using rotary encoders

Rotary encoders are electromechanical devices that are used in various electronic and mechanical devices for measuring angular position or motion of a shaft or axle in the device. The prototype system will adopt rotary magnetic absolute encoders to measure three critical motions of the crane manipulation module: boom slew and lift angles, hoist line extension and boom extension. Although the proposed motion capturing method adopts commercially available encoders, it is more flexible than other commercial solutions [71] in that the selection and deployment of the sensors are also suitable for retrofitting existing cranes in service.

4.1.3. Suspension module motion capturing using an inertia measurement unit

An inertial measurement unit (IMU) is an electronic device that measures velocity, orientation, and gravitational forces, using a combination of accelerometers and gyroscopes, sometimes magnetometers. IMU sensors were originally developed for the maneuver of aircraft and spacecraft, such as an unmanned aviation vehicle (UAV) and satellites, to report inertial measurements to the pilot system. Recently, IMU sensors have been widely used as orientation sensors for measuring human body motions in sports athlete training and movie production. A typical IMU sensor contains angular and linear accelerometers for tracking the changes in position and gyroscopes for maintaining an absolute angular reference. Generally, an IMU sensor has least one accelerometer and one gyroscope for each of the three axes: pitch (nose up and down), yaw (nose left and right) and roll (clockwise or counter-clockwise). When rigidly mounted to an object, the IMU sensor measures the linear and angular acceleration and automatically calculates the

orientation of the attached object. In the particular case of load sway, it is assumed that the cable length is known and the cable is rigid. Therefore, the load sway motions can be simplified to a typical 3-dimensional (3D) pendulum motion (Figure 15a). Given the measured angular orientation of each axis (Figure 15b) and the cable length, the estimated position of the load relative to the fixed point can be calculated by converting the Euler angle measurements to Cartesian coordinates in the local coordinate system (Figure 15c).

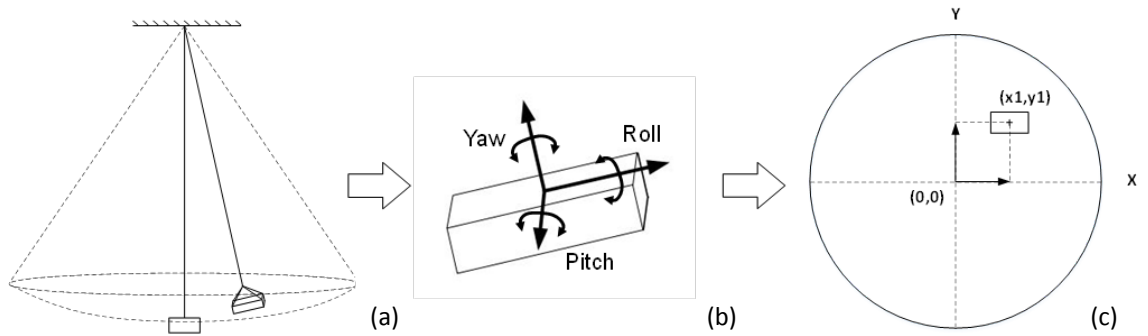


Figure 15: Transforming the angular measurements to absolute positions

This process of converting the Euler angle measurements to Cartesian coordinates is demonstrated in the following steps. Firstly, one single load orientation measurement can be decomposed into three elemental rotations, yaw, pitch, and roll. The yaw, pitch, and roll rotations can comprehensively represent a 3D rigid body in any orientation. These three elemental rotations and the individual rotation matrices are defined as follows: a yaw is a counterclockwise rotation of α about the z-axis; a pitch is a counterclockwise rotation of β about the y-axis; a roll is a counterclockwise rotation of γ about the x-axis. The rotation matrices for the three elemental rotations are given in Eq. 1, 2 and 3.

$$R_z(\alpha) = \begin{bmatrix} \cos\alpha & -\sin\alpha & 0 \\ \sin\alpha & \cos\alpha & 0 \\ 0 & 0 & 1 \end{bmatrix} \quad (\text{Eq. 1})$$

$$R_y(\beta) = \begin{bmatrix} \cos\beta & 0 & \sin\beta \\ 0 & 1 & 0 \\ -\sin\beta & 0 & \cos\beta \end{bmatrix} \quad (\text{Eq. 2})$$

$$R_x(\gamma) = \begin{bmatrix} 1 & 0 & 0 \\ 0 & \cos\gamma & -\sin\gamma \\ 0 & \sin\gamma & \cos\gamma \end{bmatrix} \quad (\text{Eq. 3})$$

Therefore, a single rotation matrix, as shown in Eq. 4, can be formed by multiplying the yaw, pitch, and roll rotation matrices.

$$R(\alpha, \beta, \gamma) = R_z(\alpha) \cdot R_y(\beta) \cdot R_x(\gamma) =$$

$$\begin{bmatrix} \cos\alpha \cdot \cos\beta & \cos\alpha \cdot \sin\beta \cdot \sin\gamma - \sin\alpha \cdot \cos\gamma & \cos\alpha \cdot \sin\beta \cdot \cos\gamma + \sin\alpha \cdot \sin\gamma \\ \sin\alpha \cdot \cos\beta & \sin\alpha \cdot \sin\beta \cdot \sin\gamma + \cos\alpha \cdot \cos\gamma & \sin\alpha \cdot \sin\beta \cdot \cos\gamma - \cos\alpha \cdot \sin\gamma \\ -\sin\beta & \sin\beta \cdot \cos\gamma & \cos\beta \cdot \cos\gamma \end{bmatrix} \quad (\text{Eq. 4})$$

Since the load sway motion is a simple 3-dimensional pendulum motion, the load trajectory lies on the internal surface of a sphere with the radius of the cable length. Hence, the unit vector on local z-axis always points to the center of the sphere. Therefore, converting the Euler angle measurements to Cartesian coordinates is simplified to converting this unit vector on the local z-axis to a vector in the global coordinate system according to the single rotation matrix containing three elemental rotations. Thus, the load position can be estimated by multiplying the rotation matrix with a unit vector (0, 0, 1) and the cable length L using Eq. 5.

$$P(x, y, z) = R(\alpha, \beta, \gamma) \cdot \begin{bmatrix} 0 \\ 0 \\ 1 \end{bmatrix} \cdot L = \begin{bmatrix} \cos\alpha \cdot \sin\beta \cdot \cos\gamma + \sin\alpha \cdot \sin\gamma \\ \sin\alpha \cdot \sin\beta \cdot \cos\gamma - \cos\alpha \cdot \sin\gamma \\ \cos\beta \cdot \cos\gamma \end{bmatrix} \cdot L \quad (\text{Eq. 5})$$

It should be noted that the initial orientation measurement (α, β, γ) is not necessarily the origin since the surface where the sensor is placed might not be completely leveled. Therefore, a deviation from the origin can be expected in the estimation of the load trajectory based on this method. To minimize this error, the initial load orientation is taken into consideration. The orientation data measured when the load is static is averaged and introduced to the calculation as an offset for correcting the deviation.

4.4. Error Estimation and Sensitivity Analysis for Crane Pose Reconstruction

When analyzing the error of the final load positioning, error propagation as a result of the changes in boom lift angle, slew angle, and boom extension must be considered. The goal of this section is to understand how the error of each sensor will affect the result of the motion reconstruction, namely the position of the crane load. Given that the load position is dependent on boom lift angle, boom length and boom slew angle, a load position in X-Y plane can be calculated as shown in Eq. 6, 7 and 8.

$$X = L_b \cdot \cos \theta_l \cdot \sin \theta_s + L_h \cdot \sin \alpha \quad (\text{Eq. 6})$$

$$Y = L_b \cdot \cos \theta_l \cdot \cos \theta_s + L_h \cdot \sin \beta \quad (\text{Eq. 7})$$

$$Z = L_b \cdot \sin \theta_l - L_h \cdot \cos \alpha \cdot \cos \beta \quad (\text{Eq. 8})$$

in which,

θ_l : boom lift angle

θ_s : boom slew angle

L_b : boom length

Each angle and length measurements were considered as a random variable with a standard deviation based on the sensor measurement accuracy (Table 2). The accuracy of each sensor indicates the measurement uncertainty.

Table 2: Accuracy and range of sensor measurements

Measurement	Type (unit)	Accuracy	Range
Boom slew angle (θ_s)	Angle (degree)	± 0.3 deg	0 to 360 deg
Boom lift angle (θ_l)	Angle (degree)	± 0.3 deg	0 to 78 deg
Boom length (L_b)	Length (m)	± 0.05 m	11 to 38 m
Hoist line length (L_h)	Length (m)	± 0.08 m	0 to 40 m
Load pitch angle (α)	Angle (degree)	± 0.7 deg	0 to 8 deg
Load roll angle (β)	Angle (degree)	± 0.7 deg	0 to 8 deg

Eq. 9 shows a variance formula to calculate error propagation, where σ_f is the uncertainty of model output, X and Y are model inputs, and σ_x and σ_y are the uncertainty of input X and Y. Since the measurements from the sensors are independent, it is assumed that there is no covariance between each input.

$$\sigma_f = \sqrt{\left(\frac{\partial f}{\partial x} \cdot \sigma_x\right)^2 + \left(\frac{\partial f}{\partial y} \cdot \sigma_y\right)^2 + \left(\frac{\partial f}{\partial z} \cdot z\right)^2 + \dots} \quad (\text{Eq. 9})$$

The following presents the results in calculating the uncertainty of the load positioning in X-axis using Eq. 6 and 9. Following the presented method, the uncertainties of the load positioning in Y and Z-axis can be calculated similarly. We take partial derivatives of X with respect to each input in the function (i.e., $L_b, \theta_l, \theta_s, L_h, \alpha$) as follows:

$$\frac{\partial X}{\partial L_b} = \cos \theta_l \cdot \sin \theta_s \quad (\text{Eq. 10})$$

$$\frac{\partial X}{\partial \theta_l} = -L_b \cdot \sin \theta_l \cdot \sin \theta_s \quad (\text{Eq. 11})$$

$$\frac{\partial X}{\partial \theta_s} = L_b \cdot \cos \theta_l \cdot \cos \theta_s \quad (\text{Eq. 12})$$

$$\frac{\partial X}{\partial L_h} = \sin \alpha \quad (\text{Eq. 13})$$

$$\frac{\partial X}{\partial \alpha} = L_h \cdot \cos \alpha \quad (\text{Eq. 14})$$

Using Eq. 9, the variance of X is calculated as follows:

$$\begin{aligned} \sigma_X^2 &= \left(\frac{\partial X}{\partial L_b} \cdot \sigma_{L_b} \right)^2 + \left(\frac{\partial X}{\partial \theta_l} \cdot \sigma_{\theta_l} \right)^2 + \left(\frac{\partial X}{\partial \theta_s} \cdot \sigma_{\theta_s} \right)^2 + \left(\frac{\partial X}{\partial L_h} \cdot \sigma_{L_h} \right)^2 + \left(\frac{\partial X}{\partial \alpha} \cdot \sigma_{\alpha} \right)^2 \\ &= (\cos \theta_l \cdot \sin \theta_s \cdot \sigma_{L_b})^2 + (-L_b \cdot \sin \theta_l \cdot \sin \theta_s \cdot \sigma_{\theta_l})^2 + (L_b \cdot \cos \theta_l \cdot \cos \theta_s \cdot \\ &\quad \sigma_{\theta_s})^2 + (\sin \alpha \cdot \sigma_{L_h})^2 + (-L_h \cdot \cos \alpha \cdot \sigma_{\alpha})^2 \end{aligned} \quad (\text{Eq. 14})$$

It should be noted that the variance of X changes as each input values change (i.e., $L_b, \theta_l, \theta_s, L_h, \alpha$). This means in different crane configurations, the error of load positioning is different. To consider the overall uncertainty in load positioning under different crane configurations, Monte Carlo method was used to generate 10,000 combinations of input values (Figure 16). Using Eq. 14, the standard deviation of X in each combination of input values was calculated. Results show that the mean error of load positioning in x-axis is 0.2141 m with standard deviation of 0.0908 m. The minimum error is 0.0215 m and the maximum is 0.4095 m.

A random configuration
given input ranges

	Low	High	RAND	sin	cos	σ	
L_b	11	38	17.90274	NA	NA	0.05	
θ_l	0	78	0.537549	0.512032	0.858966	0.005236	
θ_s	0	360	2.263766	0.769352	-0.63882	0.005236	
L_h	0	40	6.93783	NA	NA	0.08	
α	0	8	0.004527	0.004527	0.99999	0.012217	
β	0	8	0.000637	0.000637	1	0.012217	

Errors in 10,000 random
configurations

Run	$\frac{\partial X}{\partial L_b}$	$\frac{\partial X}{\partial \theta_l}$	$\frac{\partial X}{\partial L_h}$	$\frac{\partial X}{\partial \alpha}$	$\frac{\partial X}{\partial \beta}$	σ_X^2	σ_X
	0.00193	0.000298	0.002348	1.22E-06	0.002291	0.006868	0.082875
1	0.001838	0.003066	0.000734	4.95E-05	0.063937	0.069624	0.263864
2	0.001133	0.006027	0.000169	5.28E-05	0.106869	0.114251	0.338011
3	8.05E-05	6.11E-05	0.025567	8.2E-05	0.110915	0.136706	0.369737
4	0.002316	0.001065	1.44E-05	4.3E-07	0.053791	0.057188	0.239139
5	9.64E-06	0.000103	0.000446	5.53E-06	0.1057	0.106265	0.325983
6	1.91E-05	3.78E-05	0.003224	4.88E-05	0.059082	0.062412	0.249823
7	0.001412	1.41E-05	0.001441	5.97E-06	0.020123	0.022996	0.151645
8	0.000448	0.010809	0.005671	2.84E-05	0.006106	0.023061	0.15186

Figure 16: Error estimation using Monte Carlo Method

For each sensor measurement, the error is increased or decreased by 20% while other measurement errors remain the same. We calculated the change of the load positioning result for all five measurements one by one, and Figure 17 shows how the load positioning error changes as each input measurement error changes. It is obvious that the measurement of load pitch orientation has the biggest impact on the uncertainty of load positioning. The measurements of hoist line length and boom length have a minimal impact on the uncertainty of load positioning.

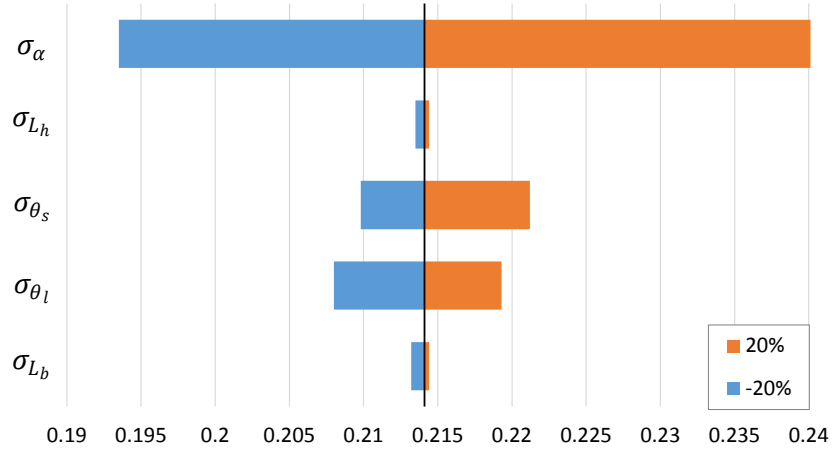


Figure 17: Sensitivity analysis of load positioning in X-axis

On top of sensor measurement errors, data collection and synchronization might increase the error if they are not handled properly. The data from the encoders are first synchronized in a processing unit so that the game engine program on the tablet receives the packet that includes the measurements from all encoders at a frequency of 50Hz. In addition, the processing unit and the program will detect and reject corrupted or incomplete packets. Given that all the encoders are connected to the processing unit by cables, delay in data collection and transmission is negligible. All these measures ensure the error related to data collection and synchronization is minimized.

4.5. Field Test and Discussion

To validate the proposed method for crane motion reconstruction, a prototype system was developed and deployed on a 70-ton telescopic boom mobile crane. The prototype system adopted rotary magnetic encoders to measure three critical motions: boom slew, hoist line extension and boom extension (Figure 18). The boom slew angle was measured by attaching a small measuring gear on the rotary encoder to the main slewing gear underneath

the crane cabin. Similar to the slewing angle, the length of the hoist line was calculated based on the rotation of the crane hoist winch measured by another rotary encoder. The boom extension was obtained using another rotary encoder by measuring the length of a wire with one end fixed at the middle of the boom and the other end attached to the tip of the boom. Unlike other motion measurements, the boom lift angle was directly measured by an inclination sensor attached to the crane boom. All the rotary encoders and inclination sensor were powered by the crane battery and connected to a microcontroller.

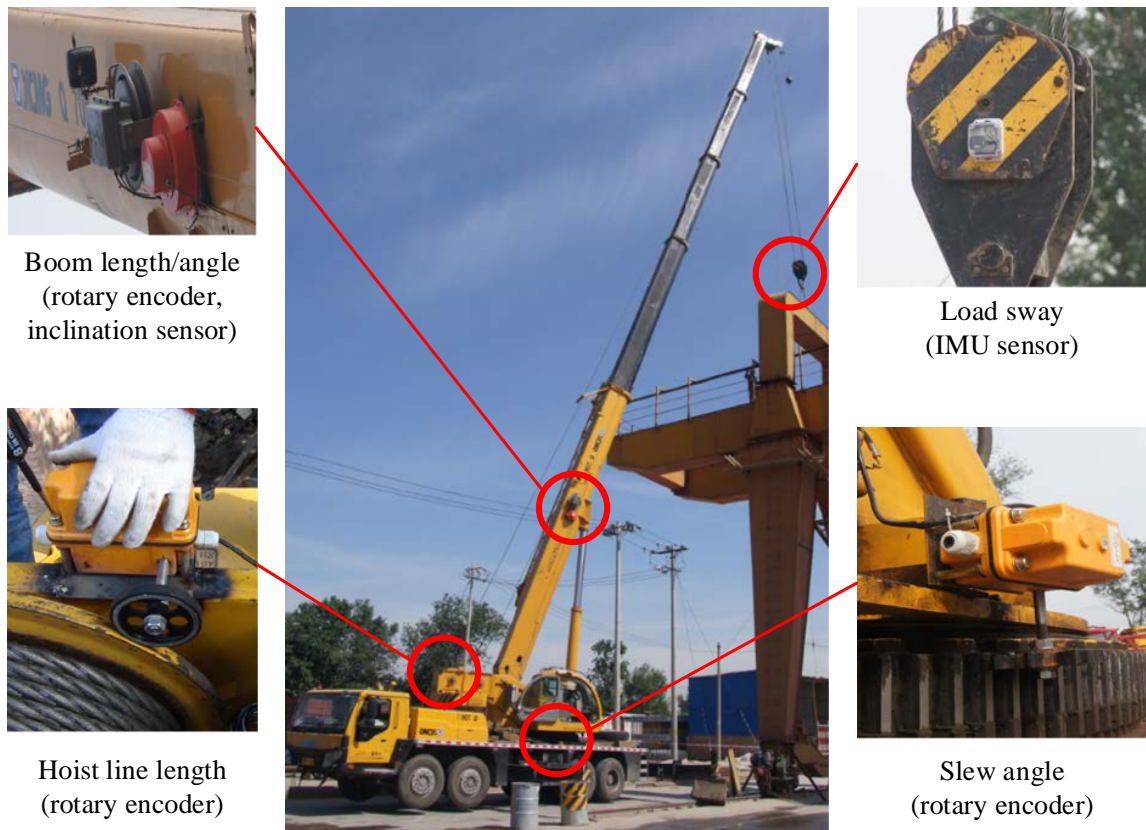


Figure 18: Sensor configuration for critical motion capturing

A wireless IMU sensor was used to measure the position of the lifted load. As shown in Figure 19, the IMU sensor was powered by a small power bank battery and they

were enclosed in a waterproof case that is NEMA 4X / IP66 rated. The case can be attached to the side of the hook block using heavy-duty tapes or bolts. The wireless IMU continuously measures and transmits load orientation to the tablet for data processing.

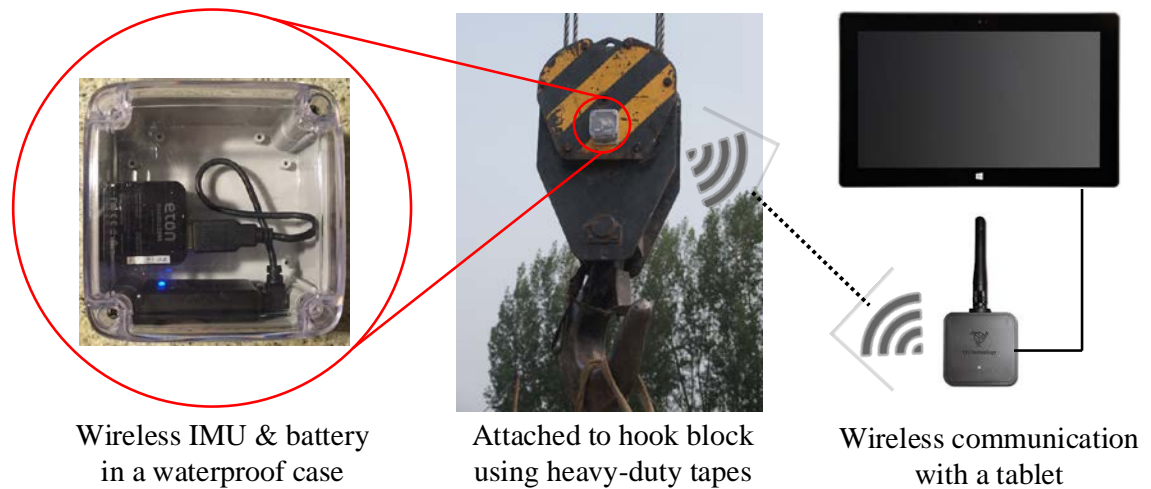


Figure 19: IMU sensor configuration for load position measurement

A tablet served as a computation device for hazard analysis while displaying the reconstruction lifting site to the operator. Although visualization delay was expected because of data transmission and computation, the test operators observed no noticeable delay during the test. The visualization results were validated by comparing the reconstructed crane boom and load motions to site camera recordings from two view angles: site overview and top view from the crane boom head. The site overview comparison demonstrates the accuracy in reconstructing crane boom motions (Figure 20) and the top view from boom head comparison demonstrates the accuracy in reconstructing crane load sway motions (Figure 21). In these figures, the solid cube indicates the lifted load and the circle indicates the target drop off location.

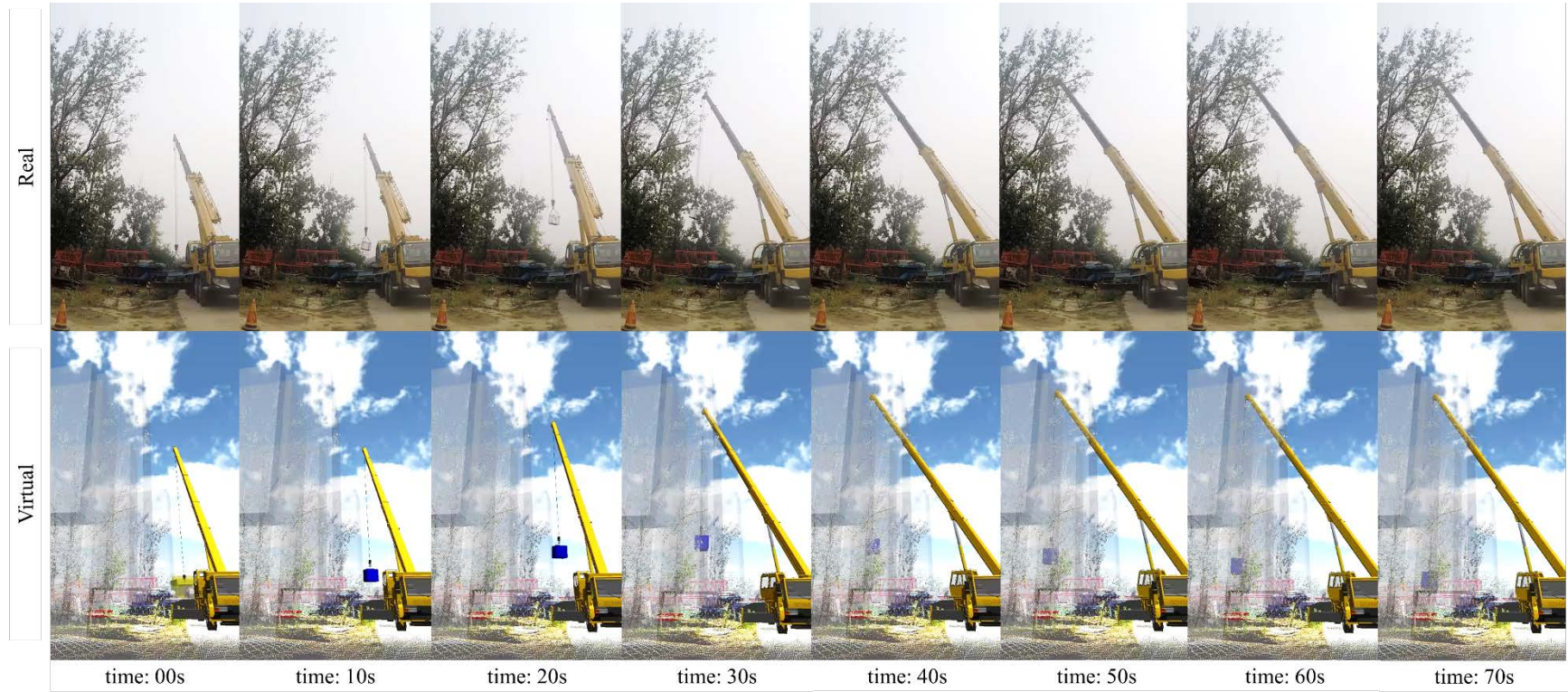


Figure 20: Comparison between actual lifting (upper) and reconstructed lifting process (lower) in site overview

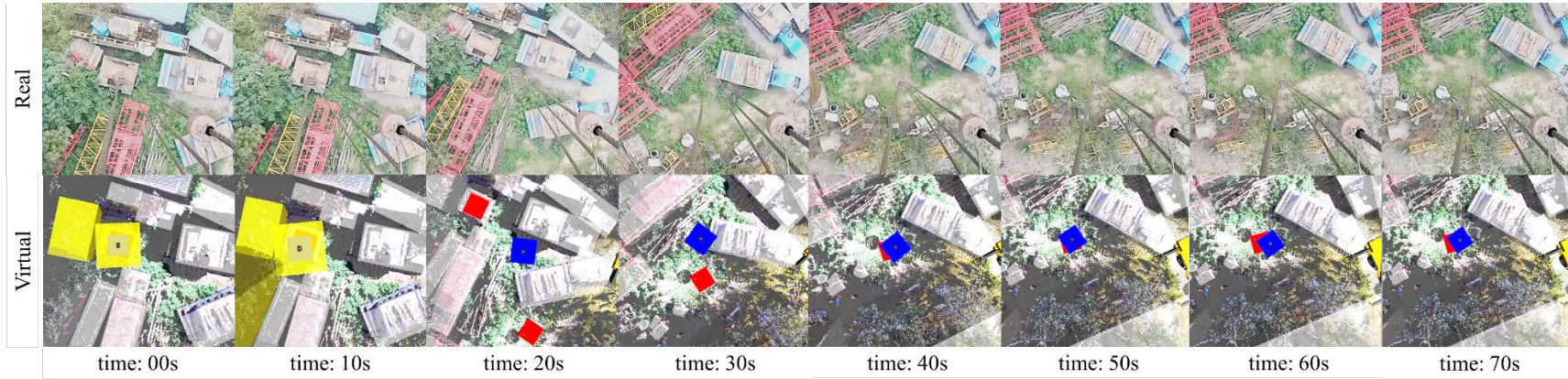


Figure 21: Comparison between actual load sway motion (upper) and reconstructed load sway motion (lower) from the boom's top view.

Since it is very difficult to measure the error during the lift, the overall reconstruction error of the system was represented by the error of load positioning at the end of each lift. This assumption is reasonable as the final load position is greatly affected by the reconstruction accuracy of both the boom and load motion. Furthermore, it also reflects the overall error that may accumulate during the lift. As the load was always placed at the exact same drop off location, the load positioning error is the horizontal distance between the actual and planned drop off location. Figure 22 plots the load positioning errors in 92 consecutive lifts, and the maximum, minimum, median, first and third quartile of the errors are shown in the box plot to the right. The average error for reconstruction is 0.43 m and the maximum error for reconstruction is 0.93 m. Compared to theoretical error calculated based on the propagation of nominal sensor errors, the average value of the actual errors is higher (0.43m vs. 0.21m) and the variances are bigger as well (0.49m vs. 0.09m). Differences between the actual and theoretical errors are mainly due to variances in sensor setup or system calibration as well as possible measurement errors. The logarithmic trend line indicates a slightly increasing tendency of the errors over the 92 lifts. It should be noted that no re-calibration was conducted during the test lifts. This indicates the system error did accumulate over time in extensive usage conditions, and thus re-calibration is necessary for actual field implementation in the long-term.

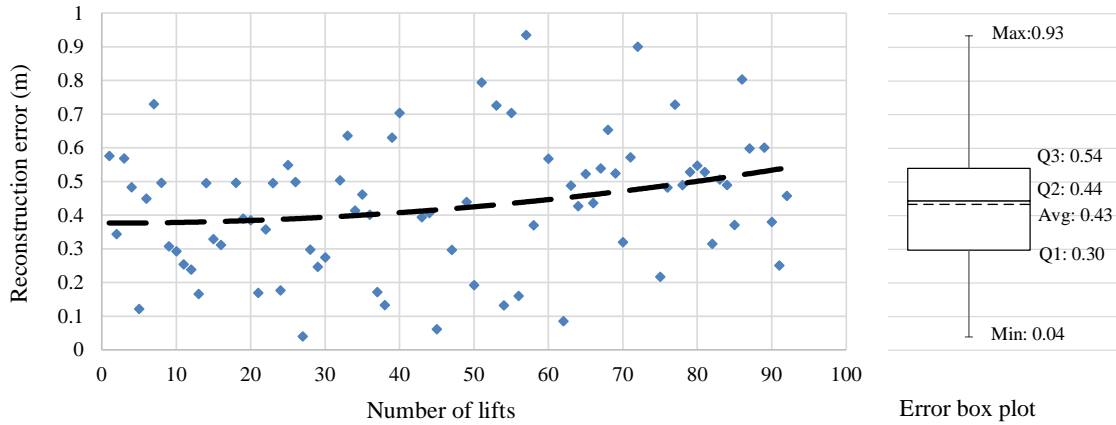


Figure 22: Errors of virtual lift reconstruction during 92 lifting tasks

Accurate motion capturing and reconstruction are essential for enabling real-time hazard analysis and visualization. The error of load positioning mainly comes from three sources: sensor measurement error, error propagation in motion reconstruction, and accumulated system error due to sensor setup. Sensor measurement error can be reduced by using sensors that are more accurate and durable. Error propagation in motion reconstruction varies in different crane configurations (e.g., boom length and angle) and thus can be hard to reduce. The accumulated system error can be reduced by improving the way the sensors are deployed. For example, the length of the hoist line is measured by attaching a small wheel to the edge of the hoist line winch. Although the contact between the wheel and the winch is perfectly firm in the beginning, it might become loose in the long term and thus increase the error in the length measurement of the hoist line. This problem can be solved by deploying a rotary encoder directly on the axle on the winch with an enclosure. Such improvement in system deployment will be addressed in the future study.

Another critical issue that can significantly compromise the effectiveness of real-time systems is the delay or latency in data processing and visualization. Crane lifting operations are so dynamic that an accident can develop in a couple of seconds. The tested prototype system showed no noticeable delay or latency based on the operator feedback and the comparison between the actual and reconstructed crane motion (see Figure 9 and 10). This is partially because the communication between sensors (except the IMU sensor) and the computer were via wired connection. In addition, delay in data processing or lagging in visualization can be expected if a less powerful tablet is used for data processing and visualization.

4.7. Conclusions

This chapter presents a novel sensor system for real-time crane motion capturing. Based on kinematics analysis for mobile cranes, crane motions can be represented by multiple critical angle and length values in the manipulation and suspension modules. Using different sensors, these values are synchronized and processed by an algorithm to automatically reconstruct crane motion in real-time. A prototype system was developed and deployed on a real crane to validate the performance of real-time motion capturing with respect to accuracy and latency. The test results show that the prototype system achieved 0.43 m accuracy with negligible latency across 92 lifts during a period of 5 days. These results indicate that the sensor system is able to reliably and accurately capture crane motion in real-time. These capabilities are essential for an assistance system to carry out a realistic visualization of crane motion, reliable and timely analysis of unsafe conditions, and effective warnings to the operator.

CHAPTER V AS-IS SITE CONDITION MODELING AND UPDATING

Cranes' lift capability and maneuverability are greatly affected by the geometric constraints in the surrounding environment, especially for mobile cranes as their location and workspace change quite frequently as a project proceeds. A major limitation in traditional lift planning approaches is the lack of information to represent the as-is lifting site condition. This chapter introduces a series of novel algorithms for as-is site condition modeling and updating based on point cloud and visual data.

5.1. As-is Geometric Data Collection

Recent advances in rapid geometry data acquisition make it possible to obtain massive 3-dimensional geometric data in a short amount of time with minimal efforts. A point cloud is a set of points containing coordinate data (XYZ) and color data (RGB) representing the geometry of objects in the captured scene. A terrestrial laser scanner collects point cloud data with good accuracy ($\pm 2\text{mm}$) and efficiency (up to 976,000 points per second) [72]. However, one drawback of laser scanning is the cost of owning or renting a laser scanner. An alternative for rapid generation of point cloud data is using Structure from Motion (SfM) photogrammetry technology. The first step in SfM method involves collecting aerial images of a construction site from a UAV at multiple viewpoints. The construction site images are highly-overlapping and encircle the site in order to cover the full 3D structure of construction-related entities. Next, the 3D point cloud of the construction site (see Figure 2a) is generated based on the image data using a Structure from Motion (SfM) algorithm adopted from [73]. This algorithm detects common features

across each camera frames using Scale Invariant Feature Transform (SIFT) [74], which finds point correspondences between images and solves for point coordinates and camera poses in a bundle adjustment procedure.

5.2. Site Condition Modeling based on Point Cloud

To model the as-is lifting site, the point cloud acquired by laser scanning or photogrammetry technologies is converted into bounding boxes to represent the dimension and location of mobile assets (e.g., vehicles, materials) and obstructions (e.g., building structure, power lines, trees). The pipeline of obtaining oriented bounding boxes for various objects in point clouds involves the steps of segmentation, clustering, and orientation estimation. The input point cloud is first down-sampled from its original number of points to around 10,000 points by performing voxel grid filtering. Individual points in the original point cloud are projected onto a grid of 1cm-sized voxels and only a single point representing the center of each occupied voxel is preserved in the point cloud while the extraneous points are filtered out. Next, ground plane segmentation is performed using Random Sample Consensus (RANSAC) [75]. Points from the ground plane are filtered out so that object points can be separated nicely in the clustering step. The RANSAC algorithm iteratively computes an estimate of the ground plane parameters by randomly sampling points from the point cloud. The best estimate in terms of the number of inliers is determined and all points located within 0.4m of the calculated plane are filtered out. The ensuing clustering step involves grouping points that are contained within the same neighborhood together and labeling each group as an individual cluster. The threshold parameter used in this study is 0.4m but it can also be manually adjusted so that the points

belonging to the same object would not be split into separate clusters and the points belonging to different objects would not be grouped into the same cluster. Even with carefully tuned clustering parameters, this step may occasionally face problems with over-segmentation or under-segmentation, which affects the tightness of fit and orientation accuracy of the bounding boxes. However, the final bounding box span in 3D space to determine collisions remains largely the same. Finally, an oriented bounding box is computed for each point cluster by considering the physical spread of points in the z-axis (vertical axis) and the x-y-plane. Principal Component Analysis (PCA) [76] is used to determine the two principal directions in which points in the cluster vary the most in the x-y-plane. The principal directions are used to determine the orientation of the objects bounding box in the x-y-plane. The final bounding box is then computed by determining the maximum and minimum length along the vertical axes and the horizontal principal axes. The total computation time for the whole process largely depends on the down-sampling ratio but it only takes a few minutes to down sample a site point cloud of around 30 million points. Regardless of the original point cloud resolution, a final point cloud with a size of around 10,000 points is considered sufficient and efficient for obstruction identification since it is only necessary to recover a rough outline of each detected object.

Once the bounding boxes for obstructions are automatically created, they are prepared for visualization with the adjustment of the surface transparency level and being labeled as obstructions in a game engine. The workflow for lift scene reconstruction is illustrated in Figure 23. As the mobile assets and obstructions in the as-is lifting site are represented by bounding boxes, the site condition can be easily updated.

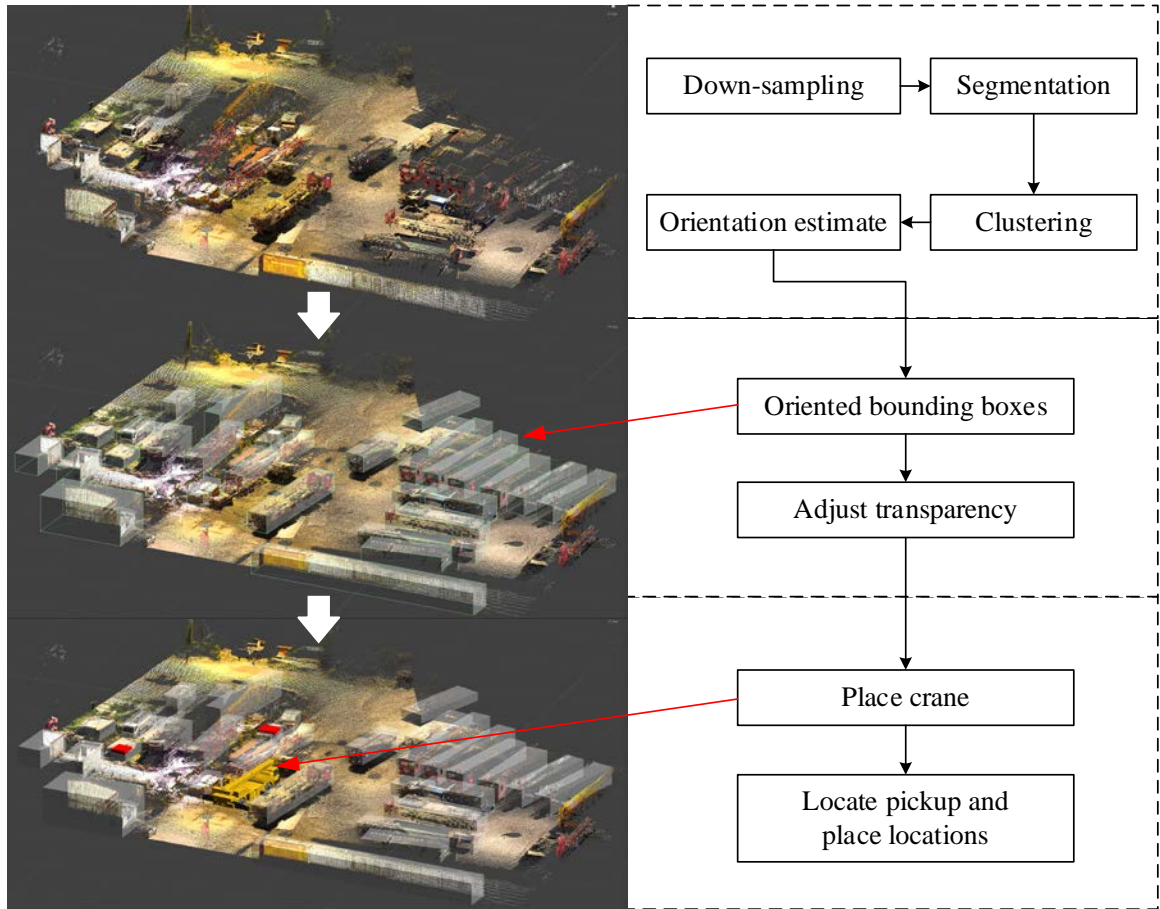


Figure 23: Lifting site condition modeling process based on point cloud data

5.3. Site Condition Updating Using a Point Cloud-Vision Hybrid Approach

Updating the site condition in dynamic crane lifting site is important for hazard detection, collision avoidance, and 3D visualization for operators of heavy equipment such as cranes. Point cloud data captures complete 3D information but requires a long period of time to acquire and process; On the other hand, visual data can be collected quickly but lacks depth information. To address these shortcomings, this section introduces a point cloud-vision hybrid approach to track the location of mobile to update the conditions in crane workspace.

First, the point cloud data collected by a laser scanner or SfM method was projected onto a 2D plane to generate a synthetic image (Figure 24a). Feature points can be calculated from the synthetic image using a point based method [77]. Then a depth buffer is created based on the 3D point cloud data, where bright points indicate points that are close to the camera while darker points indicate points that are further away from the camera (Figure 24b). This enables us to calculate the 3D position of each feature point on the synthetic image. The 2D time-lapse images captured by a UAV or a wide-angle camera mounted on crane boom are matched to the synthetic image to obtain a corresponding set of 3D point features. Finally, a camera pose estimate is calculated for each 2D image by minimizing the least-squares re-projection error of 3D point features in the image.

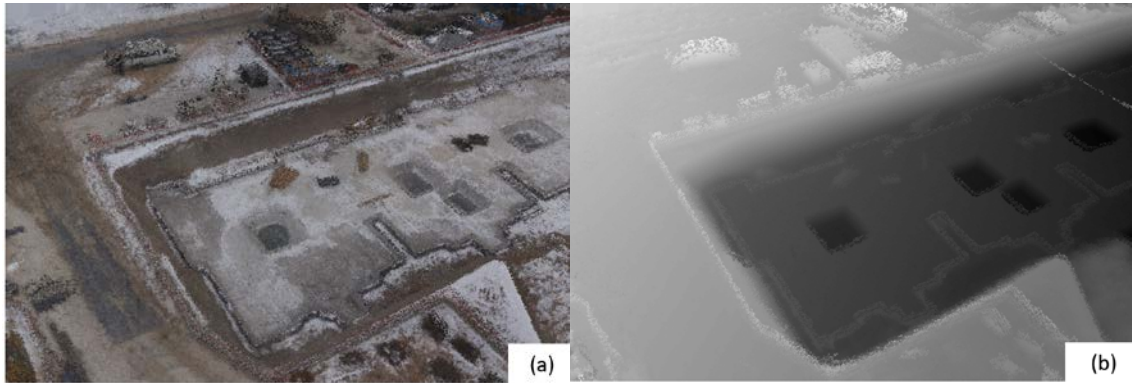


Figure 24: (a) synthetic image and (b) depth buffer generated from point cloud

The next step in the processing pipeline is object detection. For each 2D image taken in the previous step, the pixel coordinates of objects to be tracked are identified through a point-based method, namely matching of SIFT feature points. This process is semi-automated by the user specifying interested objects in the reference image. As shown

in Figure 3, bounding boxes are drawn around the two vehicles to be tracked in the reference image (Figure 25a) while the same objects are detected in the tracking image through feature point matching (Figure 25b). The process can potentially be fully automated by having a database of possible objects to be tracked or training an object detection classifier.

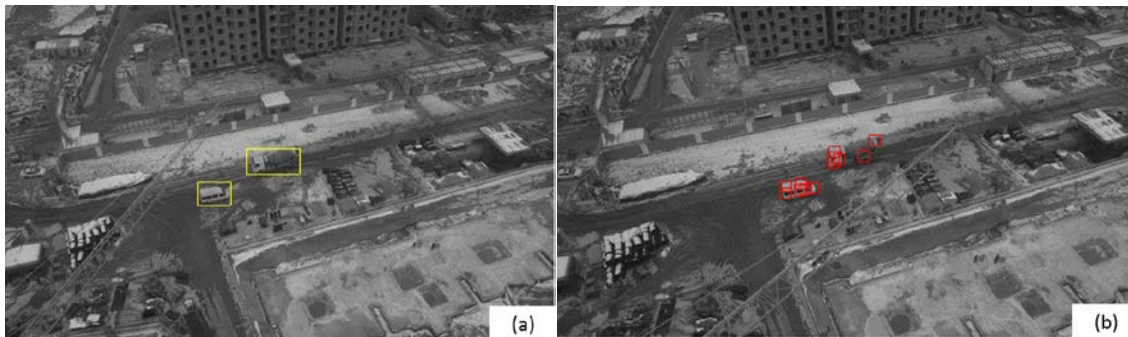


Figure 25: Object detection using feature point matching with a reference image, (a) objects of interest, (b) feature points identified

In the last step, the location of each detected object in global coordinates is calculated based on the recovered camera pose and its image coordinates. A ray casting method is used where the object location is determined by the intersection of a line formed by an image projection vector originating from the camera with the point cloud surface. For each detected object in the image, a corresponding projection vector is determined based on its pixel coordinates and camera parameters such as focal length and image size. Figure 26 shows the projection of detected objects from image coordinates to 3D space. Successfully matched objects have their bounding boxes updated in the point cloud based on the estimated 3D location.



Figure 26: Projection of image coordinates into 3D space from camera origin

An ongoing construction project was selected as a case study of the proposed method. Two vehicles (i.e., a concrete mixer truck and a minivan) were chosen as the targeted mobile assets to be tracked. Both vehicles moved in random patterns in an area of 40 m by 20 m. This case study employed an 8-axis UAV (octocopter) equipped with a mirrorless digital camera. In total 169 images at a resolution of 4912 x 3264 were used to generate the 3D point cloud of the site. Table x shows the computation time involved in each step of the proposed pipeline. The step of SfM computation and point cloud generation takes the longest amount of time but only needs to be carried out once at the start of the experiment. On the other hand, the tracking and location updating step involve a trade-off between accuracy and computation time. Using high-resolution images for tracking will potentially improve the tracking accuracy since more feature points can be detected but this will also increase the computation time.

Figure 27 shows the results obtained from tracking two vehicles over time using images captured from the UAV. The left column shows the 2D image annotated with feature points for each detected object. The right column shows the updated 3D site model (point cloud) corresponding to each captured image. The 3D site model is generated using a top-down view of the site 3D point cloud with bounding boxes formed around each tracked object. Results from the case study indicate that the proposed method dynamically updates the 3D location of two vehicles in a construction site by using the images captured from a UAV and matching them to a 3D site model in the form of a point cloud. The first four and the last images (time: 0s to 44s and 144s) show the cases of successful tracking where the bounding box for the two vehicles are shown in green. The result at time 73s shows a case when the matching algorithm lost track of a vehicle due to insufficient feature points. The corresponding bounding box is drawn based on the previous location estimate but is highlighted in red to indicate uncertainty in location.

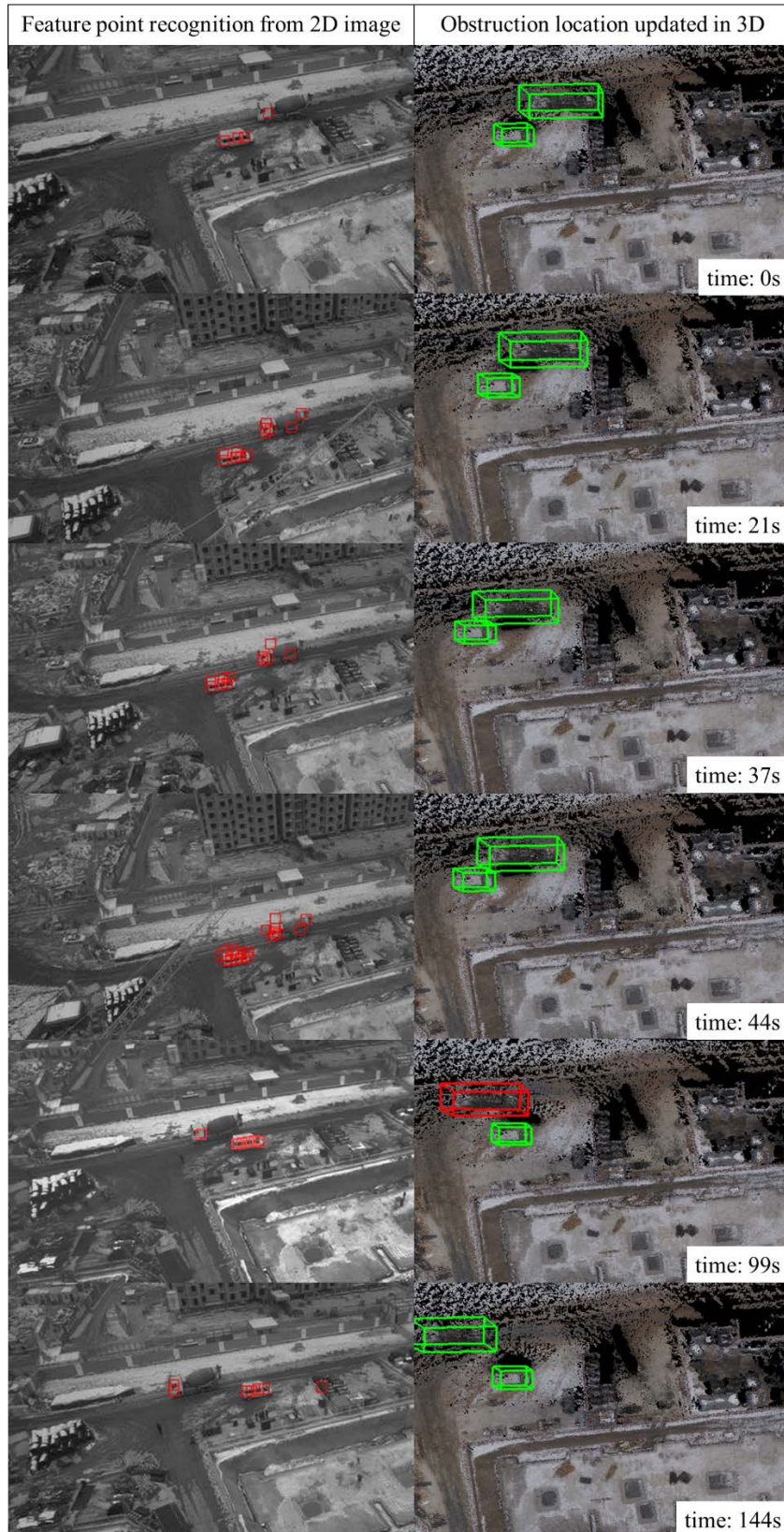


Figure 27: Results of 3D location updating of two vehicles: image captured from UAV (left) and updated 3D site model (right)

As limited by the data collection and computation time, this method cannot update the 3D site model in real-time. Nevertheless, it is not always necessary to update the site condition in real-time. First, workers as the most dynamic assets on a construction site do not need to be tracked on the lifting site considering that workers except the lift crew are not allowed to be in the lift zone. Secondly, although other mobile assets such as equipment and vehicles might be present in the lift workspace for material delivery, their location and movement are fairly predictable during the lifting operation. As such, frequent updates for the site condition, as needed, is regarded sufficient to address the changes on the lifting site.

5.5. Conclusions

To integrate environment constraints into the hazard analysis in the assistance system, this chapter describes two novel methods that enable as-is lifting site condition modeling and updating. Two technologies for rapid collection of point cloud data on lifting site are introduced. A processing pipeline is introduced to model site condition based on point cloud data. To overcome the shortcomings in location tracking using visual data and point cloud, a point cloud-vision hybrid method is introduced to track the location of mobile assets on lifting site and update the 3D site model based on the condition changes.

CHAPTER VI HAZARD ANALYSIS AND REAL-TIME VISUALIZATION

Hazard analysis and warning are the core of a safety assistance system. This chapter introduces a pro-active hazard analysis algorithm and a visualization framework for effective safety warning and user interaction.

6.1. Hazard Analysis based on Crane Motion and Site Condition

Once crane motions are captured and a lifting site is reconstructed with the recognized obstructions, the next task in this framework is to analyze potential hazards in real-time based on pre-defined proximity thresholds. The pro-active hazard analysis is enabled by the four steps as follows. First, the algorithm considers four crane parts as the objects subject to collision hazards: crane cabin, boom, hoist line, and load. Second, the obstructions present on the site are categorized into three levels of severity based on the potential consequences if the collision occurs. For example, power lines in the crane workspace fall into the highest level of severity while trees fall into the lowest level of severity. In the third step, based on safety regulations from the Occupational Safety and Health Administration (OSHA) [78] and industry best practices [11], different safe proximity thresholds are assigned to each severity levels as shown in Table 3. Lastly, the game engine keeps track of the proximity between each crane part and each obstruction. The proximity is defined as the distance between the closest points on the surfaces of each object. To minimize the delay in real-time visualization, the hazard analysis needs to be conducted in an efficient manner. As such, the program only monitors the crane parts and the obstructions within a distance less than 5 m; this input can be changed based on the

size of the crane, types of lifting work, and conditions of the job site. When the proximity between the crane part and the obstruction is beyond the respective threshold, the program will highlight the objects of interest and send visual and auditory warnings through the graphical user interface to the operator. The process of hazard identification is illustrated in a flowchart as shown in Figure 28.

Table 3: Proximity thresholds in the hazard analysis based on level of severity

Level of severity	Proximity threshold	Examples
High	4 m	Energized power lines
Moderate	2 m	Building structures, equipment
Low	1m	Trees

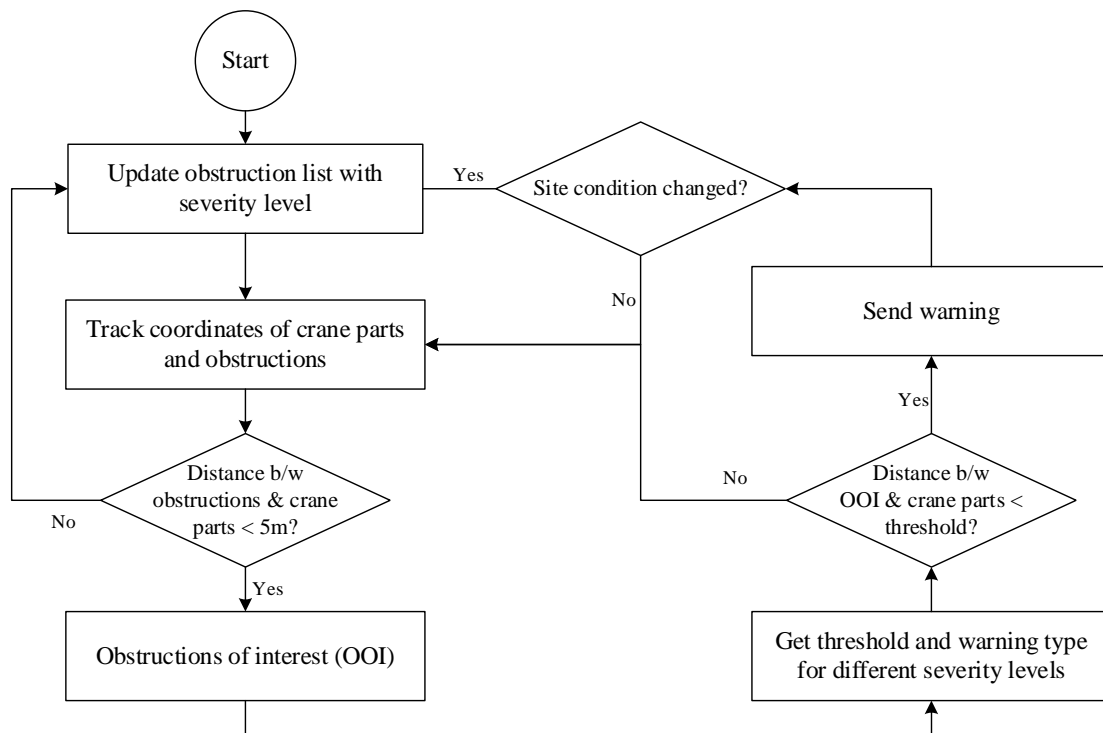


Figure 28: Flowchart of collision hazard identification

6.2. Real-time Visualization and Warnings

A user interface (UI) is the main channel of the communication between the operator and the system. The information presented by the UI has to be concise and easily understandable so that the operator can perceive the information with minimal cognitive workload. The UI of the developed system will consist of three main views of the virtually reconstructed lift scene: a voice control free view, an elevation view and a top view. All views simultaneously show the virtually reconstruction lift scene in real-time that consists of the crane movement and the environment conditions (Figure 29). The main free view will be controlled by the voice commands from the operator (e.g., zoom in/out, left/right, up/down, reset) so that the operator can easily focus on the objects of interest from an occlusion-free angle. The elevation view and the top view are useful to understand the elevation and position of crane load and parts. In addition to the three view, the UI will be augmented by information including visual warnings for collision hazard and excess load sway, highlighted obstructions in proximity to the load or crane parts, previous lift path, and 4) a voice control panel.

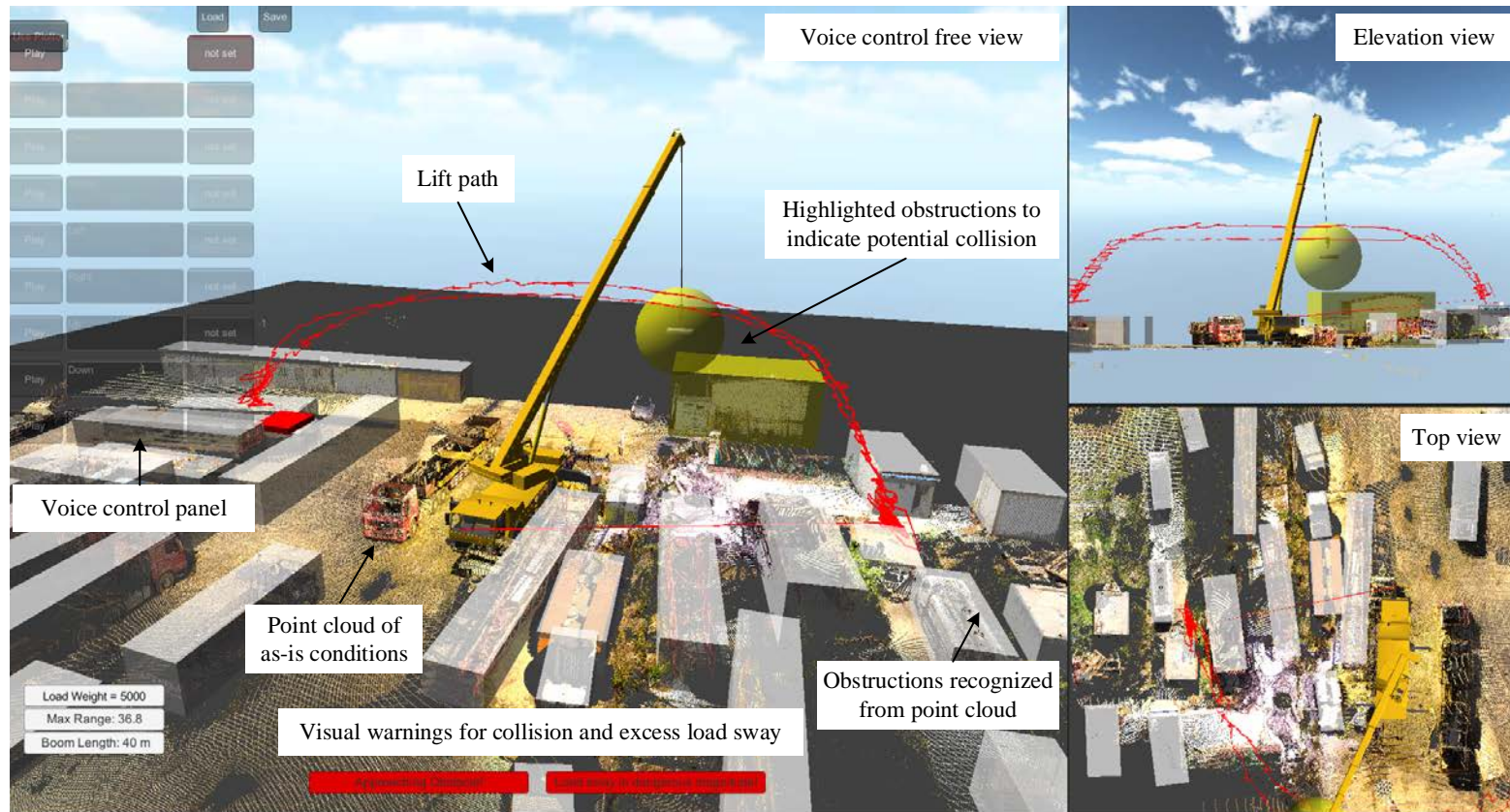


Figure 29: A Graphical User interface (GUI) for real-time visualization and warning

In the prototype system, the tasks of hazard analysis and visualization were accomplished using an on-board tablet computer. The tablet is equipped with an Intel Core i7 1.7GHz processor, Intel 5000 integrated graphic card, 8 GB RAM, and 512 GB storage. The tablet offered a bright 11-inch display so that the user interface is visible to the operator even under normal sunlight conditions (Figure 30). The tablet was mounted on a fully adjustable monitor holder, which makes it very flexible to be configured to what the operator considers fit. A game engine Unity 3D [79] was used as the program for real-time data processing and 3D visualization. To minimize the distraction to the main lifting tasks, a commercial voice recognition program was integrated into Unity3D to enable voice control over the user interface.



Figure 30: Graphical user interface deployed in a mobile crane cabin

6.3. Conclusions

This chapter describes the development of a hazard analysis approach that continuously monitors the crane motion and site condition and pro-actively detects collision hazards

based on a set of pre-defined clearance thresholds. With the aim of minimizing distraction to the main lifting task, an interactive UI was designed to provide both auditory and visual warnings that can effectively alert the operator about potential hazards during the lift.

CHAPTER VII EFFECTIVENESS VALIDATION OF LIFTING ASSISTANCE

This chapter presents five key performance indexes (KPIs) to quantify the operator's performance and introduces an online query-based technique to assess the operator's SA. In addition, perceived workload during the lifting operation was measured using NASA-TLX. These methods were used to validate the effectiveness of a prototype of the assistance system in a series of field tests.

7.1. Effectiveness Assessment Approach

Previous efforts in evaluating a crane assistance system mainly focused on measuring tracking accuracy and ease of use. Very few emphasized the system's impact on operator performance and effectiveness in improving the operators' SA. This is partly because the performance and SA of crane operator are difficult to define and quantify. In addition, most of these tests were validated in a simulated environment instead of utilizing real lift tasks with actual pressure and constraints (Hwang 2012; Chi et al. 2012; Li et al. 2013). The following sections introduce an effectiveness assessment approach consist of three methods for quantifying and measuring the operator's workload, lifting performance, and situation awareness. Section 7.2 introduces two field tests and analyzes the test results using the assessment approach.

7.1.1. Assessment of perceived workload

During the crane lifting operation, operators' performance and SA can be affected by the workload imposed by the assigned lifting task including mental, physical, and temporal

demands. Given the same lifting task, different operators may perceive different workload because of subjective, individual differences in training, experience, and cognitive capability. The perceived workload of the individual operator can be measured using NASA Task Load Index (NASA-TLX) [80]. The NASA-TLX is a widely used, subjective, multidimensional assessment tool that allows users to perform subjective workload assessments on operators working with various human-machine systems. NASA-TLX derives an overall workload score based on a weighted average of the ratings on six dimensions, including Mental Demands, Physical Demands, Temporal Demands, Own Performance, Effort, and Frustration. It has been used to assess workload in various human-machine environments such as aircraft cockpits, command, control, and communication (C3) workstations; supervisory and process control environments; and simulations and laboratory tests [81].

In the assessment of perceived workload, participants were instructed to place an “X” on each of the six scales at the point that matches their experience. Each scale has two endpoint descriptors such as “bad” and “good”, or “low” and “high”. These numerical ratings for each scale reflect the magnitude of the factors in a given task. Then, the participants were presented with a series of pairs of rating scale tiles (for example, Effort vs. Mental Demands) and asked to choose which of the items was more important to their experience of the workload in the lifting task they just performed. This was used to evaluate the contribution of each factor (its weight) to the workload of a specific task. Given the numerical rating and the weight of each factor, an adjusted rating can be computed for quantifying the overall perceived workload of the rated task.

7.1.2. Quantitative assessment of lifting performance

Crane lift performance has multiple dimensions and thus it is difficult to be defined and quantified. This section proposes a quantitative assessment method to measure lift performance with respect to efficiency and safety criteria, including collision avoidance, load sway control, lift time minimization, lift path selection, and load placement accuracy. Accordingly, five key performance indexes (KPIs) are proposed to evaluate the performance in these safety and efficiency criteria. These five KPIs are concluded based on a review of the literature and practices in operator training and qualification, as well as interviews with multiple experienced crane operators and lift supervisors. The five KPIs are defined as follows.

Collision avoidance: Colliding with surrounding obstructions (e.g., structure, equipment) is a major cause of crane-related accidents. The operator's performance in keeping the load from proximity to surrounding obstructions is quantified by the percentage of total lift time when the clearances between the load and other crane parts to surrounding obstructions are within a series of pre-defined thresholds depending on the type of obstructions ($\sum T_{\text{clearance}}$).

Load sway control: Excess load sway can lead to crane instability or boom failure, and thus should be avoided in crane operations. The operator's performance in controlling load sway is quantified by the percentage of time when the load swings beyond the threshold of 2 m in the total lift time ($\sum T_{\text{sway}}$) .

Lift time efficiency: Cranes are responsible for most vertical and horizontal transportation of structural elements, materials, and equipment. Thus, efficient execution of a lifting operation is critical to the productivity of other activities and the overall project efficiency. For clarity purposes, the total lift time in seconds (T_{lift}) for a particular task is used to quantify the efficiency of a crane lifting operation.

Lift path efficiency: Choosing the appropriate lift path is very important for a lifting operation. A short path might reduce the lift time but increase the chance of an accident as it is close to surrounding obstructions, while a longer path might be free of collisions but take more time to complete. Lift path selection is a rather subjective decision depending on many factors such as the preference of the individual operator, site condition, and crane capability. Therefore, it is difficult to evaluate the path chosen by an operator solely based on the length of the lift path. In our method, the lift path selection is assessed together with other safety and efficiency measurements (e.g., clearance to obstructions, lift time) to obtain a more comprehensive understanding of the operator performance. From an efficiency perspective, operator's performance in selecting the shortest lift path is quantified by the total distance the hook travels during the lifting task (D_{path}).

Load placement accuracy: Delivering the load to the desired position is an essential task for crane operators, and a skilled operator can place the load more accurately so that less effort is needed from ground workers to guide and stabilize the load. Thus, the cycle of one lift will be shortened and the overall lift efficiency will be improved. Operator performance

in placing the load accurately is quantified by placement error between the actual and expected positions ($D_{\text{placement}}$).

Given the five KPIs defined above, a lift performance equation is constructed as below:

$$\text{Operator performance} = f(\sum T_{\text{clearance}}, \sum T_{\text{sway}}, T_{\text{lift}}, D_{\text{path}}, D_{\text{placement}}) \quad (\text{Eq. 15})$$

$\sum T_{\text{clearance}}$ - percentage of total lift time when the load is in a dangerous clearance to obstructions

$\sum T_{\text{sway}}$ - percentage of total lift time when load sway is beyond the allowable magnitude

T_{lift} - time spent for the lifting task

D_{path} - distance the hook travels during the lifting task

$D_{\text{placement}}$ - placement error between the actual and expected positions

Each lifting task has its unique management requirement (e.g., productivity pressure) and environment constraints (e.g., wind condition, spatial conflicts) that influence the lift performance. Therefore, the results of the lift performance equation cannot be applied across different sites and cranes. For a particular lifting task, the lift performance equation can be used to track the lift performance of a single operator over time or benchmark the lift performance among multiple operators.

7.1.3. Online assessment of situation awareness

SA has been widely considered as an important factor in dynamic decision-making, and several indirect or subjective methods (e.g., physiological measurement, performance measures, self-rating) have been proposed and used in the SA research of aircraft pilots and air traffic controllers. This research employed an online query-based SA measurement method adapted from SPAM [82]. In this method, the operator will be presented with queries about the situation while the situation remains present and while they continue to perform the primary task. Figure 31 shows the steps in the query process. The questioner will indicate the operator that he intends to ask a query. Once the operator is ready to take the query, he or she will suspend the operation and indicate the questioner that he is ready. Then, the questioner will ask the question. The duration between the time the questioner finishes the question and the time operator start answering the question is considered the response time. Once the questioner records the operators' answer to the query, he will indicate the operator to resume the operation. The operator's level of SA will be quantified by the response time and response correctness.

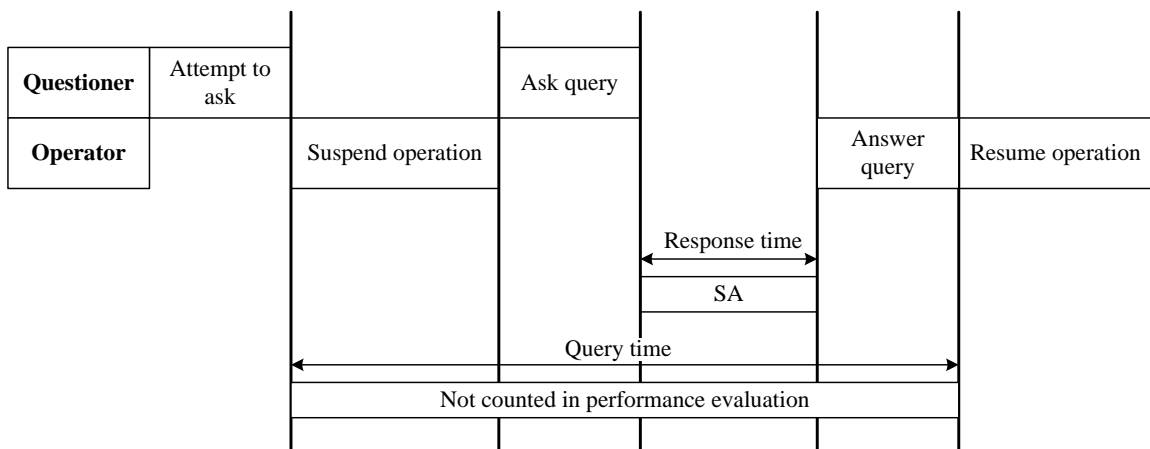


Figure 31: Query process in online SA measurement

Two major challenges that are addressed in this research when using this method are 1) designing proper queries that can effectively reflect the level of SA in crane lifting operations, and 2) choosing the proper timing to make the queries so that it does not interfere the primary lifting tasks while remains effective for real-time SA assessment. A list of queries is shown in Table 4, in which two queries focus on past events, three queries focus on present events, and one query focuses on future events. These queries were designed based on a discussion with safety experts, crane supervisors, and crane operators to ensure they reflect the most essential understanding of the lifting task and associated risks. During each lifting operation, one of the queries is chosen to ask according to the concurrent situation. For example, when the load is being lifted above a tree, the questioner can ask the current clearance between load or boom and tree.

Table 4: Query list for online SA measurement

	Type	Query
1	Past	What is the maximum sway distance so far?
2	Past	How many warnings have you received from the system so far?
3	Present	What is the current boom reach?
4	Present	What is the current clearance between load/boom and obstructions?
5	Present	How far is the load placed from its target placement location?
6	Predictive	How long do you anticipate this lifting task will take?

7.2. Field Tests and Validation Results

7.2.1. Field test 1 overview

The objective of field test 1 is to explore the impact of system usage on lift performance. Based on the system architecture, a prototype system was developed and deployed on a 70-ton telescopic boom mobile crane. Four operators with lifting experiences ranging from 13 years to 21 years participated in the test. They performed in total 92 lifting tasks on two lifting sites with different conditions and constraints. Three test scenarios were created with different assistance levels. Prior to the tests, all the operators were trained to become familiar with the display and voice control of the system; they were asked to practice with the system until they reported feeling comfortable using it. During each lifting task, their performance in safety and efficiency was recorded and quantified based on the criteria proposed in the previous section. It should be noted that the experiments were conducted in real lift jobs with actual temporal and spatial constraints, and the participating operators were exposed to real-lift pressure and risks. Compared to virtual simulations or surveys that have been commonly used in previous research, the data collected and presented in this research is more realistic and therefore the results are closer to the actual effectiveness of the assistance system.

Two lifting tasks were chosen to assess the prototype system as shown in Figure 32 and Figure 33. Lifting tasks in both sites contain blind spots where the operator does not have a direct line-of-sight to the load (test Task 1) or to the drop off location (test Task 2). In addition, the site of Task 2 is surrounded by trees which are approximately 8 m high. These confined lift workspaces present significant collision risks and challenge the operators in controlling the crane and the lifted load.

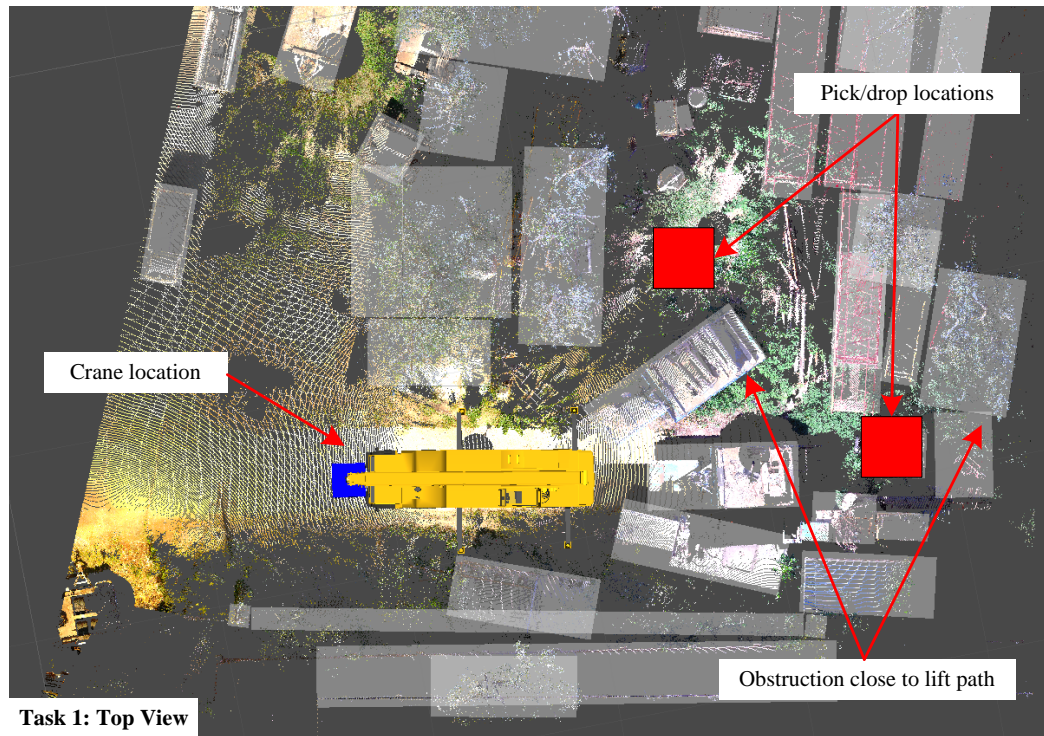


Figure 32: Illustration of Task #1 in top view



Figure 33: Illustration of Task #2 in isometric view

To evaluate the usefulness of the system, three operational scenarios were created with different assistance levels: no assistance, optional assistance, and full assistance. In the no assistance scenario, the operators performed the lifting tasks as usual without assistance from the system. In the optional assistance scenario, the operators had the option to choose how much they want to use the system based on their individual preferences. In the full assistance scenario as shown in Figure 8, the cabin window was blocked (i.e., 100% blind) so that the operator could not see the crane or the lifted load and had to fully rely on the assistance from the system. To ensure safety, a lift supervisor can stop the operation if any risk occurs.

The impact of the assistance system to operator performance in these three operation scenarios was analyzed by quantifying the lift performance with respect to safety and efficiency. Furthermore, as the operators had the freedom to determine how much they wanted to use the system in the optional assistance scenario, the relationship between the level of usage of the assistance system and the actual lift performance of each operator could be analyzed by focusing on individual differences.

7.2.2. Assessment of effectiveness in lift performance improvement

As explained in section 7.1.2, this study utilizes five KPIs to quantify the lift performance of each operator. In the tests, the five performance indicators were measured by the assistance system and recorded in a performance report after each lift. The measurements of the five KPIs for the 92 lifting tasks in no assistance, optional assistance, and full assistance scenarios are shown in the boxplots in Figure 34 and the mean value and standard deviation are summarized in in Table 5.

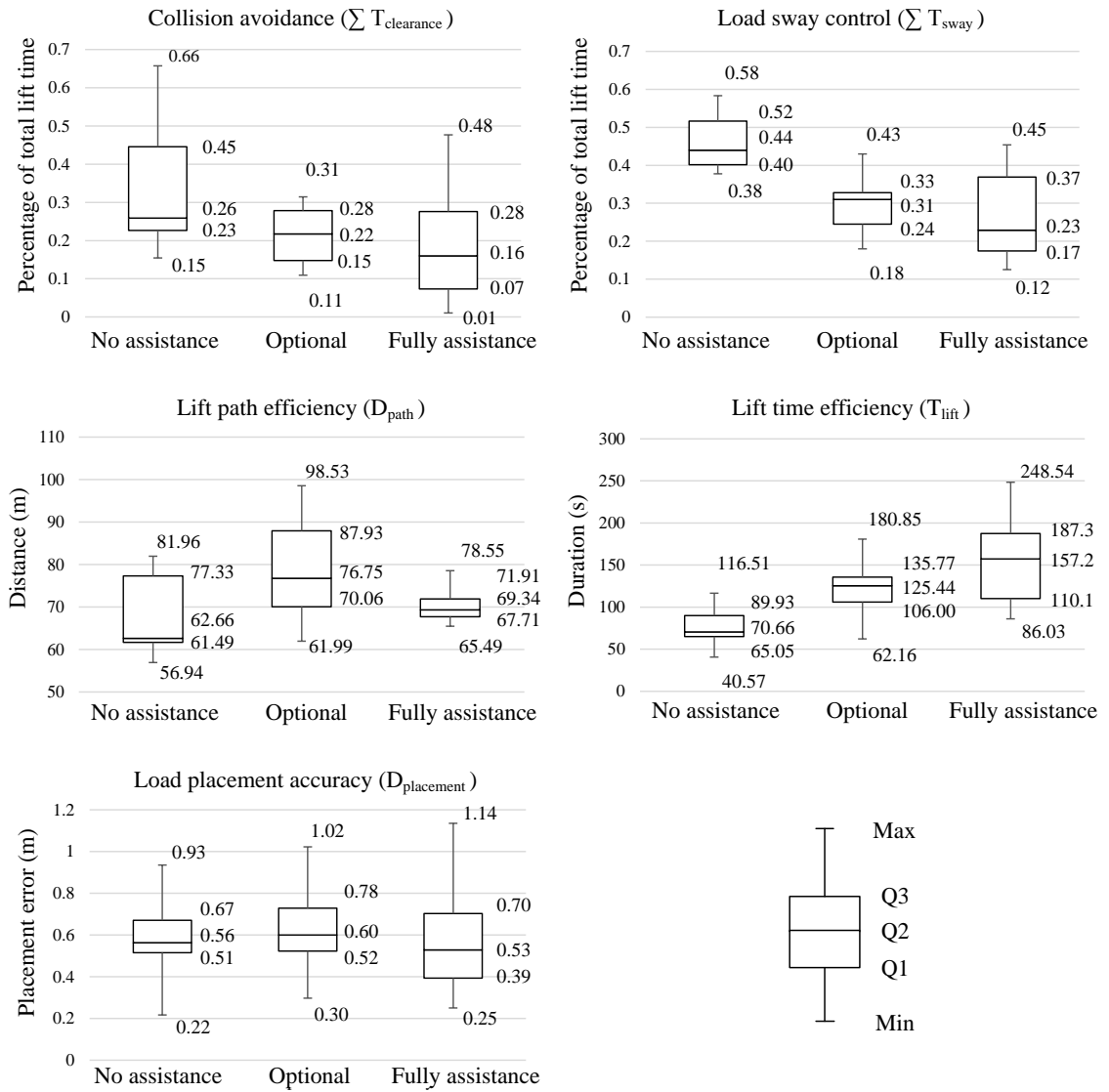


Figure 34: Boxplot of five key performance indexes (KPIs) in no assistance, optional assistance, and full assistance scenarios

Table 5: Mean and standard deviation of five KPIs in three test scenarios

KPIs	Measure	No assistance	Optional	Full assistance
Collision avoidance	Mean	33.5%	21%	19%
	STDEV	17.6%	7.9%	15.3%
Load sway control	Mean	46.3%	29%	26%
	STDEV	8.2%	8.1%	12.4%
Lift path efficiency	Mean	67.8 m	78.32 m	70.5 m
	STDEV	9.3 m	12.3 m	4.5 m
Lift time efficiency	Mean	76.7 s	120.9 s	152.8 s
	STDEV	22.5 s	32.8 s	54.9 s
Load placement accuracy	Mean	0.59 m	0.66 m	0.6 m
	STDEV	0.21 m	0.23 m	0.3 m

By examining the general trend of the results, it is observed that except for the placement error index, all of the other four KPIs were noticeably affected by the extent of operator's engagement with the assistant system. Specifically, both safety performance indexes (i.e., collision avoidance and load sway control) improved as the level of assistance increased. In the no assistance scenario, operators estimate the clearances between the load and obstructions using their direct vision or by being directed by a signal person. However, their vision capability (as well as that of the signal person) can be affected by occlusions, illumination, and the perception of depth. With the help of the system, either optional or full assistance, the operators were warned of potential collisions or excess sway proactively so that they could make a timely response to the risks. With optional assistance, the operators switched back and forth between eye observation and system visualization to confirm the observed or warned incidents, which cost them a longer response time. With full assistance, they were not allowed to check the situation with their eyes but were forced

to fully trust the system. The results show that they achieved better safety performance in the full assistance scenario; this to some extent indicates the effectiveness of the system in improving lift safety performance.

In terms of the efficiency performance, as the assistance level increased, the results show that the operators actually took longer to finish the lifting task, which is different from the authors' expectation, as the system is designed to improve the productivity of the lifting operation. Interviews with the operators revealed that this increased time may be a result of the operators feeling nervous when they were not allowed to see through the windows. In these situations, the operators tended to act more carefully, which resulted in a decreased performance in lift time efficiency. Therefore, proper training for the operators is critical for them to operate the system with confidence.

Except for lift path efficiency, operator performance in the other four categories exhibits significant variances. This is partly because the operators were not used to solely looking at the screen instead of their usual practice of looking through the cabin windows. Variance in lift path efficiency is much smaller with full assistance compared to the efficiency resulting from the no assistance and optional assistance trials. This is mainly because in the system UI, the operator can check and verify the lift path in advance with the consideration of efficiency and safety. In other words, the system allows them to optimize the lift path so that the actual paths are very close to the optimal path (i.e., shortest collision-free path). Compared to other KPIs, placement error is not as sensitive to the usage of the assistance system. Conversely, the variance of placement error increases slightly as the operators use the system more often. This is because on both lifting sites the operators had a clear line-of-sight to the locations where the loads were supposed to be

placed. It was easier for them to use their eyes than the system to check the position of the load and guide it to the designated location. When they were forced to use the system solely in the full assistance scenarios, their performance became less reliable.

7.2.3. Impact analysis of individual characteristics

The effectiveness of the assistance system can also be affected by the habits or attitudes of the individual crane operators. To understand the impact of the assistance system on the performance of operators who possess different characteristics, the 40 lifts on test site 1 who operated with optional assistance were further broken down to investigate how the usage of the system would affect the lift performance for each of the four individual operators. As the direction of the operator's eyes is a good indicator of the operator's attention focus, the level of usage was defined as a percentage of time when the operator looked at the display in the total lift time. The time the operator looked at the display was determined based on the video recordings from two cameras in the crane cabin. The relationship between the lift performance and the percentage of time the operators used the system is plotted in Figure 35.

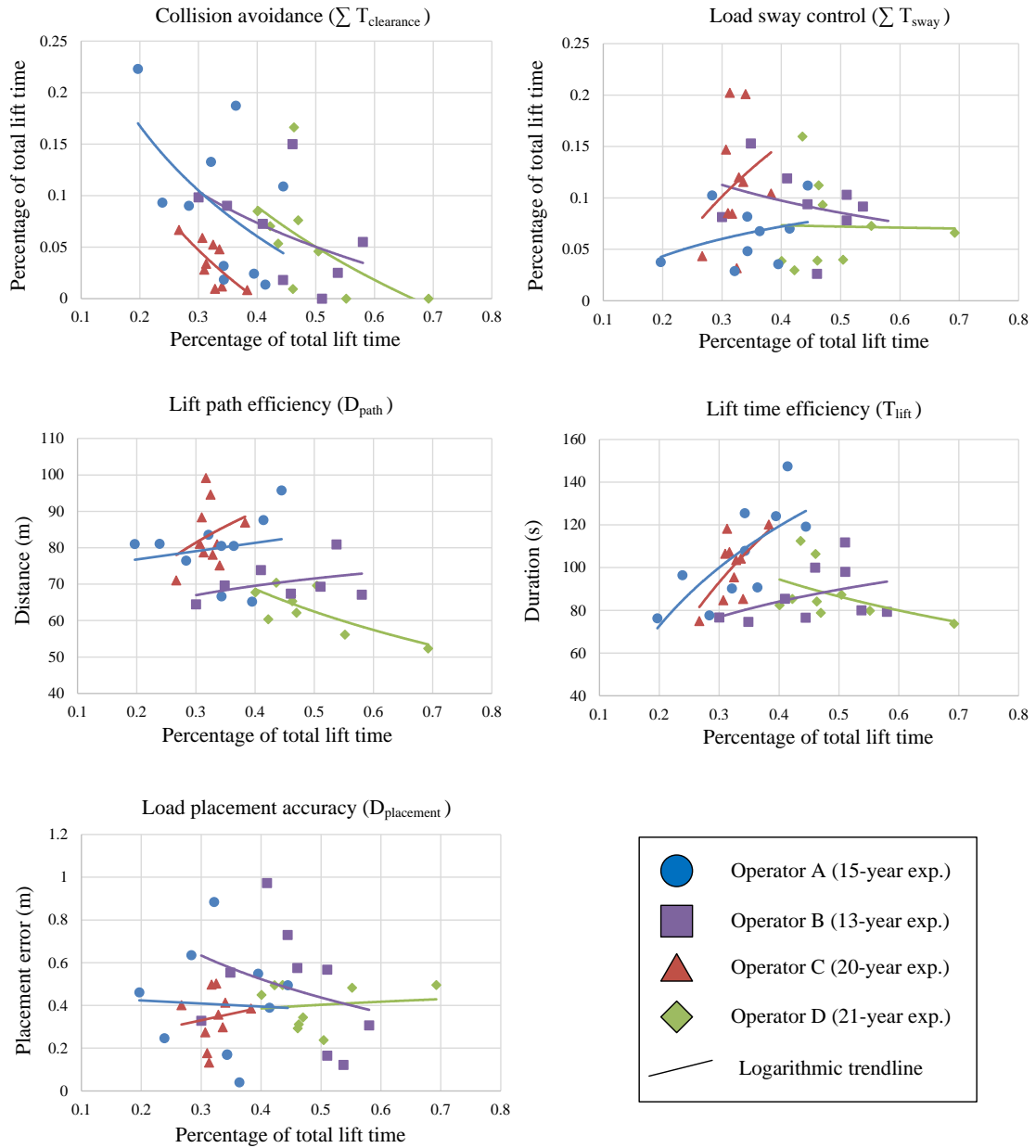


Figure 35: Relationship between system usage (percentage of total lift time in seconds) and the lift performance of each individual operator

System usage patterns were observed to be different for each operator. Operator A used the system most often (40% -70% of total lift time), while operator C and D used the system least often (20% - 45% of total lift time). For operators A, B, and D, the system

usages in each single lifting task varied by approximately 30% across individual lift iterations, while the system usage by operator C was more consistent with a 10% variance across among his 10 lift iterations. For each individual operator, variance in system usage in different iterations may be a result of the individual operator's ability to properly use the system (e.g., read information and visual representation on the display) and confidence in using the system. Although the functionalities of the system were thoroughly introduced to the operators, who had approximately 30 minutes to practice with the system before the actual test lifts, it still took several iterations for them to report feeling comfortable and confident using the system. As test results indicate, the learning curve may vary among different operators due to their individual characteristics such as learning ability and risk-taking tendencies.

The logarithmic trend lines of the performance measurements demonstrate the relationship between system usage and lift performance. In terms of safety performance, the performance of collision avoidance significantly increases as the operators use the assistance system more often. Trend lines follow a similar tendency for all four operators. As for the performance of load sway control, only operator B performed better as the system usage increased. These results demonstrate that operators A and C experienced more difficulty in controlling the load sway as they spent more time looking at the display instead of directly looking at the load. Load sway is very common during crane lifting operations. It normally occurs due to acceleration or braking in boom lifting or swing. Once load sway occurs, the operator needs to compensate the sway by moving the boom in the opposite direction. This operation requires extensive skill and a good hand-eye coordination. Although the system is reasonably accurate and fast in reconstructing the

crane motion, it is difficult for the operators to solely rely upon the system for load sway control.

The system usage has minimal impact on the lift path efficiency and the load placement accuracy. All four operators demonstrated similar results in these categories. These results are in compliance with the results from the previous section, which demonstrates that there is not much opportunity for improvement during the lift. This is probably because that the operators have already chosen a relatively optimal lift path in the beginning of the lift, through the 3D virtual reconstruction of the lift scene. The lift time efficiency, however, significantly decreases as the operators use the system more often. An analysis of the video recordings reveals that with regard to such critical moves as load sway control and blind lifts, the operators tended to be more careful and slower when using the system, which complies with the confidence issue discussed earlier.

7.2.4. Field test 2 overview

With the purpose of understanding the effectiveness of the system in improving operator's SA, field test 2 recruited five crane operators whose experience range from 8 to 16 years. Similar to field test 1, the operators were trained to be familiar with the functionalities of the assistance system in a 30-minute training session. With a different focus, field test 2 investigated how the assistance will affect the operator's SA and how the workload of different lifting tasks will influence the effectiveness. To differentiate the complexity level of the lifting operation, two lifting tasks were designed with different spatial and temporal constraints. Although surrounded by trees and other spare crane parts, lifting task 1 features a simpler lifting operation as no obstructions present between the pick and drop locations (Figure 36 and Figure 37). Lifting task 2 requires the operator to lift the load over a row of

trees of 15 m in height (Figure 38 and Figure 39). Sitting in the cabin at ground level, the operators can hardly see the load when it is above the tree and therefore estimating the clearance from the tree to the load or boom is very challenging. Two operation scenarios were created where in control scenario the operators only use traditional LMI system and in test scenario the operators use both LMI and the proposed assistance system. In total 60 lifts were conducted in the field test 2.

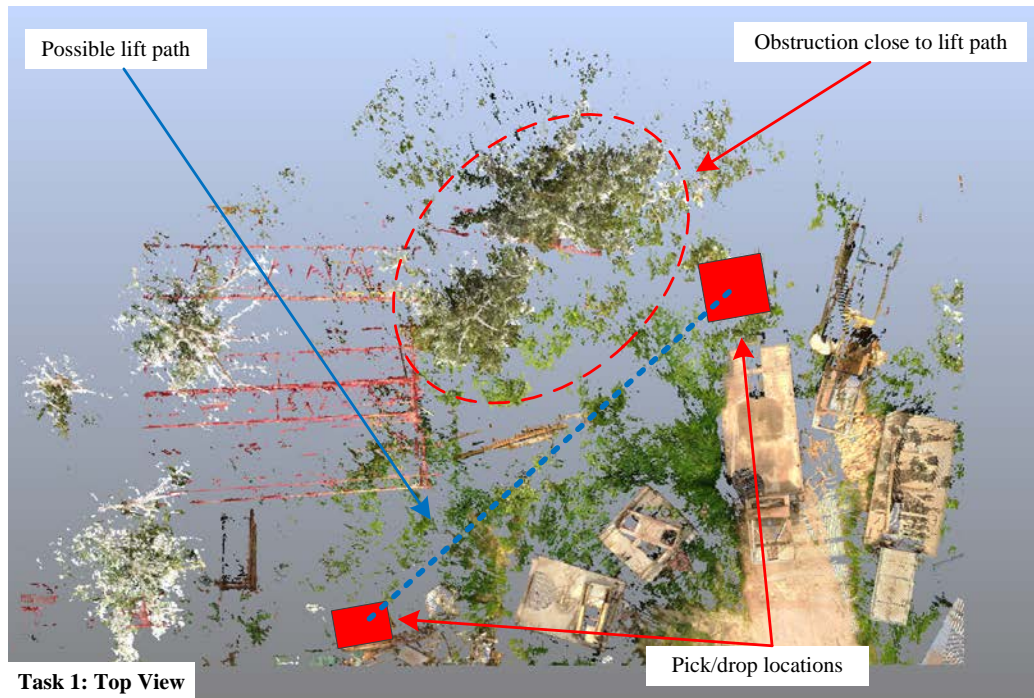


Figure 36: Illustration of lifting task #1 in top view

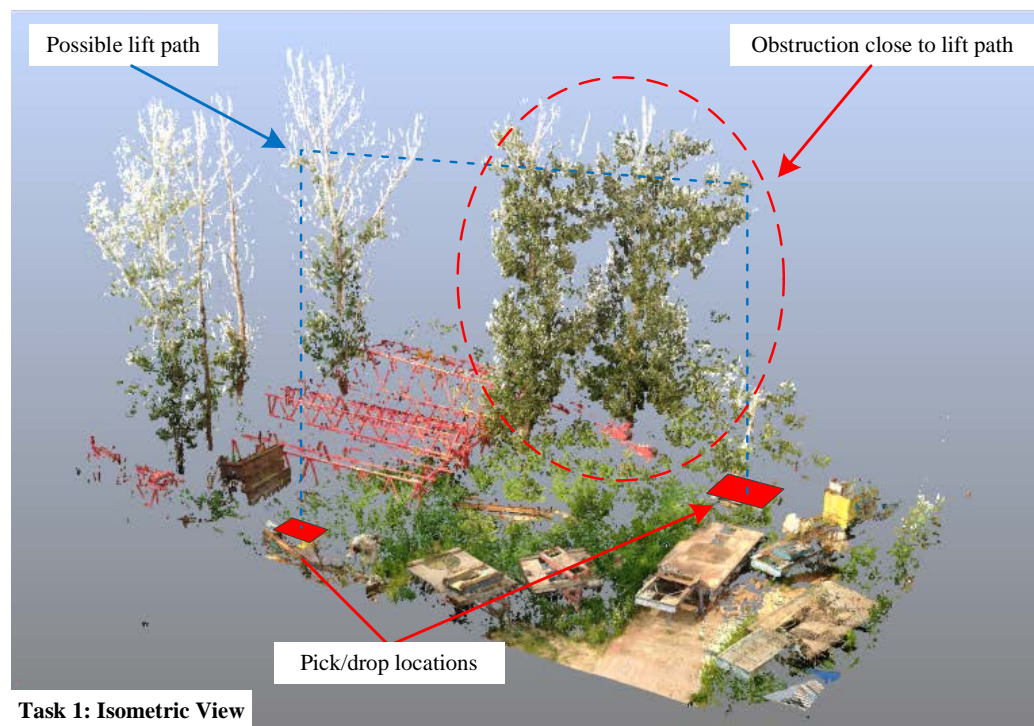


Figure 37: Illustration of lifting task #1 in isometric view

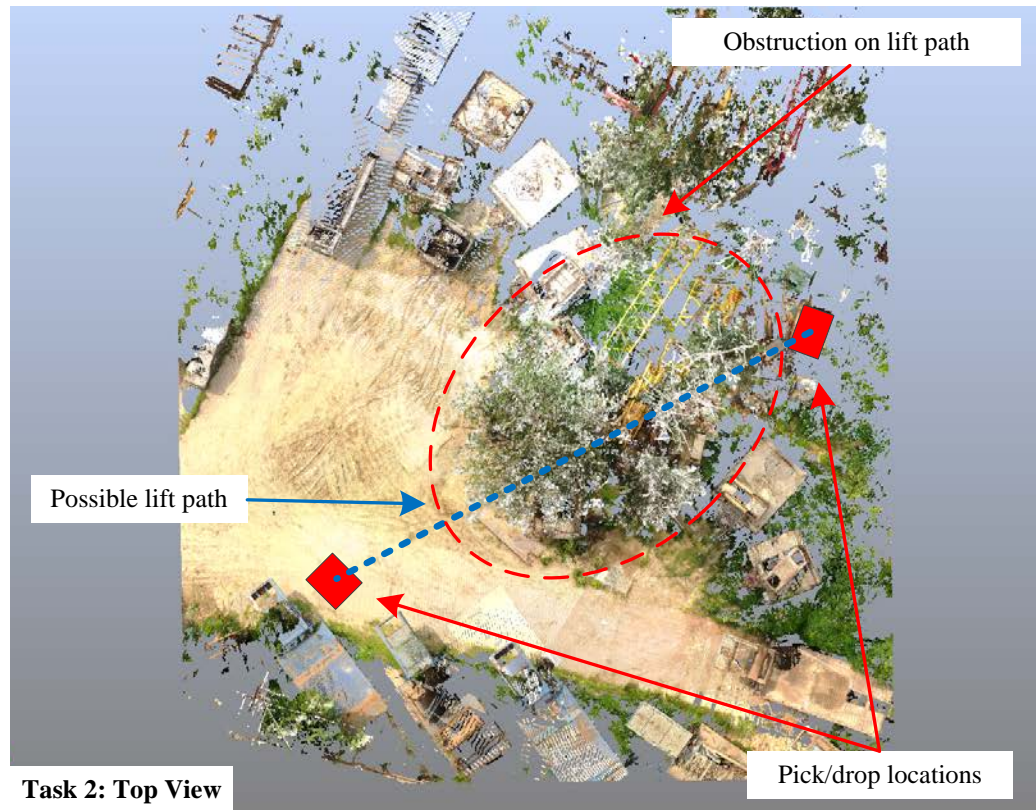


Figure 38: Illustration of lifting task #2 in top view

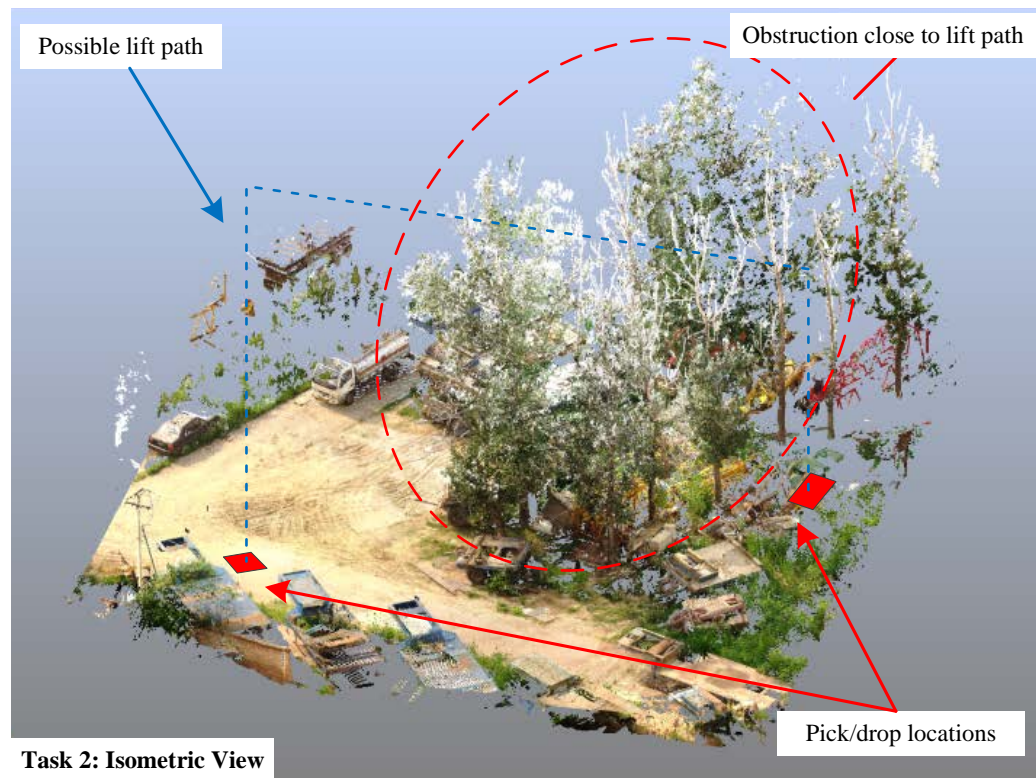


Figure 39: Illustration of lifting task #2 in isometric view

7.2.5. Workload indexes for two lifting tasks

This research adopted the NASA Task Load Index (NASA-TLX) to quantify the workload imposed on the operators in the two test lifting tasks. A NASA-TLX rating package was explained and presented to each operator after the lifting operations. They were asked to fill out the rating and weight sheets based on their experience in the lifts. As the operators vary in individual characteristics such as motivation, risk-taking tendency, and mental and physical capabilities, different operator may perceive different level of workload given the same conditions and constraints. Therefore, the workload index for each lifting task was computed based on an averaged index from the five operators. Overall, lifting task 1 received an adjusted rating of 5.42 whereas lifting task 2 received 6.65. This result indicates that lifting task 2 imposed a larger amount of workload to the operators than lifting task 1. This can be further assured by the fact that all five operators rated Task 2 higher than Task 1, with a largest difference of 2 and smallest of 0.73.

In addition to the workload indexes for the lifting tasks, it is also interesting to see how the operator rates and weights each workload dimension in general. Among the six dimensions, the largest rating difference between the two tasks lay in mental demand (5.8) whereas the smallest difference in physical demand (0.6). In the meantime, the operators weighted mental demands as the second biggest contributor (second to performance) to the workload and physical demands as the smallest. These results show that mental demand was a dominating source of workload in the two test tasks, and very likely in crane lifting operations in general as these tasks represented the common characteristics in day-to-day lifting operations.

7.2.6. Assistance effectiveness in improving lift performance

Lift performance in the two lifting tasks was quantified using the five KPIs introduced in Section 7.1.2: $\sum T_{\text{clearance}}$, $\sum T_{\text{sway}}$, T_{lift} , D_{path} , and D_{accuracy} . All five KPIs were recorded by the computer program after each lifting operation and computed based on their definitions. It should be noted that $\sum T_{\text{clearance}}$ and $\sum T_{\text{sway}}$ were normalized by dividing the accumulated time by total lift time T_{lift} of the corresponding lift. Therefore, their units are percentage. Figure 40 presents the average values of the five KPIs based on data recorded from the 60 lifts.

If we compare the KPIs in the two tasks, lift path was much longer in Task 2 (160%) and Task 2 took much longer to complete (158%). This assured the fact that Task 2 was designed to be more complex than Task 1 and the difference in complexity level will affect both the performance and the level of SA. Compared to Task 1, operators achieved better performance in Task 2 in controlling load sway (34%) and load placement accuracy (32%). This indicates that the operators were more cautious when controlling the sway and load position in a more complicated lifting task.

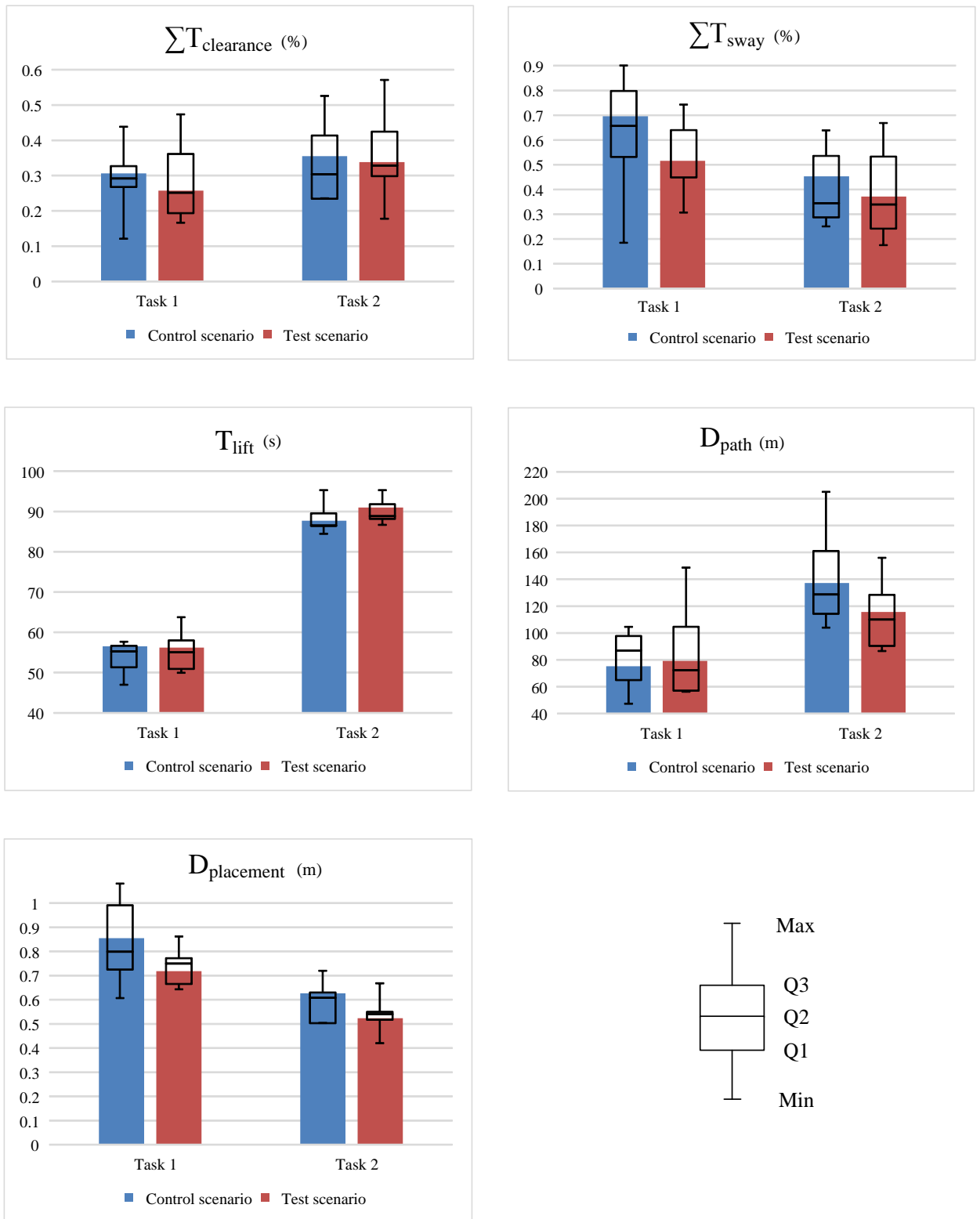


Figure 40: Key performance indexes (KPIs) in two lifting tasks under control and test scenarios

When comparing the value of each KPIs in the two scenarios, it is observed that there was a noticeable improvement in safety performance in the test scenario, especially in Task 1 where $\sum T_{\text{clearance}}$ decreased by 19.4% and $\sum T_{\text{sway}}$ decreased by 28.6%. Although the improvement of safety performance in Task 2 followed the same trend, the magnitude of improvement was less noticeable where $\sum T_{\text{clearance}}$ decreased by 5.7% and $\sum T_{\text{sway}}$ decreased by 20%. Although the operators tended to perform more safely when provided the assistance, the system had no obvious positive impact on efficiency performance except that the selection of lift path (T_{lift}) in Task 2 was more efficient (17.8%). This can be explained by that Task 1 was designed to be simple where there were not much room for improvement to shorten the lift path (see Figure 37), whereas Task 2 featured a more complicated lift and the operators had more flexibility in selecting the lift path (see Figure 39). In addition, placement accuracy ($D_{\text{placement}}$) was improved in both tasks, 17.6% in Task 1 and 19.4% in Task 2. This was mainly because the operators were able to check and adjust the load position when placing the load based on the top view provided by the assistance system.

When looking at the variances of safety KPIs, the variances of safety KPIs were consistent in Task 1 and 2 and in control and test scenarios. This suggested that the safety performance of crane lifting operations varies even for the same task in the same scenario. This also suggested that introducing the assistance system did not significantly change the operators' working pattern. For efficiency KPIs, the variances of T_{lift} and $D_{\text{placement}}$ were much smaller comparing to D_{path} , and the variances in test scenario are smaller than control scenarios. This may because that though the UI of the assistance system, the operators

obtained a better spatial awareness and therefore could plan the lift more efficiently and consistently, and place the load more accurately.

7.2.7. Assistance effectiveness in improving operator's SA

As introduced in Section 7.1.3, an online query-based SA measure was used to quantify the operators' SA during the operation. The level of SA was quantified by the response time and response correctness for each query. Figure 41 and Figure 42 present the average response time and average response correctness of the 60 queries in different tasks and scenarios. The quantile box plot indicates the variance in the results of response time and correctness. It was observed that the average response time in both tasks was remarkably reduced when the assistance system was used, 17.5% in Task 1 and 28.6% in Task 2. The quartile box plot indicates that the variances of response time in the control scenario in both tasks are much smaller than that in the test scenario. This result suggests that the operators have developed a consistent patent of understanding the situation based on their experience without the assistance. Despite the fact that overall response time was reduced, the introduction of the assistance system may change the way the operators search and understand the situation. Therefore, training plays an important role in the successful integration of the assistance system. Overall, the results show that the introduction of the assistance system facilitated the operator's ability to comprehend the situation, especially the information closely related to lift safety and efficiency.

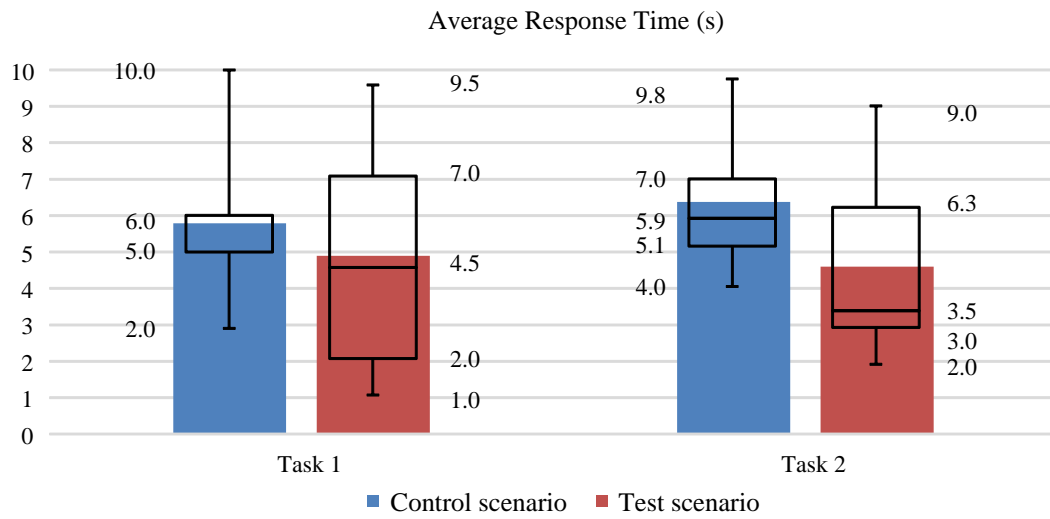


Figure 41: Average response time in two lifting tasks under control and test scenarios

Response correctness is shown in percentage and it was computed by comparing the operators' responses to the correct answer recorded in the system. The results show that average response correctness was improved in the test scenario, 2.3% in Task 1 and 9.5% in Task 2. The box plot suggests that the response correctness in test scenario was in general more consistent, especially in Task 2. Although not as obvious as the decrease in response time, the improvement of response correctness suggests that the assistance system was able to provide helpful information to augment the operator's awareness of the lifting task so that the accuracy of their decision-making can be increased.

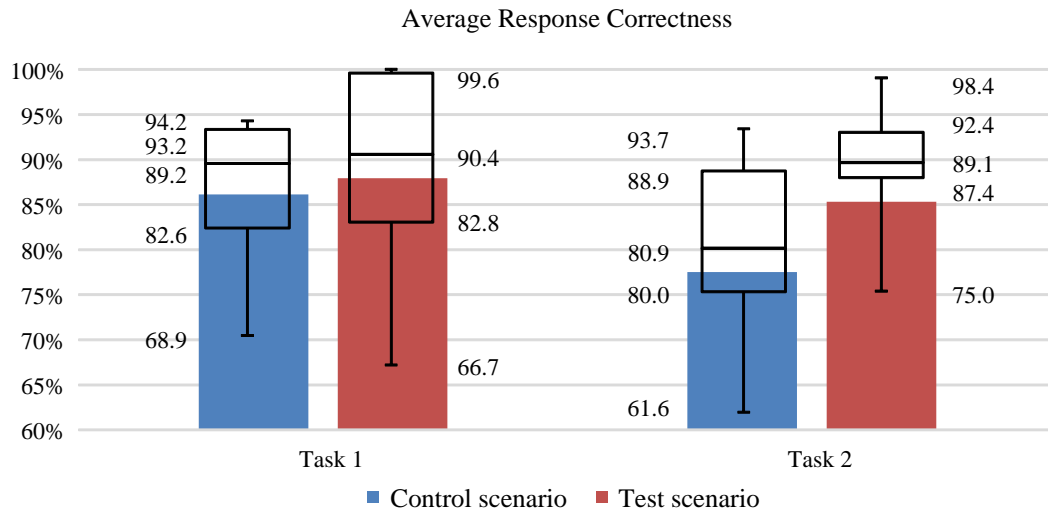


Figure 42: Average response correctness in two lifting tasks under control and test scenarios

If we break down the results of average response time into each queries (Figure 43), we notice that the estimation of incident number took the longest time for the operators to respond (6.3s), while the load displacement took the shortest time (3.6s). It is worth noting that using the system greatly reduced the response time of the prediction of lift time by 37.4% from 6.7s to 4.1s. This was because the assistance system provided a 3D representation of the crane pose and the lifting site so that the operator could easily understand the lift progress and predict the complexity and time of the remaining lift job. Also, there was noticeable response time improvement in estimating load clearance (21.1%) and boom reach distance (22.3%). This also resulted from the direct visual feedback from the user interface and the flexibility to change the view angle. There was no query asked for recalling the number of incidents and the displacement of load in the control scenario, as these queries were considered less relevant in that specific situation than other queries.

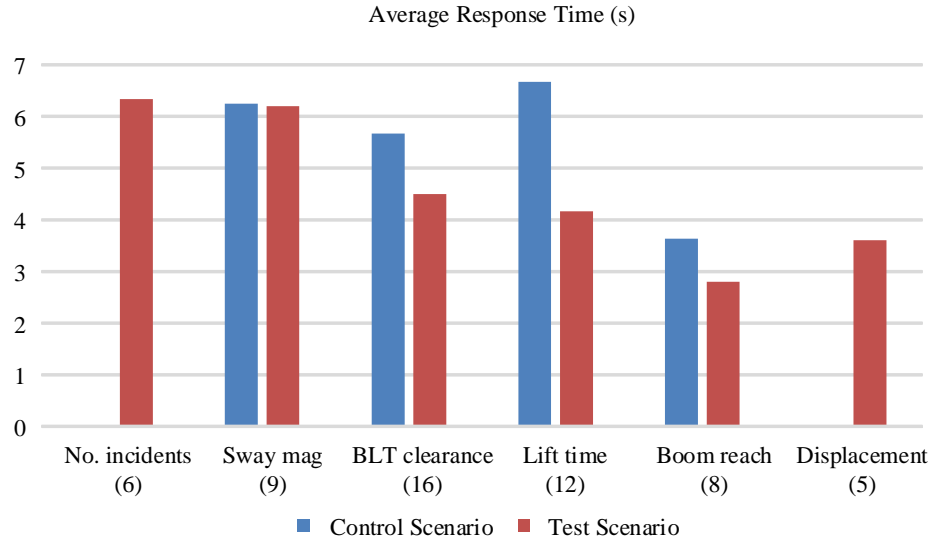


Figure 43: Average response time breakdown in each query

In the breakdown of the results of average response correctness (Figure 44), estimation of boom reach was closest to the reality (94.5%) while load displacement was least correct (74%). Overall, response correctness was improved in all recorded queries, by 6.8 % on average (3.2% for boom reach estimation, 12.3% for sway magnitude estimation, 8% for lift time prediction, and 3.7% for clearance estimation). It should be noted that the estimation correctness of load sway magnitude increased by 12.3% with the assistance of the system. This is easy to understand because the assistance system continuously monitors the load sway magnitude and warns the operator once the sway is beyond a threshold of 2 m.

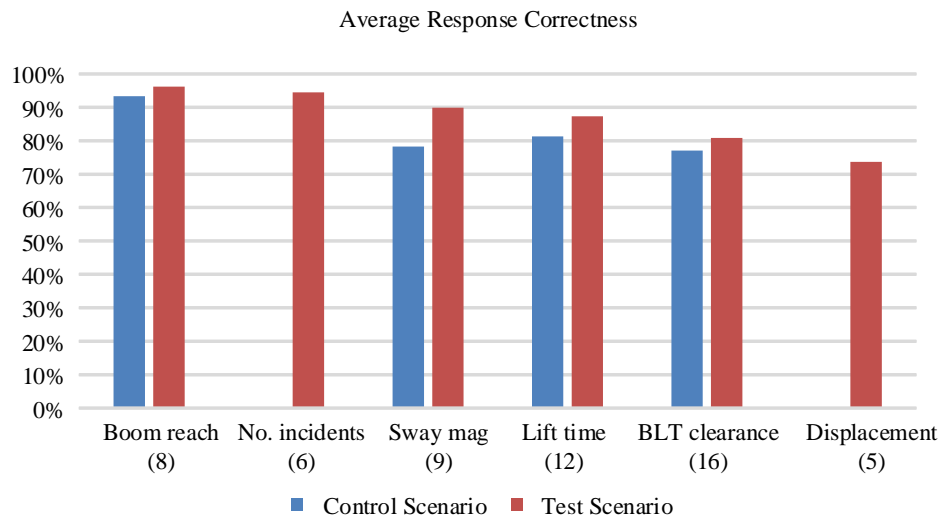


Figure 44: Average response correctness breakdown in each query

7.2.8. General feedback from the operators

Each operator participated in the field tests was asked to provide their feedback about the prototype system through a survey. The survey focused on three aspects: ease of use, impact on lift safety, and impact on lift efficiency. Table 6 summarizes the results of the survey and an average score is calculated for each statement.

Table 6: Results of general feedback survey in five Likert scale

Statement		Operator A (15-yr exp.)	Operator B (8-yr exp.)	Operator C (10-yr exp.)	Operator D (16-yr exp.)	Operator E (11-yr exp.)	Average
<i>Ease of use</i>							
1	It was easy to setup the system for a new lifting task.	4	5	3	4	4	4
2	Graphs and information displayed on the screen were informative and easy to follow.	5	4	4	4	4	4.2
3	The warnings were effective and accurate.	3	5	4	3	4	3.8
4	I was comfortable with the screen size and position.	4	5	3	4	2	3.6
5	Voice control was easy to use and I barely used the touch screen.	4	4	4	4	3	3.8
6	The virtual environment was very realistic and reflected the actual constraints.	3	5	4	4	3	3.8
7	The motion of the virtual crane matched with the real crane without delay.	4	5	4	5	4	4.4
<i>Impact on lift safety</i>							
8	I heavily relied on the system when I couldn't see the load.	4	4	3	3	4	3.6

9	I felt confident when I used the system.	4	5	4	4	3	4
10	I would perform more safely with the system.	4	5	4	3	4	4
11	I would be comfortable with using the system without a signal person.	2	5	3	3	2	3
12	I had a better understanding of the hazards associated with the lifting task	4	5	4	4	2	3.8
<i>Impact on Efficiency</i>							
13	Using the system decreased my productivity during blind lifts.	3	2	3	4	4	3.2
14	The system helped me to choose a safer and more efficient lift path	4	5	4	5	3	4.2
15	My productivity would increase if I were more used to the system.	4	4	5	5	4	4.4
16	The lift organization and planning were easier with the system.	4	5	4	5	4	4.4
<i>Others</i>							
15	I think the system should be standard on mobile cranes.	4	5	3	4	4	4
16	The lift review function will help me perform better in future lifts.	4	5	4	4	4	4.2

The system was considered easy to use in term of setting up a new lifting task and visualizing the crane motion and environment conditions in a timely manner. Nevertheless, the operators show distinct opinions about the screen size and position. Some felt the screen size and its position were just right and it would block their view otherwise, whereas others preferred a bigger screen at a higher position. This problem is expected to be solved with a head-up display or an augmented reality glass in the future.

As to the system's impact on lift safety, although the operators were not fully relying on the system, they felt confident when they used the system during the lift. They also believed that the use of the system improved the overall lift safety as they obtained a better understanding of the hazards associated with the lifting task. However, they did not think the system can completely replace the use of a signal person at this moment. The main reason for the hesitation is that they felt less secured when relying solely on a technology. The insecurity is mainly from the fact that when there is a signal person they will share the responsibility if an incident occurs, whereas when there is not the operator will be the only one to blame.

Most operators believed that viewing the lift scene in 3D and having the ability to toggle the view helped them to carry out a safer and more efficient lift plan, particularly the selection of lift path. There was a moderate opinion about whether using the system would increase or decrease the lift efficiency. Some operators argued that in less complex lifting tasks, especially when they have the direct line-of-sight to the load and obstructions, they found the warning was redundant and interrupted their job. They will have to check the source of the warnings and sometimes found the level of risk to be over-estimated. Nevertheless, all operators agreed that in complex lifts especially in blind lifts or lifts at

night, the system will play an important role in helping them to understand the collision risks. This led to a more productive lift as they save the time for communication with the signal person and they did not need to wait for the signal person to get to an observing place. It was also pointed out by the operators that they spent more time than needed on operating the system (e.g., change view angle) which could be avoided if they are more used to the system.

7.3. Conclusions

To validate the effectiveness of a safety assistance system for crane operation, this chapter introduces an assessment approach that quantifies the improvement in lift performance and SA, where lift performance is quantified by five key performance indexes (KPIs) and SA is measured by an online query-based technique. These proposed methods were tested and validated in two field tests. The first field test involved 4 operators in 92 lift iterations and it focused on the impact of system usage level to lift performance as well as the influence of individual characteristics on the system usage pattern. The second field test involved five operators in 60 lift iterations for two lifting tasks of different complexity levels. The second field test explored the impact of task complexity and operator workload on lift performance and the situation awareness (SA) of crane operators. Results from the two field tests indicate that the assistance system has a positive impact on improving lift performance as well as the operators' SA level. General feedback from the operators suggests the prototype system was easy to use and effectively assisted their safety and efficiency performance. Overall, results from the two field tests suggest that the assistance system facilitated the operator's ability to comprehend the situation, especially the information closely related to site geometric constraints, which led to a safer and more

efficient lifting operations. It should be noted that the experiments were conducted in real lift jobs with actual temporal and spatial constraints, and the participating operators were exposed to real lifting pressure and risks. Compared to virtual simulation or survey that were commonly used in previous research, the data collected and presented in this research is more realistic and therefore the results are closer to the actual effectiveness of the assistance.

CHAPTER VIII ECONOMIC ANALYSIS

Although this research mainly focuses on technical challenges in the proposed framework for real-time safety assistance, understanding the economic impact of such assistance framework is important to facilitate industry adoption. This chapter presents an indicative economic analysis of the proposed lift assistance framework. A fundamental assumption in the economic analysis is that the savings on safety and efficiency improvement (i.e., fatality and injury reduction) are calculated based on the performance improvement observed in the field tests.

8.1. Cost estimate

Costs in adopting an assistance system contain hardware purchase (e.g., tablet computer and sensors) and service costs (e.g., installation, laser scanning). Table 7 shows the cost breakdown for a prototype of the assistance system for a single crane. The total cost for one single system is estimated at \$8000. It should be noted that due to the difference in crane type and specification, the selection of sensors and the complexity of installation might vary. Therefore, the cost for adopting an assistance system might fluctuate around \$8000 for different cranes.

Table 7: Cost breakdown for a single assistance system

Item	Cost
Tablet computer	\$800
Processing unit and Encoder sensors	\$4000
IMU sensor	\$600
Installation	\$100
Laser scanning*	\$2000
Maintenance	\$500
Total	\$8000

* Assume only operation cost for laser scanning

8.2. Return estimate

There are two categories in the return, the savings due to improved lift safety and the savings due to improved lift efficiency. According to the field test results, using the system resulted in 15% reduction in collision-related near misses and 10% reduction in lift time. The following sections show the details in return calculation in these two categories. The benefits of adopting the system are estimated in US dollars per year.

8.2.1. Benefits in safety improvement

Losses in a crane accident vary due to the different consequence it may cause. Based on the level of severity, the consequences of a crane accident can be classified into the near-miss incident, property damage, injury, and fatality. Based on the data from Bureau of Labor Statistics, Waehrer et al. estimated that the cost of average construction fatality, including direct and indirect costs, is 4 million US dollars, and nonfatal days-away injuries cost \$42,000 per case [83]. Based on the records on Craneaccidents.com, claims for

damage to the crane are usually not less than \$100,000. Therefore \$100,000 is taken in this analysis for the saving in each property damage case. These numbers are adopted to estimate the savings in different types of incidents.

The occurrence of different types of incidents is estimated based on historical data of crane-related accidents. The number of fatalities in crane-related accidents per year is estimated based on the BLS statistics from 1997 to 2004, which averages 74 fatalities per year. Using the occurrence of crane-related fatalities in historical data as the basis, the “Iceberg” or “Pyramid” theory [84] is utilized to estimate the occurrence of injuries, property damage, and near misses. The “Iceberg” or “Pyramid” theory implies a ratio of 1:10 between deaths and injuries, a ratio of 1:30 between death and property damage, and a ratio of 1:600 between death and near misses (Figure 45). Therefore, the annual occurrence of crane-related fatalities is 76 cases, annual occurrence of injuries is 760 cases, annual occurrence of property damage is 2280 cases, and annual occurrence of near misses is 22800 cases.

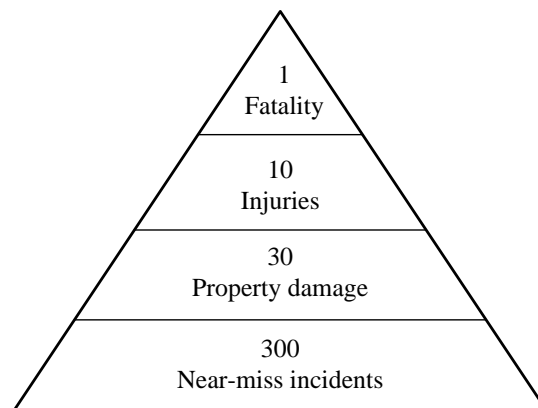


Figure 45: Incident pyramid [84]

As the field test results indicate that using the system resulted in 15% reduction in collision incidents. If we consider these collision incidents as near-misses, it is assumed that the system has the potential to reduce property damage cases by 1.5%, injury cases by 0.5%, and fatality cases by 0.05%.

Eq. 16 is used to calculate the total saving in safety improvement. The annual saving in safety improvement by using the system is \$3.7 million among all cranes in the construction industry. Although it is difficult to estimate the exact number of cranes in the construction industry, OSHA suggested there are approximately 125,000 cranes in operation [2]. Therefore, the annual return in safety improvement for a single crane is \$29.6. Although the return in safety improvement seems negligible in its pecuniary value, reduction in fatalities, injuries, and other such losses have a massive social impact that is intangible and unfair to be monetized.

$$Saving = \sum annual\ occurrences \times reduction\ rate \times saving\ per\ case \quad E.q.\ 16$$

8.2.2. Benefits in efficiency improvement

The field test results indicate that the system could potentially accelerate the lifting operation by 10%. This will generally result in 10% saving in crane rental and daily operation costs. Assuming the average rental cost for a crane is \$300,000 per year and assuming the working time of a crane is 10% in a year, the system could save the crane owner or renter \$3,000 per year by reducing the lifting time.

8.3. Return of investment analysis

Based on the cost and return analyses, for a single crane, the investment in the system is \$8000, while the return in safety improvement is \$29.6 and the return in efficiency improvement is \$3000. Without considering inflation, the investment will be returned in 2.6 years.

8.4. Conclusions

This chapter presents an indicative economic analysis of the proposed lift assistance framework. Hardware and service costs for implementing a real-time assistance system are presented and the returns in safety and efficiency improvement are estimated based on safety record assumptions and actual test data acquired from the field tests. Given a cost of \$8000 and returns of \$3029.6 for adopting a real-time assistance system on a single crane, the investment will be returned in 2.6 years. It should be noted that this economic analysis is intended to be an indicative assessment, instead of an accurate assessment. In addition, it should be emphasized that the decrease in fatalities, injuries and other such losses have a massive, positive impact on the company's reputation and morale which is difficult to be monetized.

CHAPTER IX CONCLUSIONS AND DISCUSSION

This chapter aims to summarize the work in this doctoral research and to conclude the research findings that address the research questions and objectives. This chapter also discusses the limitations in this research effort and the future work needs to be conducted.

9.1. Summary

Despite many safety considerations already embedded in lift pre-planning and operation, the ability to provide real-time safety assistance to crane operators during the lifting is inadequate. Although multiple technologies have been introduced to provide safety assistance to the operator, very few of them were actually adopted in the practice. Based on a throughout review of the state-of-the-art in crane safety technologies, gaps in the knowledge are identified including the lack of a reliable real-time crane motion capturing method, inadequate consideration of environmental constraints and changes, and missing validation of the assistance systems' impact on lift performance and operators' situation awareness. To close these gaps in knowledge, this thesis introduces a framework that outlines the technical steps and requirements for enabling real-time safety assistance for crane operations, as well as a thorough system architecture to facilitate the implementation of this framework. Further, this thesis describes in detail the design, development, and testing of three major technical components including real-time crane motion capturing, as-is site condition modeling and updating, and pro-active hazard analysis and 3D visualization. A prototype system was developed based on the proposed system architecture and deployed on a real mobile crane. Field test results indicate this system was able to track and visualize crane motion in real-time with an average accuracy of 0.43 m.

Based on crane motion and as-is site conditions, the system was able to identify the potential collision hazards and provide timely warnings to the operator to mitigate the risk.

To address the need to assess the effectiveness of assistance systems, this research developed an objective approach that quantifies the improvement in lift performance and SA, where lift performance is quantified by five key performance indexes (KPIs) and SA is measured by an online query-based technique. This assessment approach was tested in two field tests to validate the effectiveness of a prototype of the proposed safety assistance system based on the system architecture. The first field test focuses on the impact of system usage level to lift performance as well as the influence of individual characteristics on the system usage pattern. The second field test explored the impact of task complexity and operator workload on lift performance and the situation awareness (SA) of crane operators. Results from the two field tests indicate that the assistance system has a positive impact on improving lift performance as well as the operators' SA level. General feedback from the operators suggests the prototype system was easy to use and effectively assisted their safety and efficiency performance.

9.2. Research Contribution and Impacts

The primary goal of this research is to reduce crane accidents related to operator errors. To achieve this goal, a framework along with multiple innovative hardware design and computation algorithms are presented for enabling real-time safety assistance.

Findings in this research supplements and enhances existing knowledge in both research and practices concerning crane safety. As a summary, major contributions of this doctoral research are concluded as follows:

- A scientific framework is created to outline the requirements and technical roadmap for effective and reliable safety assistance for crane operations. As this framework address several common challenges in equipment operation monitoring and analysis, this framework is essential for the development of real-time assistance for construction equipment in general. To be specific, this research presents an IMU-based sensing method and a computation algorithm for crane load positioning, a point cloud-vision hybrid approach for quick site condition modeling and mobile asset location updating, and a hazard recognition algorithm for collision risk analysis and pro-active warning.
- A practical system architecture enabled by the creation of novel methods and computation algorithms for sensor data processing and real-time visualization is presented. The proposed system architecture enables easy deployment of cost-effective sensors that can be equipped with a new crane as well as retrofit a used crane. In addition, a UI design was created for effective warning and hands-free interaction with the assistance system.
- An assessment approach is introduced for validating the effectiveness of safety assistance systems. This approach quantifies the lift performance, measures the level of SA during the operation, and considers the impact of workload on performance and SA. This approach can be further used to validate the effectiveness of emerging technologies that work closely with a human operator or function with human decision-making.

9.3. Discussion and Recommendation for Future Research

- Despite that many methods developed for mobile cranes can be applied for other crane types, designing the assistance system for other crane types should identify their unique requirements such as sensing range, crane kinematics, and the scenario where multiple cranes need to work together.
- The methods developed for site condition updating are able to continuously track the change of site conditions, but it cannot update the 3D site model in a very high frequency or in real-time. Ideally, the site condition is preferred to be updated in real-time to capture any tiny changes at any given moment. In reality, technology limitations such as data acquisition rate and computational capability make real-time 3-dimension geometry updating very challenging and expensive even if possible. Nevertheless, with the advance in sensing technology and improvement of computation capability, continuous data collection, and real-time computation can be anticipated in the near future.
- The effectiveness of a prototype assistance system was validated in two field tests and the test results show the improvement in lift performance and operators' situation awareness. Nevertheless, based on the principle of statistical analysis, the sample size of operators participated in the field tests were not large enough to show the statistical significance of the improvement. Particularly, the variances in the measurements tend to be large due to the limited number of subjects and the significant difference in experience and maneuver pattern among them. That being said, results in these field tests reflect the general trend in the improvement of lift performance and SA by introducing the assistance system. The conclusions are

meaningful to understand the strengths and limitations of the current design and to guide the future work.

- Another limitation in the SA measurement in field test 2 is that the query process was not blind to the questioner. This means potentially the questioner could intentionally select the easy query to get a better result in the test scenario. These biases in the results can be minimized by asking multiple queries and randomly selecting part of them for SA measurement.
- Although this thesis reported the cost breakdown for a prototype assistance system, a thorough economic analysis is not conducted. This is mainly because the return of investment for adopting such assistance system is difficult to estimate. In particular, savings in safety performance improvement is always hard to quantify, and most likely cannot be monetized. That said, a rough economic analysis is presented in the thesis based on extensive assumptions. The results can be used as a reference but should not be taken as a dependable proof for technology adoption.

REFERENCES

- [1] Technavio Insights, “2012-2016 Global Crane Market Report,” 2016.
- [2] Occupational Safety and Health Administration, “Crane and Hoist Safety,” 2016. [Online]. Available: <https://www.osha.gov/archive/oshinfo/priorities/crane.html>. [Accessed: 22-Aug-2016].
- [3] Bureau of Labor Statistics (BLS), “Census of Fatal Occupational Injuries,” *U.S. Department of Labor, Bureau of Labor Statistics, News*, 2016. [Online]. Available: <http://www.bls.gov/iif/oshcfoi1.htm>.
- [4] CPWR, “Crane-Related Deaths in Construction and Recommendations for Their Prevention,” 2009.
- [5] R. L. Neitzel, N. S. Seixas, and K. K. Ren, “A review of crane safety in the construction industry,” *Appl. Occup. Environ. Hyg.*, vol. 16, no. 12, pp. 1106–17, Dec. 2001.
- [6] J. E. Beavers, J. R. Moore, R. Rinehart, and W. R. Schriver, “Crane-Related Fatalities in the Construction Industry,” *J. Constr. Eng. Manag.*, pp. 901–910, 2006.
- [7] A. Suruda, M. Egger, and D. Liu, “Crane-Related Deaths in the U.S. Construction Industry, 1984-94,” *J. Constr. Eng. Manag.*, vol. 132(9), pp. 901–910, 1997.
- [8] K. Tantisevi and B. Akinci, “Automated generation of workspace requirements of mobile crane operations to support conflict detection,” *Autom. Constr.*, vol. 16, no. 3, pp. 262–276, May 2007.
- [9] Y. K. Cho and C. T. Haas, “Rapid geometric modeling for unstructured construction workspaces,” *Comput. Civ. Infrastruct. Eng.*, vol. 18, no. 4, pp. 242–253, 2003.
- [10] Y. K. Cho, C. T. Haas, K. Liapi, and S. V. Sreenivasan, “A framework for rapid local area modeling for construction automation,” *Autom. Constr.*, vol. 11, no. 6, pp. 629–641, 2002.
- [11] L. K. Shapiro and J. P. Shapiro, *Cranes and Derricks*. New York: McGraw-Hill, 2011.
- [12] R. A. King, “Analysis of Crane and Lifting Accidents in North America from 2004 to 2010,” 2012. [Online]. Available: <https://dspace.mit.edu/handle/1721.1/73792>. [Accessed: 19-Aug-2016].
- [13] G. Raviv, B. Fishbain, and A. Shapira, “Analyzing risk factors in crane-related near-miss and accident reports,” *Saf. Sci.*, vol. 91, pp. 192–205, 2017.
- [14] W. C. Hornaday, C. T. Haas, J. T. O’Connor, and J. Wen, “Computer-aided planning

- for heavy lifts,” *J. Constr. Eng. Manag.*, vol. 119, no. 3, pp. 498–515, 1994.
- [15] P. Zhang, F. C. Harris, P. O. Olomolaiye, and G. D. Holt, “Location Optimization for a Group of Tower Cranes,” *J. Constr. Eng. Manag.*, vol. 1, no. April, pp. 115–122, 1999.
 - [16] V. Kamat and J. Martinez, “Visualizing Simulated Construction Operation in 3D,” *J. Comput. Civ. Eng.*, no. October, pp. 329–337, 2001.
 - [17] M. Al-Hussein, M. Athar Niaz, H. Yu, and H. Kim, “Integrating 3D visualization and simulation for tower crane operations on construction sites,” *Autom. Constr.*, vol. 15, no. 5, pp. 554–562, Sep. 2006.
 - [18] K. Lin and C. T. Haas, “Multiple heavy lifts optimization,” *J. Constr. Eng. Manag.*, vol. 122, no. 4, pp. 354–362, 1996.
 - [19] M. Al-Hussein, S. Alkass, and O. Moselhi, “Optimization Algorithm for Selection and on Site Location of Mobile Cranes,” *J. Constr. Eng. Manag.*, vol. 131, no. 5, pp. 579–590, May 2005.
 - [20] J. Irizarry and E. Karan, “Optimizing Location of Tower Cranes on Construction Sites through GIS and BIM Integration,” *J. Inf. Technol. Constr.*, vol. 17, no. March, pp. 351–366, 2012.
 - [21] C. M. Tam and T. K. L. Tong, “GA-ANN model for optimizing the locations of tower crane and supply points for high-rise public housing construction,” *Constr. Manag. Econ.*, vol. 21, no. 3, pp. 257–266, 2003.
 - [22] Z. Lei, H. Taghaddos, U. Hermann, and M. Al-hussein, “A methodology for mobile crane lift path checking in heavy industrial projects,” *Autom. Constr.*, vol. 31, pp. 41–53, 2013.
 - [23] A. R. Soltani, H. Tawfik, J. Y. Goulernas, and T. Fernando, “Path planning in construction sites: performance evaluation of the Dijkstra, A and GA search algorithms,” *Adv. Eng. Informatics*, vol. 16, no. 4, pp. 291–303, Oct. 2002.
 - [24] P. L. Sivakumar, K. Varghese, and N. R. Babu, “Automated Path Planning of Cooperative Crane Lifts Using Heuristic Search,” *J. Comput. Civ. Eng.*, vol. 17(3), pp. 197–207, 2003.
 - [25] Y.-C. Chang, W.-H. Hung, and S.-C. Kang, “A fast path planning method for single and dual crane erections,” *Autom. Constr.*, vol. 22, pp. 468–480, Mar. 2012.
 - [26] J. J. Kuffner and S. M. LaValle, “RRT-connect: An efficient approach to single-query path planning,” *Proc. 2000 ICRA. Millenn. Conf. IEEE Int. Conf. Robot. Autom. Symp. Proc. (Cat. No.00CH37065)*, vol. 2, no. Icr, pp. 995–1001, 2000.
 - [27] Y. Lin, X. Wang, D. Wu, X. Wang, and S. Gao, “Lift Path Planning for Telescopic

- Crane Based-on Improved hRRT,” *Int. J. Comput. Theory Eng.*, vol. 5, no. 5, pp. 816–819, 2013.
- [28] C. Zhang and A. Hammad, “Improving lifting motion planning and re-planning of cranes with consideration for safety and efficiency,” *Adv. Eng. Informatics*, vol. 26, no. 2, pp. 396–410, Apr. 2012.
 - [29] H. AlBahnassi and A. Hammad, “Near real-time motion planning and simulation of cranes in construction: Framework and system architecture,” *J. Comput. Civ. Eng.*, vol. 26, no. 1, pp. 54–63, 2012.
 - [30] S. W. Kwon, F. Bosche, C. Kim, C. T. Haas, and K. a. Liapi, “Fitting range data to primitives for rapid local 3D modeling using sparse range point clouds,” *Autom. Constr.*, vol. 13, no. 1, pp. 67–81, 2004.
 - [31] S. Kang and E. Miranda, “Physics Based Model for Simulating the Dynamics of Tower Crane,” *Int. Conf. Comput. Civ. Build. Eng.*, vol. 8, pp. 248–253, 2004.
 - [32] W.-H. Hung and S.-C. Kang, “Configurable model for real-time crane erection visualization,” *Adv. Eng. Softw.*, vol. 65, pp. 1–11, Nov. 2013.
 - [33] J. Reason, *Human Error*. Cambridge University Press, 1990.
 - [34] X. Luo, F. Leite, and W. J. O’Brien, “Requirements for Autonomous Crane Safety Monitoring,” *Comput. Civ. Eng.*, pp. 331–338, 2011.
 - [35] C. Zhang, A. Hammad, and S. Rodriguez, “Crane Pose Estimation Using UWB Real-Time Location System,” *J. Comput. Civ. Eng.*, pp. 625–637, 2012.
 - [36] S. Hwang, “Ultra-wide band technology experiments for real-time prevention of tower crane collisions,” *Autom. Constr.*, vol. 22, pp. 545–553, Mar. 2012.
 - [37] H. Li, G. Chan, and M. Skitmore, “Integrating real time positioning systems to improve blind lifting and loading crane operations,” *Constr. Manag. Econ.*, vol. 31, pp. 1–10, Jan. 2013.
 - [38] X. Luo, F. Leite, and W. O’Brien, “Location-Aware Sensor Data Error Impact on Autonomous Crane Safety Monitoring,” *J. Comput. Civ. Eng.*, vol. 29, no. 4, p. B4014010, 2014.
 - [39] N. Li and B. Becerik-Gerber, “Performance-based evaluation of RFID-based indoor location sensing solutions for the built environment,” *Adv. Eng. Informatics*, vol. 25, no. 3, pp. 535–546, 2011.
 - [40] Y. K. Cho, J. H. Youn, and D. Martinez, “Error modeling for an untethered ultra-wideband system for construction indoor asset tracking,” *Autom. Constr.*, vol. 19, no. 1, pp. 43–54, 2010.

- [41] C. Feng, S. Dong, K. M. Lundeen, Y. Xiao, and V. R. Kamat, "Vision-Based Articulated Machine Pose Estimation for Excavation Monitoring and Guidance," *Proc. 32nd Int. Symp. Autom. Robot. Constr.*, 2015.
- [42] J. Yang, P. A. Vela, J. Teizer, and Z. Shi, "Vision-Based Tower Crane Tracking for Understanding Construction Activity," *ASCE J. Comput. Civ. Eng.*, vol. 28, no. 1, pp. 103–112, 2013.
- [43] Y. K. Cho and M. Gai, "Projection-Recognition-Projection Method for Automatic Object Recognition and Registration for Dynamic Heavy Equipment Operations," *J. Comput. Civ. Eng.*, vol. 28, no. 5, p. A4014002, Sep. 2014.
- [44] C. Wang and Y. K. Cho, "Smart scanning and near real-time 3D surface modeling of dynamic construction equipment from a point cloud," *Autom. Constr.*, vol. 49, pp. 239–249, 2015.
- [45] G. Lee, J. Cho, S. Ham, T. Lee, G. Lee, S. H. Yun, and H. J. Yang, "A BIM- and sensor-based tower crane navigation system for blind lifts," *Autom. Constr.*, vol. 26, pp. 1–10, Oct. 2012.
- [46] W. Ren and Z. Wu, "Real-Time Anticollision System for Mobile Cranes during Lift Operations," *J. Comput. Civ. Eng.*, pp. 1–12, 2012.
- [47] U.-K. Lee, K.-I. Kang, G.-H. Kim, and H.-H. Cho, "Improving Tower Crane Productivity Using Wireless Technology," *Comput. Civ. Infrastruct. Eng.*, vol. 21, no. 8, pp. 594–604, Nov. 2006.
- [48] G. Putnik, V. Shah, V. Spasojević-Brkić, C. Alves, and H. Castro, "A proposal for installation architecture for video cameras and screens in an integrated vision system for crane cabins," *9th Int. Qual. Conf.*, no. June, pp. 633–640, 2015.
- [49] A. Shapira, F. Asce, Y. Rosenfeld, and I. Mizrahi, "Vision System for Tower Cranes," *J. Constr. Eng. Manag.*, no. May, pp. 320–332, 2008.
- [50] G. Lee, H.-H. Kim, C.-J. Lee, S.-I. Ham, S.-H. Yun, H. Cho, B. K. Kim, G. T. Kim, and K. Kim, "A laser-technology-based lifting-path tracking system for a robotic tower crane," *Autom. Constr.*, vol. 18, no. 7, pp. 865–874, Nov. 2009.
- [51] X. Wang, Y. Y. Zhang, D. Wu, and S. De Gao, "Collision-Free Path Planning for Mobile Cranes Based on Ant Colony Algorithm," *Key Eng. Mater.*, vol. 467–469, pp. 1108–1115, Feb. 2011.
- [52] X. Su, J. Pan, and M. Grinter, "Improving Construction Equipment Operation Safety from a Human-centered Perspective," *Procedia Eng.*, vol. 118, pp. 290–295, 2015.
- [53] H. L. Chi, Y. C. Chen, S. C. Kang, and S. H. Hsieh, "Development of user interface for tele-operated cranes," *Adv. Eng. Informatics*, vol. 26, no. 3, pp. 641–652, 2012.

- [54] R. Stiefelhagen and J. Zhu, "Head orientation and gaze direction in meetings," *CHI 02 Ext. Abstr. Hum. factors Comput. Syst. CHI 02*, no. 1, p. 858, 2002.
- [55] A. Furnham, *Personality at work: the role of individual differences in the workplace*. New York: Routledge, 1994.
- [56] D. B. Kaber and M. R. Endsley, "The effects of level of automation and adaptive automation on human performance, situation awareness and workload in a dynamic control task," *Theor. Issues Ergon. Sci.*, vol. 5, no. 2, pp. 113–153, 2004.
- [57] D. G. Jones and M. R. Endsley, "Sources of situation awareness errors in aviation," *Aviat. Sp. Environ. Med.*, vol. 67, no. 6, pp. 507–512, 1996.
- [58] M. R. Endsley, "Situation awareness global assessment technique (SAGAT)," in *Proceedings of the IEEE 1988 National Aerospace and Electronics Conference*, 1988, pp. 789–795.
- [59] F. T. Durso and S. D. Gronlund, "Situation Awareness," *Handb. Appl. Cogn.*, pp. 283–314, 1999.
- [60] G. Hauland, "Measuring Individual and Team Situation Awareness During Planning Tasks in Training of En Route Air Traffic Control," *Int. J. Aviat. Psychol.*, vol. 18, no. 776112470, pp. 290–304, 2008.
- [61] F. T. Durso, K. M. Geldbach, and P. Corballis, "Detecting Confusion Using Facial Electromyography," *Hum. Factors J. Hum. Factors Ergon. Soc.*, vol. 54, no. 1, pp. 60–69, 2012.
- [62] F. T. Durso, K. M. Geldbach, and P. Corballis, "Detecting Confusion Using Facial Electromyography," *Hum. Factors J. Hum. Factors Ergon. Soc.*, vol. 54, no. 1, pp. 60–69, 2012.
- [63] M. A. Vidulich, M. Stratton, M. Crabtree, and G. Wilson, "Performance-based and physiological measures of situational awareness," *Aviat. Space. Environ. Med.*, 1994.
- [64] G. Wilson, "Strategies for psychophysiological assessment of situation awareness," in *Situation Awareness Analysis and Measurement*, Lawrence Erlbaum Associates, 2000, pp. 158–169.
- [65] M. R. Endsley, "Toward a Theory of Situation Awareness in Dynamic Systems," *Hum. Factors J. Hum. Factors Ergon. Soc.*, vol. 37, no. 1, pp. 32–64, 1995.
- [66] M. R. Endsley, "Measurement of Situation Awareness in Dynamic Systems," *Hum. Factors J. Hum. Factors Ergon. Soc.*, vol. 37, no. 1, pp. 65–84, 1995.
- [67] E. Jeannot, C. Kelly, and D. Thompson, "The Development of Situation Awareness Measures in ATM Systems," *System*, vol. 1.0, no. {HRS/HSP-005-REP-01, Ed. 1.0,

Released Issue}, p. 88, 2003.

- [68] F. T. Durso, T. Truitt, C. Hackworth, and J. Crutchfield, "En Route Operational Errors and Situational Awareness," *Int. J. Aviat. Psychol.*, vol. 8, no. 2, pp. 157–176, 1998.
- [69] F. Durso, T. Truitt, C. Hackworth, J. Crutchfield, D. Nikolic, P. M. Moertl, and D. Ohrt, "Expertise and chess: A pilot study comparing situation awareness methodologies." 1995.
- [70] K. Harwood, B. Barnett, and C. D. Wickens, "Situational awareness: A conceptual and methodological framework," in *Proceedings of the 11th Biennial Psychology in the Department of Defense Symposium*, 1988, pp. 23–27.
- [71] Baumer Group, "Cranes and Heavy Vehicles," 2016. [Online]. Available: http://www.baumer.com/fileadmin/user_upload/international/Downloads/BR-CT/Baumer_Heavy-Vehicles-Cranes_BR_EN_1108_11047951.pdf. [Accessed: 19-Aug-2016].
- [72] FARO Technology Ltd., "FARO Laser Scanner Focus 3D X330," 2015. [Online]. Available: <https://www.reproproducts.com/pdfs/brochures/faro/x330.pdf>. [Accessed: 19-Aug-2016].
- [73] N. Snavely, S. M. Seitz, and R. Szeliski, "Modeling the world from Internet photo collections," *Int. J. Comput. Vis.*, vol. 80, no. 2, pp. 189–210, 2008.
- [74] D. G. Lowe, "Distinctive Image Features from Scale-Invariant Keypoints," *Int. J. Comput. Vis.*, vol. 60, no. 2, pp. 91–110, 2004.
- [75] R. Schnabel, R. Wahl, and R. Klein, "Efficient RANSAC for point-cloud shape detection," *Comput. Graph. Forum*, vol. 26, no. 2, pp. 214–226, 2007.
- [76] N. Locantore, J. S. Marron, D. G. Simpson, N. Tripoli, J. T. Zhang, and K. L. Cohen, "Robust principal component analysis for functional data," *Test*, vol. 8, no. 1, pp. 1–73, 1999.
- [77] T. Mathes and J. Piater, "Robust non-rigid object tracking using point distribution manifolds," *Pattern Recognit.*, pp. 515–524, 2006.
- [78] Occupational Safety & Health Administration, "Cranes and Derricks in Construction (1926.1408)," 2016. [Online]. Available: https://www.osha.gov/pls/oshaweb/owadisp.show_document?p_table=STANDARDS&p_id=19. [Accessed: 19-Aug-2016].
- [79] Unity Technologies, "Unity3D," 2016. [Online]. Available: <https://www.unity3d.com>. [Accessed: 19-Aug-2016].
- [80] S. Hart and L. Staveland, "Development of NASA-TLX (Task Load Index): Results

of empirical and theoretical research,” *Adv. Psychol.*, vol. 52, pp. 139–183, 1988.

- [81] NASA, “NASA-TLX.” [Online]. Available: <http://humansystems.arc.nasa.gov/groups/tlx/>. [Accessed: 22-Aug-2016].
- [82] F. T. Durso and A. R. Dattel, “SPAM: The Real-Time Assessment of SA,” pp. 137–154, 2004.
- [83] G. Waehrer, X. Dong, T. Miller, E. Haile, and Y. Men, “Costs of Occupational Injuries in Construction in the United States,” *Accid. Anal. Prev.*, vol. 39, no. 6, pp. 1258–1266, 2007.
- [84] F. Bird, “Near miss reporting as a safety tool,” *Int. Saf. Acad.*, 1974.

VITA

Yihai Fang was born in Xi'an and grew up in Beijing, China. He received his Ph.D. from the School of Civil and Environmental Engineering at the Georgia Institute of Technology. His research revolves around leveraging information and sensing technologies to enhance construction safety and efficiency. More specifically, his doctoral thesis titles “Real-time Safety Assistance to Improve Operators' Situation Awareness in Crane Lifting Operations.” During the doctoral study, Yihai completed his Master of Science degree in Construction Engineering and Management at Georgia Tech. Prior to joining Georgia Tech, Yihai received a Bachelor's degree in Civil Engineering from Tongji University, Shanghai, China in 2011. By the time of graduation, Yihai's research findings have been published in six journal publications and numerous conference proceedings.